

İSTANBUL TECHNICAL UNIVERSITY ★ INSTITUTE OF SCIENCE AND TECHNOLOGY

**ARTIFICIAL NEURAL NETWORK APPROACHES FOR
SLOPE STABILITY**

**M.Sc. Thesis by
Mert TOLON , B.S.c**

Department : Civil Engineering

Programme: Earthquake Engineering

JUNE 2007

**ARTIFICIAL NEURAL NETWORK APPROACHES FOR
SLOPE STABILITY**

**M.Sc. Thesis by
Mert TOLON , B.S.c
501051212**

Date of submission : 4 May 2007

Date of defence examination: 13 June 2007

Supervisor (Chairman): Assoc. Prof. Dr. Derin N. URAL

Members of the Examining Committee Assoc. Prof. Dr. Recep İYİSAN (İ.T.Ü.)

Assist. Prof. Dr. Mehmet BERİLGİN (Y.T.Ü.)

JUNE 2007

**YAPAY SİNİR AĞLARI YÖNTEMİ KULLANILARAK
SEV STABİLİTESİNİN İNCELENMESİ**

**YÜKSEK LİSANS TEZİ
Mert TOLON
501051212**

**Tezin Enstitüye Verildiği Tarih : 4 Mayıs 2007
Tezin Savunulduğu Tarih : 13 Haziran 2007**

**Tez Danışmanı : Doç.Dr. Derin N. URAL
Diğer Jüri Üyeleri Doç. Dr. Recep İYİSAN (İ.T.Ü.)
Y.Doç.Dr. Mehmet BERİLGİN (Y.T.Ü.)**

HAZİRAN 2007

PREFACE

I would like to express my grateful thanks to the respectful members of Earthquake Engineering Division of the Civil Engineering Department at Istanbul Technical University for giving me the chance to study for my MSc thesis. I especially would like to express my sincere thanks to my supervisor Assoc. Prof. Derin N. URAL for her guidance and insight throughout the research. I also want to thank to Assoc. Prof. Recep IYISAN for giving valuable help during the preparation of this thesis.

Finally, I am most grateful to my family for their endless supports. Preparation of this thesis involved several months of long working hours; I could not have done it without their insight and encouragement.

June 2007

Mert TOLON

ÖNSÖZ

İstanbul Teknik Üniversitesi İnşaat Mühendisliği Bölümü Deprem Mühendisliği Anabilim Dalı'nın bana yüksek lisans yapma olanağı tanıyan saygıdeğer öğretim üyelerine minnet dolu teşekkürlerimi bildirmek isterim. Özellikle danışmanım Doç. Dr. Derin N. URAL'a çalışmalarım boyunca gösterdiği rehberlik ve anlayıştan dolayı en içten teşekkürlerimi sunmak istiyorum. Ayrıca bu tezi hazırlamam sırasında göstermiş olduğu yardımlardan dolayı Doç. Dr. Recep İYİSAN'a teşekkürü bir borç biliyorum.

Son olarak, aileme de vermiş oldukları sonsuz destekten ötürü minnettarım. Bu tezin hazırlanması aylar süren çalışma saatleri sonunda bitmiştir; onların anlayışı ve cesaretlendirmesi olmadan bunu gerçekleştiremezdim.

Haziran 2007

Mert TOLON

TABLE OF CONTENTS

ABBREVIATIONS	vii
LIST OF TABLES	viii
LIST OF FIGURES	ix
LIST OF SYMBOLS	xi
ÖZET	xii
SUMMARY	xiii
1. INTRODUCTION	1
1.1. General	1
1.2. Short History of Artificial Intelligence Method	1
1.3. Objectives	2
2. LITERATURE REVIEW	4
2.1. Introduction	4
2.2. Types of slope failure modes	4
2.2.1. Short term stability	4
2.2.2. Long term stability	5
2.3. Factors affecting slope stability analyses	5
2.3.1. Failure plane geometry	5
2.3.2. Non-Homogeneity of soil layers	6
2.3.3. Tension crack	6
2.3.4. Dynamic loading	7
2.4. Methods of analyses	7
2.4.1. Planar failure surface	9
2.4.2. Circular failure surface	10
2.4.2.1. Fellenius method	10
2.4.2.2. Bishop method	12
2.4.2.3. Spencer's method	13
2.4.2.4. Obtaining the most critical circle	16
2.4.3. Non-Circular failure surface	17
2.4.3.1. Janbu's method	17
2.4.3.2. Morgensten-Price methods	19
2.4.3.3. Location of critical failure surface	20
2.4.4. Selection of method	20
2.5. Numerical methods for slope stability analysis	21
2.5.1. Finite difference method	21
2.5.2. Finite element method	22
2.6. Computer programs based on traditional methods	24
2.7. Slope stability analyses conditions	33

3. ARTIFICIAL INTELLIGENCE APPLICATIONS WITH NEURAL NETWORKS	35
3.1 Introduction	35
3.2 Neural Network's Properties	35
3.2.1 Basic Structure Of Neural Network	35
3.2.2 Design Choices Of Neural Networks	39
3.2.3 Neural Network Architectures	40
3.2.3.1 GRNN architecture and learning algorithm	40
3.2.3.2 PNN architecture	45
3.2.3.3 Back propagation neural network architecture	47
3.2.3.4 Kohonen architecture	50
3.2.3.5 GMDH architecture	51
3.3 General Applications In Civil Engineering	52
3.3.1 Dynamic Soil–Structure Interaction Using Neural Networks For Parameter Evaluation	52
3.3.2 A Neural Network Approach For Predicting The Structural Behavior Of Concrete Slabs	52
3.3.3 Neural Network Analysis of Structural Damage Due to Corrosion	53
3.3.4 Artificial Neural Networks for Predicting The Response Of Structural Systems with Viscoelastic Dampers	54
3.3.5 Modeling Ground Motion Using Neural Networks	55
3.3.6 Analysis Of Soil Water Retention Data Using Artificial Neural Networks	55
3.3.7 Neural Network Based Prediction Of Ground Surface Settlements Due To Tunnelling	57
3.3.8 Neural Network Modeling Of Water Table Depth Fluctuations	57
3.4 General Applications In Geotechnical Engineering	58
3.4.1 Pile Capacity	59
3.4.2 Settlement Of Foundations	60
3.4.3 Soil Properties And Behaviour	63
3.4.4 Liquefaction	65
3.4.5 Site Characterization	66
3.4.6 Earth retaining structures	66
3.4.7 Tunnels And Underground Openings	67
4. NEURAL NETWORK APPROACHES FOR SLOPE STABILITY	68
4.1 Introduction	68
4.2 Input Parameters Information	68
4.3 Analysis	70
4.3.1 BPNN approaches	70
4.3.1.1 Model 1	70
4.3.1.2 Model 2	74
4.3.2 GRNN approaches	77
4.3.2.1 Model 3	77
4.3.2.2 Model 4	80
4.3.2.3 Model 5	83

5. RESULTS	87
REFERENCES	94
APPENDIX A	99
APPENDIX B	103
APPENDIX C	107
APPENDIX D	108
APPENDIX E	112
APPENDIX F	116
APPENDIX G	120
APPENDIX H	122
CURRICULUM VITAE	128

ABBREVIATIONS

AI	: Artificial Intelligence
ANN	: Artificial Neural Network
BPNN	: Back Propagation Neural Network
CPT	: Cone Penetration Test
FEM	: Finite Element Method
FS	: Factor of Safety
GRNN	: General Regression Neural Network
GMDH	: Group Method of Data Handling
KLP	: Kohonen Learning Paradigm
MAE	: Mean Absolute Errors
NN	: Neural Network
PDE	: Partial Differential Equations
PNN	: Probabilistic Neural Network
RMSE	: Root Mean Squared Errors
SCANN	: Site Characterization using Artificial Neural Network

LIST OF TABLES

	<u>Page No</u>
Table 2.1	Comparison of features of methods..... 20
Table 3.1	Summary of regression analysis results of pile capacity prediction..... 60
Table 3.2	Comparison of predicted vs measured settlements..... 63
Table 4.1	Input and output values range for neural network..... 69
Table 4.2	Model 1 approach for training..... 70
Table 4.3	The contribution factors for model 1..... 71
Table 4.4	The results of model 1..... 71
Table 4.5	A pieces of model 1 output table..... 73
Table 4.6	Model 2 approach for training..... 74
Table 4.7	The contribution factors for model 2..... 75
Table 4.8	The results of model 75
Table 4.9	The architecture and the configuration of the model 3..... 77
Table 4.10	Individual smoothing factors for model 3..... 78
Table 4.11	The results of model 3..... 78
Table 4.12	The architecture and the configuration of the model 4..... 80
Table 4.13	Individual smoothing factors for model 4..... 81
Table 4.14	The results of the model 4..... 82
Table 4.15	The architecture and the configuration of the model 5..... 84
Table 4.16	Individual smoothing factors for model 5..... 84
Table 4.17	The results of the model 5..... 85
Table 5.1	Model 1 and model 2 approach configurations and architecture..... 87
Table 5.2	Output R^2 values for model 1 and 2..... 88
Table 5.3	The first five contribution factors for model 1 and model 2..... 89
Table 5.4	The architecture and the configuration of models 3, 4 and 5..... 89
Table 5.5	Output R^2 values for model 3, 4, and 5..... 89
Table 5.6	The first five of individual smoothing factor for models 3, 4, 5 90
Table 5.7	Simulation success rates for each model..... 92

LIST OF FIGURES

	<u>Page No</u>
Figure 1.1 : A basic slope figure.....	1
Figure 2.1 : Shear characteristics of over consolidated clay and corresponding Mohr-Coulomb failure envelopes	5
Figure 2.2 : Change of minimum F.S.with depth of tension crack for constant c' & Φ'	7
Figure 2.3 : Examples of limit equilibrium methods.....	8
Figure 2.4 : Forces acting on a vertical slice.....	9
Figure 2.5 : Circular failure surface and forces acting on a single slice.....	11
Figure 2.6 : Position of line of thrust.....	13
Figure 2.7 : Forces on a slice for Spencer's method.....	14
Figure 2.8 : Variation of F_m and F_f with θ	15
Figure 2.9 : Grid search patter.....	16
Figure 2.10 : Janbu's correction factor for his simplified method	19
Figure 3.1 : Schematic diagram of a neuron's network.....	35
Figure 3.2 : Neural networks structure.....	36
Figure 3.3 : Design choices for neural network application.....	39
Figure 3.4 : The basic GRNN architecture.....	41
Figure 3.5 : The GRNN architecture.....	42
Figure 3.6 : Linear activation function.....	43
Figure 3.7 : Logistic function.....	44
Figure 3.8 : Symmetric logistic function.....	44
Figure 3.9 : Gaussian function.....	44
Figure 3.10 : The PNN architecture.....	45
Figure 3.11 : Probabilistic neural network layers.....	46
Figure 3.12 : Mismatch the function due to the overfitting.....	50
Figure 3.13 : Comparison of theoretical settlement and neural network predicton.....	61
Figure 3.14 : Settlement predicted using traditional methods.....	62
Figure 3.15 : Settlement prediction using artificial neural network.....	62
Figure 4.1 : Basic slope profile and slope parameters.....	69
Figure 4.2 : Actual – network output scatter for model 1 and error limits.....	72
Figure 4.3 : Variables error through pattern and error limits for model 1.....	72
Figure 4.4 : Test set error graph for model 1.....	73
Figure 4.5 : Actual-network output scatter for model 2 and error limits.....	75
Figure 4.6 : Variables error through pattern and error limits for model 2.....	76
Figure 4.7 : Test set error graph for model 2.....	76
Figure 4.8 : Actual-network output scatter for model 3 and error limits.....	79
Figure 4.9 : Variables error through pattern and error limits for model 3.....	79
Figure 4.10 : Test set error graph for model 3.....	80

Figure 4.11	: Actual-network output scatter for model 4 and error limits.....	82
Figure 4.12	: Variables error through pattern and error limits for model 4.....	83
Figure 4.13	: Test set error graph for model 4.....	83
Figure 4.14	: Actual-network output scatter for model 5 and error limits.....	85
Figure 4.15	: Variables error through pattern and error limits for model 5.....	86
Figure 4.16	: Test set error graph for model 5.....	86
Figure 5.1	: Test set error graph for model 1.....	88
Figure 5.2	: Test set error graph for model 2.....	88
Figure 5.3	: Test set error graph for model 3.....	90
Figure 5.4	: Test set error graph for model 4.....	91
Figure 5.5	: Test set error graph for model 5.....	91

LIST OF SYMBOLS

b	: The slice width
β	: The inclination of slope
c	: The cohesion of soil
Δl	: Length of each individual segment into which the slip surface has been subdivided
Φ	: The friction angle of soil
γ	: The unit weight of soil
γ_w	: The unit weight of water
H	: The height of slope
H_b	: The depth of firm base
H_w	: The height of water level
k_h	: Horizontal seismic coefficient
k_v	: Vertical seismic coefficient
λ	: Scaling factor
Q	: The later slice forces
P	: Total reaction to the base of the slice
P'	: The force due to the effective stress
s_i	: Available shear strength
τ	: The shear stress
u	: The water pressure acting on the base of the slice
W	: The total weight of the slice
Z_0	: Depth of the tension crack

YAPAY SİNİR AĞLARI YÖNTEMİNİ KULLANARAK ŞEV STABİLİTESİNİN İNCELENMESİ

ÖZET

Ülkemizde inşaat mühendisliği disiplinde yapay sinir ağlarını kullanmak çok yeni bir yöntemdir. Bu olgu genelde inşaat mühendisliği disiplinde hidrolik dalında ve Geoteknik mühendisliğinde kullanılmıştır. Bu çalışmada şev stabilitesinin incelenmesi yapay zeka mantığı kullanılarak incelenmiştir. Bu da şev stabilitesinde deprem etkisinin incelenmesine farklı bir bakış açısı getirecektir.

Bu çalışmada 170 tane lokal bölgenin şev profili dataları kullanılmıştır. Çalışmada kullanılan bu verilerin hazırlanışı ve kullanım şekili bölüm 4’de anlatılmıştır.

Yapay zeka mantığı yaklaşımında beş tane yapay sinir ağı mimarisi kullanılmıştır. Bunlar BPNN, geri yayımlı sinir ağı mimarisi ve GRNN, genel regresyonlu yapay sinir ağı mimarisi, GMDH, gruplama methodu, Kohonen ve PNN, olasılık yöntemidir. Ancak sadece BPNN, geri yayımlı sinir ağı mimarisi ve GRNN, genel regresyonlu yapay sinir ağı mimarisi model oluşturmakta kullanılmıştır. Bu yaklaşımlarda 9 adet girdi ve 1 tane çıkış parametreleri verilmiştir. Çıkış parametresi şev güvenlik katsayısı olup, girdi parametreleri şev yüksekliği (H), şev eğimi (β), yeraltı suyu derinliği (H_w), sağlam zemin derinliği (H_b), kohezyon (c), zemin içsel sürtünme açısı (Φ), kuru birim hacim ağırlığı (γ), düşey ve yatay sismik zemin katsayıları (K_h , K_v)’dır. Bu çalışmadaki amaç sismik zemin katsayılarının şev stabilitesindeki önemlerinin incelenmesidir.

Tüm modellemelerde ve datalarda sismik zemin katsayıları kullanılmış olup bu yaklaşımdan beklenen sismik etkinin öneminin çıkarılmasıdır.

Sonuç olarak genel regresyon yapay sinir ağı modelinin daha başarılı olduğu ve % 92.5 başarı yüzdesine sahip olduğu görülmüş, düşey ve yatay sismik zemin katsayılarının şev yüksekliği, şev eğimi ve yeraltı suyu derinliğinden sonra şev stabilitesindeki etkisinin önemli olduğu görülmüştür.

SLOPE STABILITY INVESTIGATION BY USING ARTIFICIAL NEURAL NETWORK ANALYSIS

SUMMARY

To use Neural Network approaches is a new phenomena for civil engineering disciplines in Turkey. This phenomena generally is used in Hydrology branch of civil engineering disciplines and in geotechnical disciplines, etc. In this study slope stability was discussed by using Neural Network approaches. This provides a new point of view for seeing the effects of earthquake to slope stability safety.

In this study 170 slope data and their properties are used. Preparedness of using these data in this study is discussed in chapter 4.

In Artificial Intelligence approach five neural network approaches architecture are used. These approaches are Back propagation neural network architecture (BPNN), General regression neural network (GRNN), Group method of data handling (GMDH), Kohonen learning paradigm and Probabilistic neural network (PNN) architectures. But only 2 of them used, these are the back propagation neural network architecture (BPNN) and the general regression neural network (GRNN).

There are 9 input parameters and 1 output parameter. The output parameter is the factor of the safety of the slopes (F.S.), the input parameters are the height of slope (H), the inclination of slope (β), the height of water level (H_w), the depth of firm base (H_b), the cohesion of soil (c), the friction angle of soil (Φ), the unit weight of soil (γ), but the important input parameters are horizontal and vertical seismic coefficients (k_h , k_v). Trying to be obtained is the importance of the seismic coefficients for a slope stability safety.

For all of the architecture approaches the models are solved for including the seismic coefficients (k_h , k_v) effects. From this approach it is expected to see the earthquake impact to a slope.

In conclusion this study shows that the general regression neural network (GRNN) approach is, the more appropriate model, and has a % 92.5 success rate for forecasting the effect of earthquake for slope stability safety and generally horizontal and vertical seismic coefficients importance seen after the height of the slope (H), the inclination of slope (β), the height of water level (H_w) importance.

1. INTRODUCTION

1.1 General

This study was prepared to investigate the effects seismic coefficient to a slope and the slope stability reaction with Neural Network (NN) approaches. Assessments of seismic loading and a basic slope figure given in Figure 1.1. For the purpose of engineering design, source effects generally refer to the slope parameters.

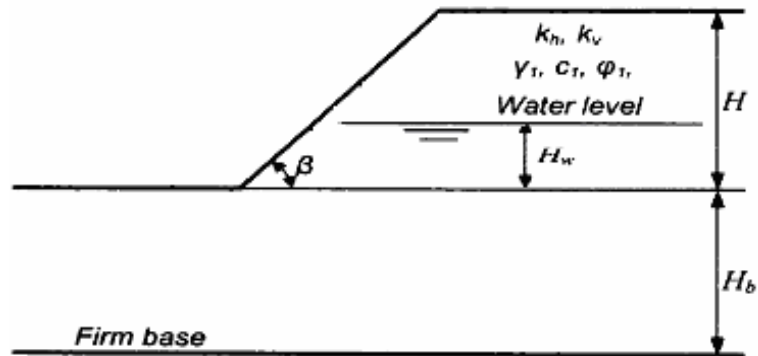


Figure 1.1 : A basic slope figure

On the other hand, the parameters of slope are determinate the safety of a slope so to find out which parameter is important we can use Neural Network (NN). These parameters are discussed in section 3 and 4.

1.2 Short History of Artificial Intelligence (AI) Method

Artificial intelligence (AI) is the study of ideas brought into machines that respond to stimulation, consistent with traditional responses from humans, given the human capacity for contemplation, judgment and intention. Each such machine should engage in critical appraisal and selection of differing opinions within itself. Produced by human skill and labor, these machines should conduct themselves in agreement with life, spirit and sensitivity, though in reality, they are imitations. Human beings have attained the ability to respond to the world by bringing previous experience, or others' experience, and AI function in this way.

Artificial Intelligence is a valuable tool of representing real-world realities. The birth of artificial intelligence is attributed to the first "intelligent" machine concept developed by Alan Turing, a scientist at Cambridge, UK. The famous "Turing Machine", from many is considered the foundation stone of artificial intelligence, and it found its first use in the, also famous, Enigma decryption project during the WWII. Nevertheless, despite the "mythological" and science fiction depictions of Artificial Intelligence (AI), its true development was closely related to the development of computers in the post-war era. The use of computers allowed Artificial Intelligence (AI) to pursue its real purpose, that is, the attempt to understand, replicate and analyze intelligent entities and processes of our world. As time progressed, the study of artificial intelligence made its first natal steps. But, the "boost" on research and analytic explorations of Artificial Intelligence became possible after the ability of researchers, organizations and institutions to perform computer-based operations and experimentations, especially in the late 1970's and 1980's. Today, artificial intelligence is a part of our everyday life. AI is used on a constantly growing number of applications and processes we use in our every-day life. Web-searches, economic models, computer games, automobile processors, etc, are only some of the most known applications that AI methods found their implementation.

1.3 Objectives

Turkey is a country where destructive earthquakes occur frequently. Since earthquakes occurs in regions at high population, earthquake loading and effects of soil are extremely important.

The purpose of this study is to examine the effect of seismic coefficients and the safety factor of a slope via artificial intelligence, rather than conventional and wellknown methodologies. Advantages of this innovative Artificial Intelligence approach can be listed as;

In future, it may provide forecasting of foundation, and soil effects or damage with earthquake loading. Events experienced can be taught to Neuroshell2 (Neural Network program used in this study) and events experienced are indicators of experiences which might occur in the future.

Like constructing robots or perceiving of human voices on mobile phone which are artificial intelligence methods; using earthquake data can be constituted knowledge programs according to high risk potentials.

By the way of Neural Network approaches, inertial interaction can be generalized and forecasted.

In this study, factor of safety and the seismic coefficients effects will be investigated with NN approaches. It should be noted that the General Regression Neural Network (GRNN) and Back Propagation Neural Network (BPNN) will be used.

2.LITERATURE REVIEW

2.1 Introduction

Slope stability is usually analyzed by methods of limit equilibrium. Historically these methods were developed before the advent of computers; computationally more complex methods followed later. These methods require information about the strength parameters and the geometrical parameters of the soil and rock mass. The factor of safety (FS) is defined as the ratio of reaction over action, expressed in terms of moments and forces and eventually in terms of stresses, depending on the geometry of the assumed slip surface. The way and methods of calculating FS values are given below.

2.2 Types of Slope Failure Modes

One knows that a stability check is made for two different failure modes when analyzing the safety of a slope. The slope can fail either during the excavation or long after the construction is completed. So for checking these slope failure modes, the stability of the slope must be checked both for short term stability and long term stability.

2.2.1 Short Term Stability

Short term stability conditions apply after a cut is made in a slope. In excavating for a cut shear stresses are induced that may cause failure in the undrained state. The total stress strength parameter cohesion, c , is used for short term stability. Based on field observations and laboratory analyses of soil samples the friction angle of the soil is zero ($\Phi = 0$) the total stress method is satisfactory for short term stability analysis of non-fissured clay. For fissured over consolidated clays, the $\Phi = 0$ analysis can also be employed by taking into account reduced shear strength due to the amount and magnitude of fissuring in soils.

2.2.2 Long Term Stability

Long term stability is encountered in natural slopes and are considered in analyzing the stability of embankments. The effective stress methods of analysis are used for the long term stability analysis of both non-fissured and over consolidated fissured clay. Effective stress parameters, c' and Φ' must be used to analyses the long term stability problem of slopes. Pore water pressure may be assumed to be in equilibrium and are determined form considerations of steady-seepage. Skempton (1964) suggested the use of the radius shear strength concept for long term slope analysis for over consolidated clays. The residual shear strength can be obtained from slow drained shear tests. Figure 2.1 shows the shear strength characteristics of an over consolidated clay in terms of effective stress. Discussions on the method of selection of the strength parameters for stability investigation are given by Lowe (1967), Schuster (1968) and Duncan – Dunlop (1969).

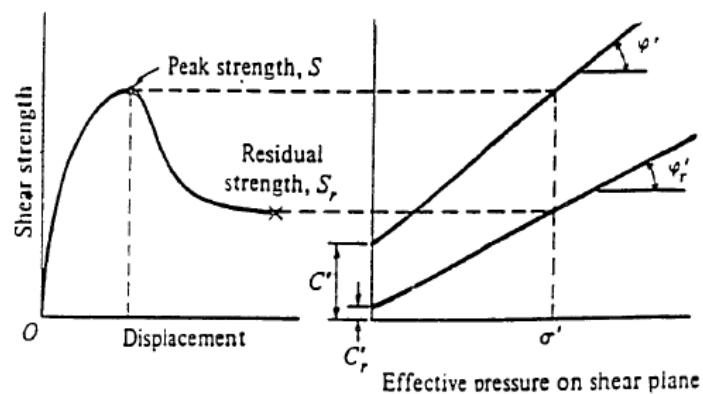


Figure 2.1 : Shear characteristics of over consolidated clay and corresponding Mohr-Coulomb failure envelopes (Fang , 1991)

2.3 Factors Affecting Slope Stability Analysis

We know that there are a number of factors that affect slope stability analysis. There are major factors like, failure plane geometry, non homogeneity of soil layers, tension cracks, dynamic loading or earthquakes and seepage flow that can affect slope stability analysis. These major factors explanations are given below.

2.3.1 Failure Plane Geometry

The geometry of the failure plane is assumed to be circular or non-circular. Non-circular surfaces include logarithmic spiral and simple wedge geometry. These are commonly known as general failure surfaces.

The use of the circular arc and logarithmic spiral failure planes for stability analysis have been discussed by Spencer (1969) and Chen (1970). Spencer (1969) suggested that the circular curve is more critical than the logarithmic spiral arc. Chen (1970) concluded that the shape of the failure plane is not sensitive in the analysis of stability in slopes .

2.3.2 Non homogeneity of Soil Layers

Depending upon the environmental condition of deposition and subsequent stress changes during geological history, soil strength parameters may be isotropic. However, most soils are unisotropic. Lo (1965) developed a general method of stability analysis for unisotropic soils, where the effect of unisotropy is small for steep slopes. For flatter slopes, the influence of unisotropy on stability is significant and can't be ignored.

2.3.3 Tension Crack

Tension crack generally occur near the crest of a slope. The crack reduces the overall stability of a slope by decreasing the cohesion which can be mobilized along the upper part of a potential failure surfaces. Therefore the factor of the safety of a slope varies with the depth of the tension crack. While the change in depth of a tension crack can be quite large, the corresponding change in the numerical values of the factor of safety is not significant. Figure 2.2 shows the change of minimum factor of safety with the change of the depth for an assumed Φ' - c' soil under drained conditions. The depth of water increases when the depth of the crack increases. The effect of water pressure in a tension crack on the position of critical circle is found to be rather small. However, the factor of safety decreases as the depth of water increases in a tension crack .

If the soil strength is purely cohesive, as for clay soils in the undrained state, the depth of the tension crack ranges from 2 to 4 times c / γ (Bromhead , 1986). The following formula can also be used to determine the depth of the tension crack

$$Z_o = \frac{2c'}{\gamma} \tan(45 + \phi' / 2) \quad (2.1)$$

where , Z_o is depth of the tension crack, tension cracks can be very deep and sometimes can even penetrate to the water table .

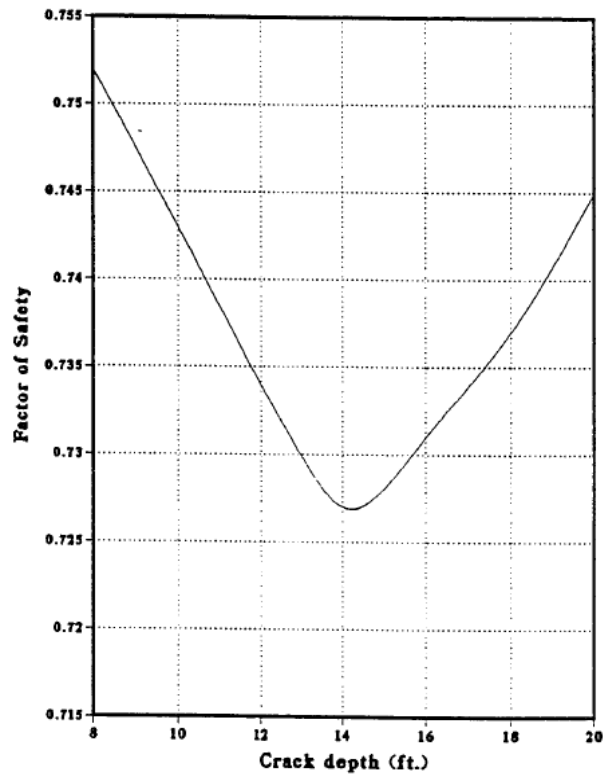


Figure 2.2: Change of minimum F.S.with depth of tension crack for constant c' & Φ' (Feng , 1991)

2.3.4 Dynamic Loading

The effect of dynamic loading including that due to earthquakes on slope stability should also be considered. So after the 1960's the researchers started to study about dynamic loading and slope stability relationship like Seed and Gogman (1967) studied the yield acceleration of slope in cohesion less soils. Finn (1966) reported the earthquake stability of cohesive slopes. Methods for evaluating slope response to earthquakes and design procedures due to earthquake are given by Seed (1966 , 1967), Sherard (1967) and Majundar (1971). Based on the laboratory tests, Ellis and Hartman (1967) reported that the dynamic strength of a soil may be less or greater than soil strength under static loadings.

2.4 Methods of Analysis

We know that, there are a number of methods available for performing slope stability analysis but the majority of these methods may be categorized as limit equilibrium methods. The basic assumption of the limit equilibrium method is that Coloumb's failure criterion is satisfied along the failure surface. It is widely used for slope

stability problems. However, it neglects soil stress – strain relationships in that the soil is assumed to move as a rigid block.

To begin the analysis, a trial failure surface for the slope is assumed. Next a free body or slice is then taken from the slope and the shear resistance is then compared to the estimated of available mobilized shear stress of the soil to give an indication of the factor of safety.

The Culman method and the Friction circle method (Taylor , 1948) consider the equilibrium of the whole free body as shown in Figure 2.3.

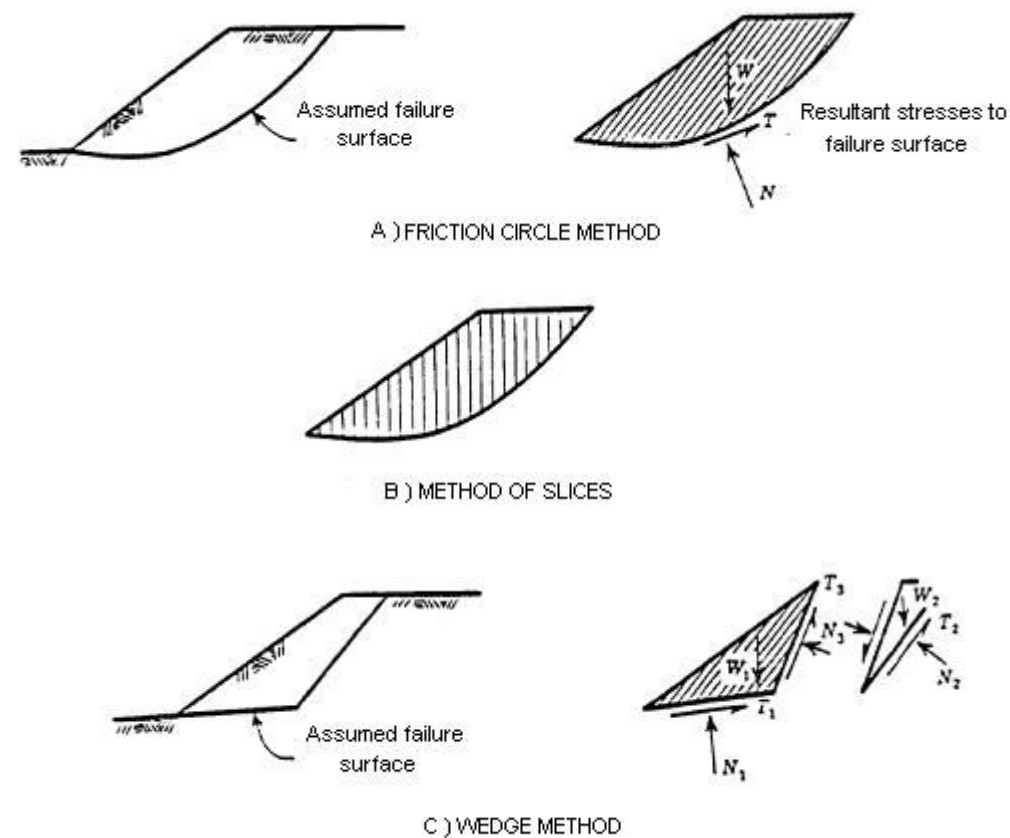


Figure 2.3 : Examples of limit equilibrium methods (Fang , 1991)

The Swedish circle method (Fellenius , 1927), the Bishop's (1955), Bishop and Morgenstern (1960), Morgenstern (1963), and Spencer's (1967) method are based on the method of slices with minor variations. The method of slices approach is to divide the free body into many vertical slices and to consider the equilibrium of each slice. The safety of the slope is found from summing the stability of all slices.

In addition to the above mentioned methods, Hunter and Schuster (1968 , 1971), Huang (1975 , 1980), and Koppular (1948) discuss limit equilibrium methods.

Lowe and Karafiath (1960) and Janbu (1954) developed methods which are also in the category of the limit equilibrium method. These methods explanations are given below by classifying them with the geometry of slope failure surface.

2.4.1 Planar Failure Surface

A slope that is uniform and very long relative t the depth of the potentially unstable layer may often be analyzed as a planar failure slope. The general model is shown in Figure 2.4.

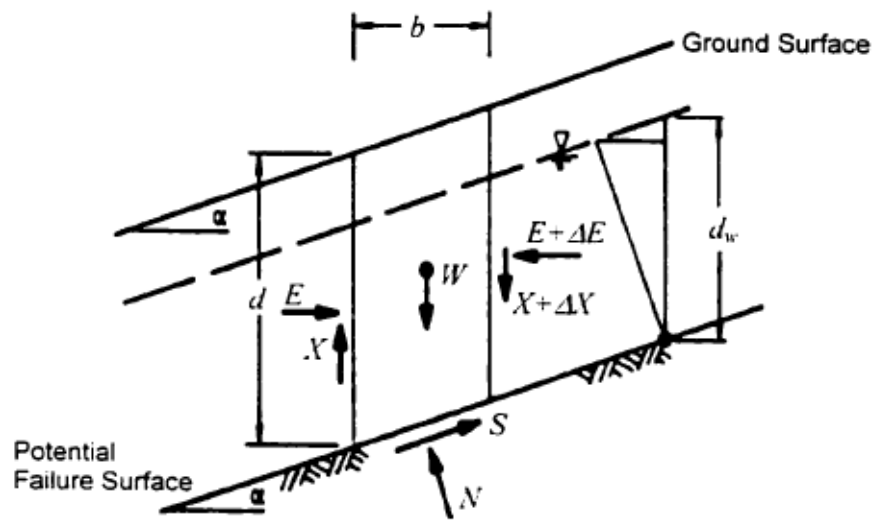


Figure 2.4 : Forces acting on a Vertical Slice (Mostyn and Small , 1987)

As can be seen, the failure plane is taken to be parallel to and at a depth, d , below the ground surface having an inclination α with the horizontal. The assumption that the slope is very long and uniform implies that any vertical slice is similar to all others. Thus the side forces must be equal in magnitude, opposite in direction and co-linear. Groundwater flow is usually taken to be parallel to the ground surface with the phreatic surface at a distance d_w , above the failure plane. For a material with a Mohr-Coloumb failure criterion the factor of safety, F_s , of the slope is given by the following expression (Das, 1993);

$$F_s = \frac{c' + (\gamma d - \gamma_w d_w) \cos^2 \alpha \tan \phi'}{\gamma d \cdot \sin \alpha \cdot \cos \alpha} \quad (2.2)$$

where c' is effective cohesion of soil, γ is the unit weight of soil, γ_w is the unit weight of water and Φ' is the effective angle of friction.

The derivation of the factor of safety for a slope with planar failure surface is presented in most textbooks on soil mechanics or slope stability. The effective cohesion is often ignored or assumed to be zero in which case equation 2.2 simplifies to :

$$F_s = \left(1 - \frac{\gamma_w d_w}{\gamma d} \right) \frac{\tan \phi'}{\tan \alpha} \quad (2.3)$$

If the water table is at or below the failure plane then the slope is at limiting equilibrium when the slope angle equals the effective angle of friction. If the water table is at the surface then the slope angle at limiting equilibrium is near half the effective angle of friction.

2.4.2 Circular Failure Surface

For many slope failures, the surfaces along which sliding takes place is found to be non-planar or curved leading to the idea of using curved failure surfaces for the analysis of slope stability (Spencer 1973, Chen and Shao 1988). Although the actual failure surfaces in most cases are bowl shaped , the representation of a failure surface as a single curve (in two dimension) greatly simplifies the analysis.

Early solutions for circular surfaces were obtained by Fellenius (1927) who used the method of slices and by Taylor (1937, 1948) who used a friction circle method to produce charts of “ stability numbers “ to determine factors of safety against slope failure. Most modern circular slip circle methods make use of the method of slices, and the major differences between these methods involve the way, in which the unknown quantities that arise in the analysis are dealt with. Some of the methods for analysis of circular failure surfaces using the method of slices are presented in the following sections.

2.4.2.1 Fellenius Method

This method assumes that for any slice, the forces acting upon its sides has a resultant of zero in the direction normal to the failure arc. This method have errors on the safe side, but is widely used in practice because of its early origins and simplicity. Figure 2.5 shows the region above the assumed circular failure surface divided into slices and a free body diagram of a single slice with all of the forces acting on it, and the unknown points of application of the forces. As there are too many unknowns to obtain a solution, some assumptions must be made about the

forces and their locations. The interslice forces ($X_n ; E_n$) are assumed to be equal and opposite to each slice and therefore they cancel each other. Taking moments about the center of the circle and assuming that everywhere along the failure surface the amount of shear stress mobilized τ_M is the same fraction of the total shear stress available ($\tau_M = (c' + \sigma' \cdot \tan \phi') / F$), we obtain :

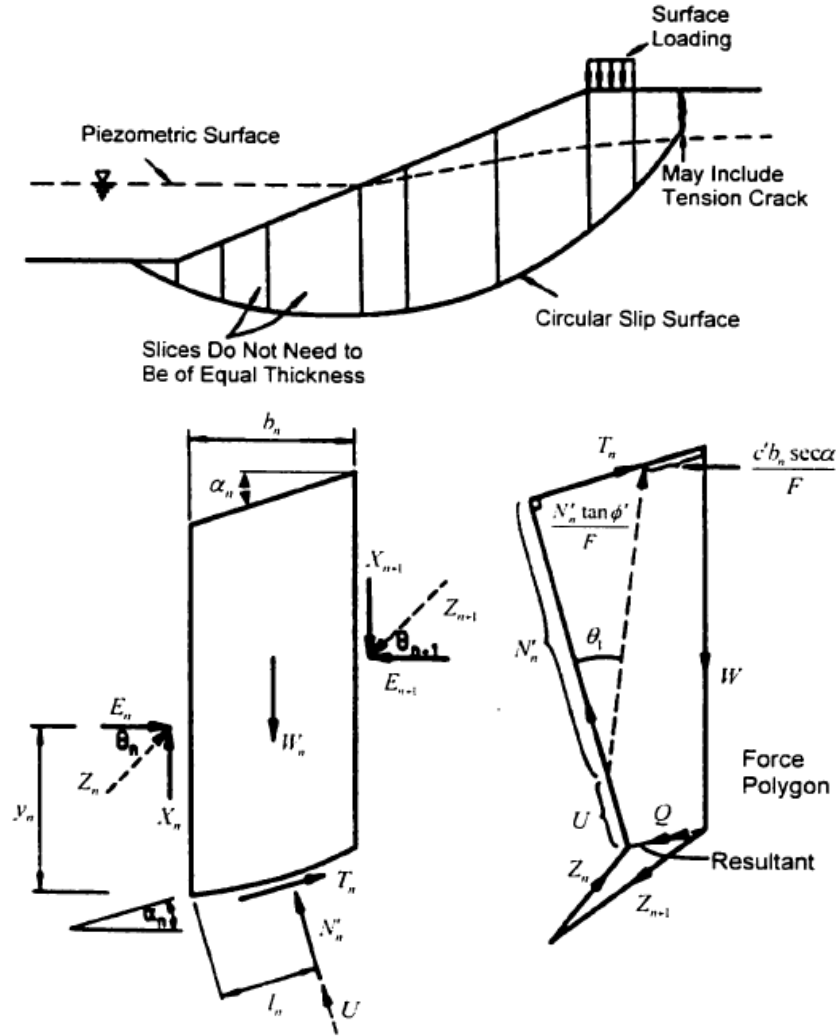


Figure 2.5 : Circular failure surface and forces acting on a single slice
(Fellenius , 1927)

$$F_s = \frac{\sum [c' b \cdot \sec \alpha + (W \cdot \cos \alpha - u b \cdot \sec \alpha) \cdot \tan \phi']}{\sum W \cdot \sin \alpha} \quad (2.4)$$

where c' is the effective cohesion, b is the slice width , α is the angle of the base of the slice to the horizontal, W is the total weight of the slice, u is the water pressure acting on the base of the slice, Φ' is the effective angle of friction, and the summation implies an addition over all slices .

2.4.2.2 Bishop's Method

This method was developed by Bishop in 1955, and improved upon the method of slices developed by Fellenius (1936). The method is based on the statical analysis of the mass which is considered to be made up of vertical slices. Equilibrium of forces in the vertical direction is satisfied for each slice and the equilibrium of moments about the center point of the trial arc is satisfied for each slice. Equilibrium is also satisfied for the entire soil mass, consisting of all slices, above the trial arc. The factor of safety is calculated by dividing the sum of the resisting moments by the sum of the moments that causes the failure.

For a mathematically correct static solution, equilibrium of forces and moments must exist for each slice as well as for all of the slices. Bishop's rigorous formulation contains too many unknowns to enable a direct solution. Some assumptions must be made regarding the distribution of some of the unknown quantities and for this method assumptions are made concerning the distribution of X force. The position of the line of thrust y_t (Figure 2.6) of these X forces must be such that the moment equilibrium of each slice is maintained. As pointed out Sarma (1979), Bishop didn't consider the point of action of the normal force on the base of the slice, thereby eliminating another group of unknowns for the problem.

Using Bishop's original and now somewhat familiar notation, the expression for the factor of safety against a slip failure is expressed as :

$$F = \frac{\sum [c'b + (W - ub + \Delta X) \cdot \tan \phi' / m_\alpha]}{\sum W \cdot \sin \alpha} \quad (2.5)$$

where ;

$$\Delta X = X_n - X_{n+1} \quad (2.6)$$

$$m_\alpha = \cos \alpha \cdot \left(1 + \frac{\tan \alpha \cdot \tan \phi'}{F} \right) \quad (2.7)$$

b is the slice width , W is the total weight of the slice, c' is the effective cohesion, ϕ' is the effective angle of friction, u is the water pressure acting on the base of the slice, α is the angle of the base of the slice to the horizontal.

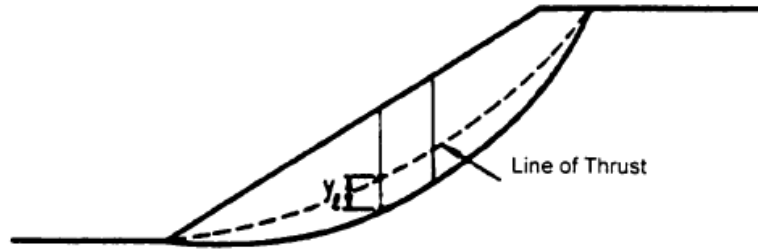


Figure 2.6 : Position of Line of Thrust (Fellenius , 1927)

2.4.2.3 Spencer's Method

Spencer developed this method in 1967 to determine the factor of safety of a slope against the failure on a trial slip surface. The analysis is in terms of effective stress. It leads to two equations of equilibrium, force equilibrium and moment equilibrium. As in Bishop's method the soil mass within the slip surface is divided into vertical slices. In each slice, the resultant of the forces and the sum of the moments of the forces must both be zero.

The factor of safety is defined as the ratio of the total shear strength available, S on the slip surface to the total stress mobilized, S_m in order to maintain equilibrium.

$$F = \frac{S}{S_m} \quad (2.8)$$

A sketch of a slice with the forces acting upon is shown in Figure 2.7. The forces are as follows :

The weight, W_i

The total reaction, P normal to the base of the slice (the force P' due to the effective stress, The force $ub.\sec\alpha$ due to the pore pressure, u),

thus;

$$P = P' + ub.\sec\alpha \quad (2.9)$$

The mobilized shear force,

$$S_m = \frac{S}{F} \quad (2.10)$$

where,

$$S = c'b.\sec\alpha + P'.\tan\phi' \quad (2.11)$$

$$S_m = \frac{c'b}{F} \sec \alpha + P' \frac{\tan \phi'}{F} \quad (2.12)$$

The interslice forces Z_n and Z_{n+1} ; from equilibrium, the resultant Q of these two forces must pass through the point of intersection of the three other forces.

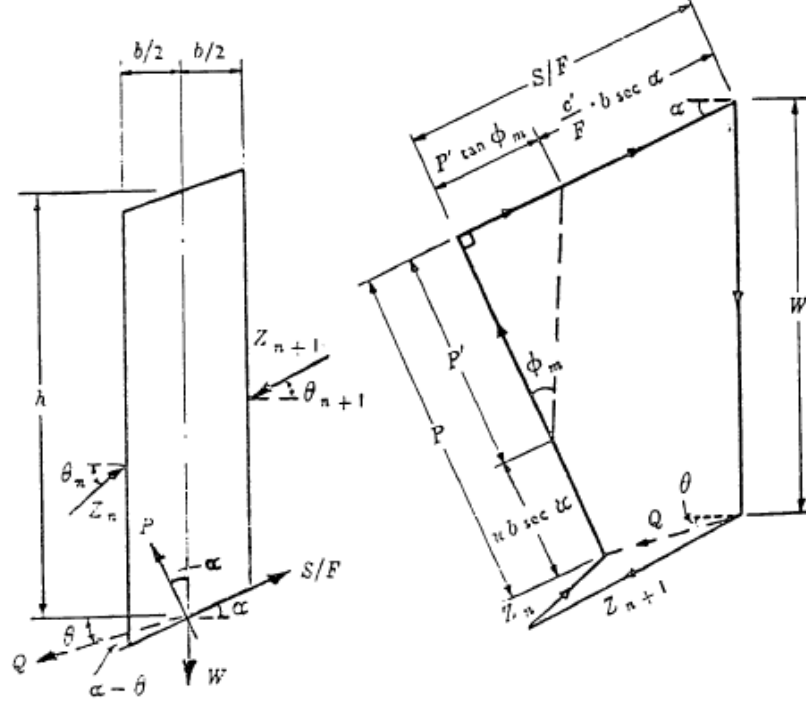


Figure 2.7 : Forces on a slice for Spencer's method (Spencer , 1967)

By resolving the forces shown in Figure 2.7 normal and parallel to the base of the slice, the resultant, Q_i of the later slice forces can be written :

$$Q_i = \frac{\frac{c'b_i}{F} \sec \alpha_i + \frac{\tan \phi'}{F} (W_i \cos \alpha_i - u_i b_i \sec \alpha_i) - W_i \sin \alpha_i}{\cos(\alpha_i - \theta_i) \left[1 + \frac{\tan \phi'}{F} \tan(\alpha_i - \theta_i) \right]} \quad (2.13)$$

(2.13)

For force equilibrium of the whole mass, the sum of both the horizontal and vertical components of the inter slice forces must be zero.

$$\sum Q_i \cos \theta_i = 0 \quad (2.14)$$

$$\sum Q_i \sin \theta_i = 0 \quad (2.15)$$

Furthermore, for moment equilibrium, the sum of the moments of the inter slice forces about the center rotation must also be zero.

$$\sum [Q_i R \cos(\alpha_i - \theta_i)] = 0 \quad (2.16)$$

Since the slip surface is assumed to be circular,

$$\sum [Q \cos(\alpha_i - \theta_i)] = 0 \quad (2.17)$$

Assuming the inter slice forces are parallel,

$$\sum Q = 0 \quad (2.18)$$

Spencer also described the following procedure to solve for F, Q and θ .

A circular slip surface is chosen arbitrarily the area inside the slip surface is divided into vertical slices of equal width. The mean height, h, and base slope α of each slice is determined graphically.

Several values of θ are chosen and for each, the value of F is found which satisfies both Equations 2.17, 2.18. The value of F obtained using Eqn. 2.18 is designated F_f , and that obtained from using Eqn. 2.17 as F_m . The value of the factor of safety obtained from moment equilibrium and taking θ as zero is designated as F_m .

The resulting value of F_f are plotted versus θ . On the same graph, a second curve is plotted as F_m versus θ . A typical graph is shown in Figure 2.8. The intersection of two curves gives the values of the factor of the safety, F, which satisfies both Eqn. 2.17 and 2.18. The corresponding slope θ of the inter slice forces is also obtained.

The values of F and θ are then substituted into Eqn. 2.13 to obtain the values of the resultant of the inter slice forces. Then, working from the first slice to the last, the values of the inter slice forces are obtained.

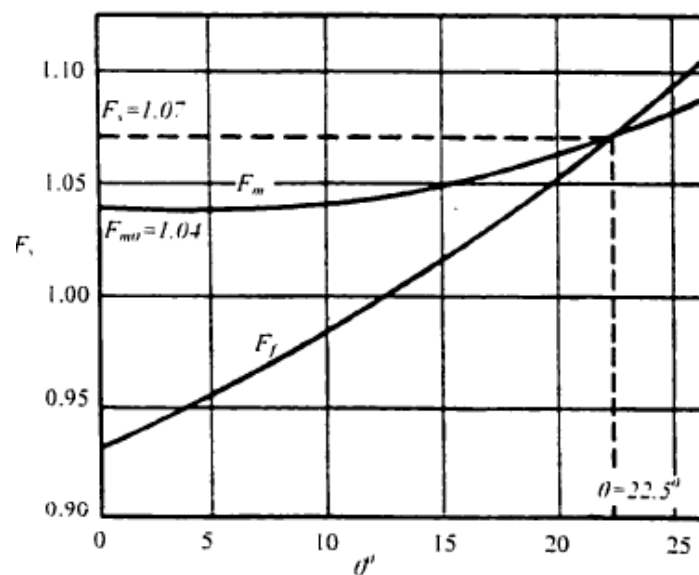


Figure 2.8 : Variation of F_m and F_f with θ (Spencer , 1967)

The required (critical) factor of safety is obtained for the case $F_m = F_f = F_S$. This factor of safety $F_S = 1,07$ and the corresponding value of the inter slice force angle $\theta = 22,5^0$ can be used to subsequently determine all the inter slice forces and their line of thrust. The difference in factor of safety obtained using the Spencer's method as compared to Bishop's method is not large. It was noted by Spencer (1968) that the difference between two methods exceeded %1.

2.4.2.4 Obtaining The Most Critical Circle

Whichever of the methods of obtaining the factor of safety is used, a number of trial circles must be taken and analyzed in order to obtain the one that gives the least factor of safety (Barker , 1980). As most analyses are done by computers the process of analyzing a few hundred trial circles may be relatively quick and inexpensive in today's computing environment.

Computer programs need some type of algorithm upon which the search for the slip surface with the minimum factor of safety is based. One of the most commonly used methods is to specify a grid on which the centers of trial slip circles lie (Figure 2.9). Contours of the minimum factor of safety at each center on the grid can be plotted in order to determine where the critical center may lie.

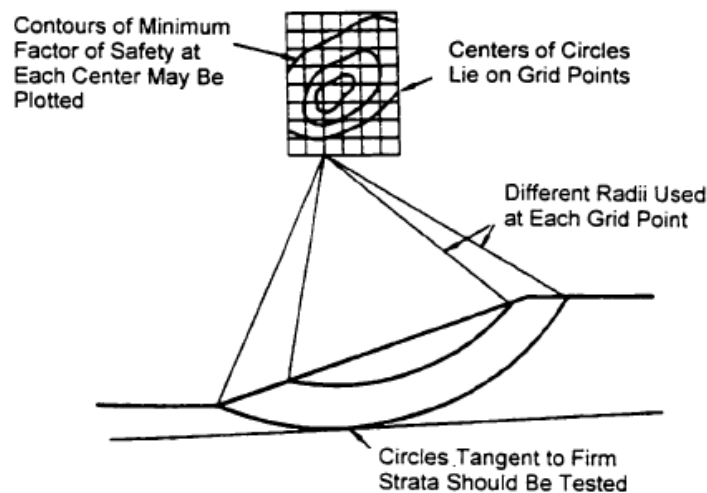


Figure 2.9 : Grid Search patten (Mostyn and Small , 1987)

The amount of computation required to find the critical circle may be greatly reduced by using a technique by which one can automatically locate the center coordinates and radius of the circle yielding the minimum factor of safety. Such a technique has been described by Boutrup and Lovell (1980), who used the simplex reflection

method. To explain how the method works, consider the problem of finding the factor of safety for a two dimensional circular slip surface. The problem basically involves finding the coordinates a , b of the center and radius r of the circle which minimize the factor of safety, F_s . This is done by evaluating F_s at the four corners of a tetrahedron defined in x , y , r space. The value of factor of safety found at each corner may then be used to decide in which direction to move to obtain a lower factor of safety. Obviously this will be away from the vertex of the tetrahedron with the highest factor of safety. Depending on the coordinates and radii given to start the search, the minimum factor of safety can be found quite quickly.

2.4.3 Non – Circular Failure Surface

If the shear strength is non- uniform within a slope then the failure surface with the minimum factor of safety will not necessarily be a circle but the shape will depend on the distribution of shear strength. Sometimes the general shape of the critical failure surface will be highly constrained by the distribution of weak zones within the slope; other times it may require a lot of insight or work to find the critical surface or at least some surface with similar stability.

Analysis of circular failure surfaces is easier than that of non-circular or generalized failure surfaces. This is because moments taken about the center of a circular failure surface result in a zero moment arm for the normal forces acting on the failure surface and a constant moment arm for the cohesive forces on the failure surface. Nevertheless the moments for the entire mass or each slice can be taken about any point or points that are convenient and failure surface of any shape can be adopted. This approach is used in analyzing generalized failure surfaces. Some of these methods are given below.

2.4.3.1 Janbu's Method

From the mid-50s to the early 70's, Janbu developed generalized and simplified methods which are best described in Janbu (1973). In the generalized method, a line of thrust is assumed and the equations of equilibrium solved. Sarma (1979) pointed out that this is not a rigorous solution because moment equilibrium of the last slice is not satisfied; this affects the line of thrust but does not greatly affect the factor of safety. Janbu (1973) noted that the factor of safety is relatively insensitive to the assumption regarding the location of the line of thrust as long as it is

reasonable. According to Janbu (1973) in the line of thrust should be near one third the height of the slice for cohesion less soils. It should be below this level in the active zone and above it in the passive zone for cohesive soils. This method sometimes gives answers that differ quite markedly from those obtained by other methods such as Bishop method. Janbu's method is based on satisfying only force equilibrium and assumes zero inter slice shear forces and does not satisfy moment equilibrium. However, the simplified Janbu method does satisfy vertical force equilibrium and overall horizontal force equilibrium.

The normal effective stress at the base of each slice can be determined with the following equations:

$$N' = \frac{-U_{\alpha} \cos \alpha - S_m \sin \alpha + W(1 - k_v) + U_{\beta} \cos \beta + Q \cos \delta}{\cos \alpha} \quad (2.19)$$

The overall horizontal force equilibrium for the slide mass is determined from the following:

$$\sum_{i=1}^n [F_H]_i = \sum_{i=1}^n [(N' + U_{\alpha}) \sin \alpha + Wk_h + U_{\beta} \sin \beta] + \sum_{i=1}^n \left[Q \sin \delta - \frac{C + N' \tan \phi}{F} \cos \alpha \right] = 0 \quad (2.20)$$

It then follows that the Factor of Safety F can be determined with the following equation:

$$F = \frac{\sum_{i=1}^n [C + N' \tan \phi] \cos \alpha}{\sum_{i=1}^n A_4 + N' \sin \alpha} \quad (2.21)$$

$$A_4 = U_{\alpha} \sin \alpha + Wk_h + U_{\beta} + Q \sin \delta \quad (2.22)$$

The Simplified Janbu Method does not satisfy moment equilibrium for the slide mass, as mentioned earlier. Therefore, Janbu performed more rigorous solutions and compared the result to those found using his simplified method. He then presented the following chart as seen in Figure 2.10 to correct for his over-determined solution.

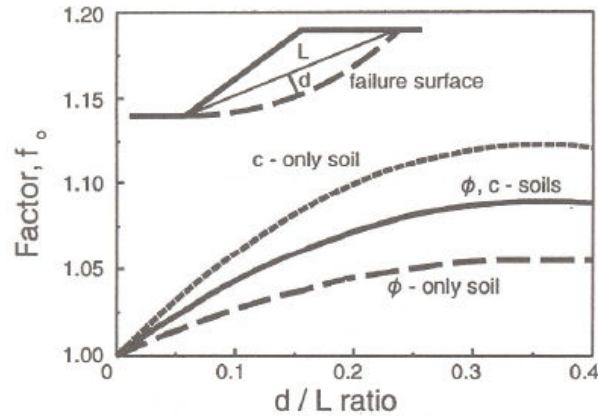


Figure 2.10 : Janbu's Correction factor for his simplified method

$$F_{Janbu} = f_o * F_{calculated}$$

2.4.3.2 Morgenstern - Price Method

This is perhaps the best known and most widely used method developed for analyzing generalized failure surfaces. The method was initially described by Morgenstern and Price (1965). It satisfies all static equilibrium requirements and is, therefore, a rigorous method, but the solution obtained must be checked for acceptability. The overall problem is made determinate by assuming a functional relationship between the inter slice shear force and the inter slice normal force. The function is referred to as $f(x)$ and most programs implementing the method provide a choice of such functions. Choosing such a function actually over determined the problem and thus part of the solution is to determine a scaling factor, λ . The function $f(x)$ defines the relative inclination of the inter slice forces, while λ defines their absolute magnitude. Thus the inter slice forces on the left hand side of slice are related by following equation :

$$X = \lambda \cdot f(x) \cdot E \quad (2.23)$$

The solution procedure proposed by Morgenstern and Price (1965) differs from that adopted by most investigators in that the problem was formulated using differential equations that were integrated over each slice. Morgenstern and Price (1965) method doesn't make the assumption that the normal force on the base of each slice acts at the center of the slice. Thus, the accuracy of the other methods increases as the slice become thinner. A reasonable number of slices should be adopted in any analyses.

2.4.3.3 Location of Critical Failure Surface

Initially, methods of analysis were based on circular surfaces. However, development of methods for non-circular surfaces followed soon. For the most part, non-circular methods may also be used for the analysis of circular failure surfaces, since a circle is merely a special type of curved failure surface.

The equivalent problem of determining the generalized failure surface having minimum factor of safety is considerably more complex and routine procedures are uncommon. It is often necessary to locate the critical failure surface by an intelligent selection of potential failure surfaces and manual iteration until the critical surface has been established. This may often be the most efficient means of locating the critical surface.

2.4.4 Selection of Method

Some methods of slope stability analysis are more rigorous and should be favored for detailed evaluation of final designs. Some methods (Spencer, Swedish, wedge) can be used to analyze noncircular slip surfaces. Some methods (Bishop, Swedish, wedge) can be used without the aid of a computer and are therefore convenient for independently checking results obtained using computer programs. Also when these latter methods are implemented in software they extremely fast and are useful where very large numbers of trial slip surfaces are to be analyzed. Table 2.1 can be helpful in selecting a suitable method for analysis.

Table 2.1 : Comparison of features of methods

Feature	Ordinary method of slices	Simplified Bishop	Spencer	Modified Swedish	Wedge	Infinite slope
Accuracy		X	X			X
Plane slip surfaces parallel to slope face						X
Circular slip surfaces	X	X	X	X		
Wedge failure mechanism			X	X	X	
Non-circular slip surfaces – any shape			X	X		
Suitable for hand calculations	X	X		X	X	X

2.5 Numerical Methods For Slope Stability Analysis

With the rapid development of computational technologies, alternative numerical approach have been sought for developing new modeling techniques. Among them, finite difference method and finite element method are being widely used by consulting firms as computing facilities become cheaper and more readily available. Although they are more complex to use than the conventionally limit equilibrium methods, they nevertheless can provide a detailed insight into the way how a slope will deform and fail and therefore provide a valuable addition to methods of analyzing slope behavior.

2.5.1 Finite Difference Method

The application of the limit equilibrium methods gives an insight of the stability of the slope at the state of failure and gives no information about the stress – strain history of the slope prior and after failure has occurred. The limit equilibrium methods generally do not satisfy the stress equilibrium at any given point in the slope at any given time, thus the methods are inappropriate to model progressive failure mechanisms. Finite element and difference methods can model the deformation of the slope and the stress caused by the deformations throughout the failure. There are some computer programs based on these methods that can solve such problems, however these methods still require an interpretation of the results of analysis, and it has not widely used for general slope stability analysis. However, with advanced computer technology and interactive visualization of the results of such analyses, the methods have a place among the general methods used in stability analysis. Finite difference methods content is given below.

Finite difference method widely used to obtain approximate solutions of many boundary value problems whose exact solutions are mathematically complex and in come cases impossible. Response of a structure system is often represented by the governing differential equations. These equations involve derivatives of functions using finite difference approach these derivatives can be easily evaluated at discrete points. The partial differential equations (PDE) can then be solved in the domain with respect to some given boundary conditions. Cundall (1976) gave an example of how finite difference methods might be applied to the problems of slope stability.

Finite difference method is an approximate method for determining derivatives of a function. Depending upon circumstances, the finite difference method may give exact results. However, frequently it yields only approximate results. The extent of error in using finite difference method in finding derivatives of a function depends on various including order of derivative, type of function, type of finite difference mesh.

This method has the following advantages over the traditional methods : Failure mode develops naturally no need to specify trial surfaces; No parameters need to be given as input. Multiple failure surfaces evolve naturally.

2.5.2 Finite Element Method

The finite element method (FEM) represent a powerful alternative approach for slope stability analysis. This method is accurate, versatile and requires fewer assumptions especially regarding the failure mechanism. The FEM can solve problems with irregular boundaries and complex variation of potential and flow lines. The region to be analyzed is divided into elements which are jointed at nodes. The unknown displacements at each node may be computed and from these the strain and stress fields within the body may be found.

The finite element method (FEM) can be used to compute displacements and stresses caused by applied loads. However, it does not provide a value for the overall factor of safety without additional processing of the computed stresses. The principal uses of the finite element method for design are as follows:

(1) Finite element analyses can provide estimates of displacements and construction pore water pressures. These may be useful for field control of construction, or when there is concern for damage to adjacent structures. If the displacements and pore water pressures measured in the field differ greatly from those computed, the reason for the difference should be investigated.

(2) Finite element analyses provide displacement pattern which may show potential and possibly complex failure mechanisms. The validity of the factor of safety obtained from limit equilibrium analyses depends on locating the critical potential slip surfaces. In complex conditions, it is often difficult to anticipate failure modes, particularly if reinforcement or structural members such as geotextiles, concrete retaining walls, or sheet piles are included. Once a potential failure mechanism is

recognized, the factor of safety against a shear failure developing by that mode can be computed using conventional limit equilibrium procedures.

(3) Finite element analyses provide estimates of mobilized stresses and forces. The finite element method may be particularly useful in judging what strengths should be used when materials have very dissimilar stress-strain and strength properties, i.e., where strain compatibility is an issue. The FEM can help identify local regions where “overstress” may occur and cause cracking in brittle and strain softening materials. Also, the FEM is helpful in identifying how reinforcement will respond in embankments. Finite element analyses may be useful in areas where new types of reinforcement are being used or reinforcement is being used in ways different from the ways for which experience exists. An important input to the stability analyses for reinforced slopes is the force in the reinforcement. The FEM can provide useful guidance for establishing the force that will be used.

Use of finite element analyses to compute factors of safety. If desired, factors of safety equivalent to those computed using limit equilibrium analyses can be computed from results of finite element analyses. The procedure for using the FEM to compute factors of safety are as follows:

- (1) Perform an analysis using the FEM to determine the stresses for the slope.
- (2) Select a trial slip surface.
- (3) Subdivide the slip surface into segments.
- (4) Compute the normal stresses and shear stresses along an assumed slip surface. This requires interpolation of values of stress from the values calculated at Gauss points in the finite element mesh to obtain values at selected points on the slip surface. If an effective stress analysis is being performed, subtract pore pressures to determine the effective normal stresses on the slip surface. The pore pressures are determined from the same finite element analysis if a coupled analysis was performed to compute stresses and deformations. The pore pressures are determined from a separate steady seepage analysis if an uncoupled analysis was performed to compute stresses and deformations.
- (5) Use the normal stress and the shear strength parameters, c and Φ or c' and Φ' , to compute the available shear strength at points along the shear surface. Use total normal stresses and total stress shear strength parameters for total stress analysis and

effective normal stresses and effective stress shear strength parameters for effective stress analyses.

(6) Compute an overall factor of safety using the following equation:

$$F_s = \frac{\sum s_i \Delta l_i}{\sum \tau_i \Delta l_i} \quad (2.24)$$

$$\tau_f = c' + \sigma_n \tan \phi' \quad \text{and} \quad F_s = \frac{\tau_s}{\tau_n} \quad (2.25)$$

where ;

s_i = Available shear strength computed in step (4)

τ_i = Shear stress computed in step (3)

Δl = Length of each individual segment into which the slip surface has been subdivided.

The summations in Equation 2.24 are performed over all the segments into which the slip surface has been subdivided.

Finite element analyses require considerably more time and effort, beyond that required for limit equilibrium analyses and additional data related to stress-strain behavior of materials. Therefore, the use of finite element analyses is not justified for the sole purpose of calculating factors of safety.

Another method is that the shear strength reduction technique is a new method to use finite element method in the slope stability analysis, and assumed that the failure mechanism of slope is directly related to the development of the shear strain. In this method, the shear strength (c, ϕ) of the geomaterial is divided by the shear strength reduction ratio, F_s , and use the reduced shear strength (c', ϕ') to replace the primary shear strength to bring the slope to the verge of failure. When the verge of failure arrives, the strain or displacement in the sliding zone will break, and this kind of break will lead the convergence of finite element fail. The expression of the reduction can be described as:

$$c' = c / F_s \quad (2.26)$$

$$\phi' = \text{atan}(\tan \phi / F_s) \quad (2.27)$$

Where, c and ϕ are the shear strength parameters, c' and ϕ' are the reduced shear strength parameters, F_s is the shear strength reduction ratio. During the calculation, the shear strength reduction ration, F_s , is increased step by step, and the shear

strength of the geomaterial is also changed. When the convergence is failed, the shear strength ratio, F_s , is the safety factor of the slope, and the plastic zone corresponds to the sliding face of the slope.

2.6 Computer Programs Based on Traditional Methods

Program : CLARA-W

Description : CLARA-W is a program for geotechnical slope stability analysis in two or three dimensions, using Bishop, Janbu, Spencer and Morgenstern-Price methods. Features include: 2D and 3D analysis of rotational or non-rotational sliding surfaces, ellipsoids, wedges, compound surfaces, fully specified surfaces and searches. Other features include point loads, tension cracks, earthquake loading, anisotropic and non-linear material strength models and the possibility to use digital elevation model (DEM) files to specify ground surface topography. It also includes 3D extensions of the Spencer's method and the Morgenstern-Price method. (Geotechnical & Geoenvironmental Software Directory - <http://www.ggsd.com>)

Program : XSLOPE for Windows

Description : XSLOPE for Windows computes the stability of an earth slope using Bishop's (1955) simplified method for circular failure surfaces or Morgenstern and Price's (1965, 1967) analysis for non-circular failure surfaces. The slope may be divided into a number of different soil layers with different properties. In the Bishop analysis a circular surface of rupture is assumed and then the equilibrium of the sliding mass of soil is considered by dividing this mass into a number of slices. This process is repeated for a large number of circles and the minimum factor of safety determined. Pore pressures within each soil layer can be calculated by a number of different methods, from the depth below a piezo metric surface, by using a pore pressure coefficient ru , from a user specified grid of pore pressures, or from a grid of pore pressures generated by program FESEEP. External normal and shear tractions can be applied to segments along the surface of the slope. The effect of an earthquake is modeled by applying a set of horizontal and vertical forces at the centroid of each slice. These forces are calculated using the horizontal and vertical seismic coefficients which are assumed to vary with depth. (<http://www.ggsd.com>)

Program : SVDynamic

Description : SVDynamic carries out slope stability analyses using the dynamic programming method to determine the location of the slip surface and factor of safety of a slope based on a finite element analysis. It has been verified against traditional slope stability analysis methods such as Morgenstern-Price, GLE (General Limit Equilibrium - Fredlund et al. 1982), Spencer, Simplified Bishop's, Janbu, and the Ordinary method. (<http://www.ggsd.com>)

Program : GeoStru

Description : Slope (GeoStru) carries out the analysis of soil slope stability both in static and seismic states utilising the limit equilibrium methods of Fellenius, Bishop, Janbu, Bell, Sarma, Spencer, Morgenstern and Price. The discrete element method (DEM) is also used for circular and non-circular failures by which it is possible to determine movement in the slope, examine a gradual failure, and employ various models of force-deformation. Program is doing automatic computation of Safety Factor for surfaces that are tangential to a straight line (automatically varying the inclination), or that pass through one, two, or three given points, and back analysis. (<http://www.ggsd.com>)

Program : SLOPE/W Basic Edition

Description : SLOPE/W Basic Edition has the essential features for solving slope stability analyses, including: Ordinary, Bishop, Janbu Simplified, Spencer, Morgenstern-Price and Generalized Limit Equilibrium methods. Pore-water pressure conditions specified using a piezometric line. Soil strength specified as undrained, cohesive and frictional, no strength, or impenetrable. Ground surface surcharge pressures. It has horizontal and vertical seismic coefficients analyses. (<http://www.ggsd.com>)

Program : DC-Slope

Description : DC-Slope carries out slope stability analysis according to Krey-Bishop (friction circle) and Janbu (arbitrary sliding planes) methods. Main features include: Freely defined ground surface and layers, ground water and seepage paths, different load cases with concentrated and distributed loads, dead and live loads or earthquake loads. Program have automatic iteration of center and/or radius, optionally with predefined range, to find the minimum safety factor. (<http://www.ggsd.com>)

Program : Slope (ejgeSoft)

Description : Slope is a program for carrying out slope stability analysis by the Bishop method and has the following features: Any shape of soil profile can be considered; Change any parameter for immediate re-calculation; Any consistent unit system can be used (SI is default); Several soil layers with different properties can be considered; Single circle can be specified; Single center can be specified and R range scanned by the program; A grid of centers can be specified for minimum FS search; Output of details can be requested, down to slice weights; Pore pressures are specified either by an ru coefficient or a fixed ground water table elevation. (<http://www.ggsd.com>)

Program : CADS Re-Slope

Description : CADS Re-Slope is a general slope stability software package supplied as a complete suite or as a series of modules. The Full Slope Stability module features: Circular and user defined slip surfaces; Swedish method of slices; Bishops method (No interslice shear, moment equilibrium); Janbu method (No interslice shear, horizontal equilibrium); Rigorous method (interslice shear, full equilibrium); Also program have Seismic analysis (horizontal and vertical acceleration). (<http://www.ggsd.com>)

Program : GGU-STABILITY

Description : GGU-STABILITY for slope failure calculations and soil nailing. Considers circular slip surfaces (Bishop or Krey) and polygonal slip surfaces (Janbu), in addition to rigid body failure mechanisms and block sliding methods. Slip stability. Overturning stability. Base failure safety. Slope failure safety (Bishop). Calculation of maximum "nailing forces". (<http://www.ggsd.com>)

Program : GeoStar

Description : GeoStar supports standard and improved limit equilibrium methods. Cylindrical or general shaped (polygonal) shear surface. Progressive failure. General shaped layers. Variable inter-slice forces. Ground water influence calculated from groundwater levels, pore pressure coefficient (Bishop - Morgenstern), pore pressure value for layer or explicit field of pore pressure values (i.e. imported from a finite element calculation). (<http://www.ggsd.com>)

Program : TSTAB

Description : TSTAB conducts limit equilibrium slope stability analyses of circular slip surfaces by the Simplified Bishop or Spencer methods and searches for the critical circular slip surface. Provides for application of line loads and pressures to the slope and this capability allows for modeling of both anchors and internal reinforcement, such as that provided by geogrids. Automatically computes the pressures on submerged slopes and the pressures due to fluid in tension cracks. Provides several alternatives for specifying shear strengths, allows anisotropic undrained shear strengths and allows specification of local residual factors. Provides a choice of automatic computation of pore pressures from a specified phreatic surface or from the average pore pressure ratio or specification of pore pressures as contours or specification of pore pressures on a grid. Includes an interactive pre-processor for generating input files and generates plots of slope geometry, soil layers, pore pressures, specified slip circles or trial slip circles, with critical circles highlighted. (<http://www.ggsd.com>)

Program : Geo-Tec B

Description : Geo-Tec B is a cross platform (Windows and Macintosh) slope stability analysis program using the Janbu, Bishop and Fellenius methods. It can automatically calculate a series of circles between two defined extreme circles. Circles may be defined by identifying three points or a center and radius. Seismic analysis is carried out by a pseudo-static method. When using the Janbu method, it is possible to apply an external horizontal force to the slope. (<http://www.ggsd.com>)

Program : PCSTABL 6

Description : PCSTABL 6 is a computer program for the general solution of slope stability problems by two-dimensional limiting equilibrium methods and includes the analysis of reinforced soil slopes with geosynthetics, nailing, and tiebacks. The calculation of the factor of safety against instability of a slope is performed by the simplified Bishop method, applicable to circular shaped failure surfaces, the simplified Janbu method, applicable to failure surfaces of general shape, and the Spencer method, applicable to any type of surface. The simplified Janbu method has an option to use a correction factor, developed by Janbu, which can be applied to the factor of safety to reduce the conservatism produced by the assumption of no

interslice forces. It features random techniques for generation of potential failure surfaces for subsequent determination of the more critical surfaces and their corresponding factors of safety. (<http://www.ggsd.com>)

Program : STABGM

Description : STABGM is a program for the slope stability analysis of reinforced embankments and slopes with circular slip surfaces, using the Ordinary Method of Slices and Bishop's Modified Method. (<http://www.ggsd.com>)

Program : Stabl for Windows

Description :Stabl for Windows is the Windows version of PCSTABL 6 program for the general solution of slope stability problems by two-dimensional limiting equilibrium methods and includes the analysis of reinforced soil slopes with geosynthetics, nailing, and tiebacks. The calculation of the factor of safety against instability of a slope is performed by the simplified Bishop method, applicable to circular shaped failure surfaces, the simplified Janbu method, applicable to failure surfaces of general shape, and the Spencer method, applicable to any type of surface. The simplified Janbu method has an option to use a correction factor, developed by Janbu, which can be applied to the factor of safety to reduce the conservatism produced by the assumption of no interslice forces. It features random techniques for generation of potential failure surfaces for subsequent determination of the more critical surfaces and their corresponding factors of safety. (<http://www.ggsd.com>)

Program : Slope stability (Fine)

Description : Slope stability (Fine) solves the slope stability problem in a two dimensional environment. The slip surface can be modeled in two different ways - circular (Bishop or Petterson method), or polygonal (Sarma method). Features include:

- Simple input of geometry of layers
- Built-in database of soils and rocks
- Optimization of circular and polygonal slip surfaces
- An arbitrary number of surcharges (strip, trapezoidal, concentrated loading)
- Simple modeling of rigid bodies
- Possibility to model earthquake effects

- Possibility to consider foliation of soils (soil anisotropy)
- Possibility to introduce geo-reinforcement into the analysis
- Analysis in effective and total parameters of soils
- An arbitrary number of analyses within one stage of construction
- Possibility to introduce restrictions on the slip surface optimization
- Analysis according to the theory of limit states or safety factor

(<http://www.ggsd.com>)

Program : STABLE

Description : STABLE carries out slope stability analysis by the methods of Bishop, Morgenstern-Price and Sarma. Analyses may include: point loads, line reinforcement forces, flexible soil geometry for representation of lenses, inclusions, clay cores etc. Pore pressures may be specified as: piezometric surface, R_u values in each soil, absolute or excess values in each soil. Automatic slip-circle generation., location of critical circle, earthquake analysis. (<http://www.ggsd.com>)

Program : SLOPE 12R

Description : SLOPE 12R is a computer program for analysing the stability of slopes, also applicable to earth pressure and bearing capacity problems. Main Features are : Automatically generates slip surfaces to find the critical failure mechanism. The ground can be described in terms of up to nine soil strata with different strength properties. Multiple water tables or piezometric surfaces modeled. In simple cases pore pressures are calculated from the position of the water table but in more complicated flow conditions local values of pore pressure can be defined. Circular and non-circular slip surfaces can be analysed. A group of circular slip surfaces can be analysed by defining a rectangular grid of centres. For each centre a number of different radii can be specified. Two and three part wedges can be analysed. A group of wedges can be analysed by defining a rectangular grid of wedge nodes. Analysis methods: Swedish Circle (or Fellenius') method; Bishop's method; Spencer's method; Janbu's method. External forces (due to buildings or strut forces in excavations) can be applied to the ground surface. Earthquake forces can be modeled in a quasi-static manner by specifying horizontal and vertical acceleration factors. (<http://www.ggsd.com>)

Program : XSTABL

Description : XSTABL performs a two dimensional limit equilibrium analysis to compute the factor of safety for a layered slope. The Generalized Limit Equilibrium (GLE) method allows factors of safety to be calculated for force and moment equilibrium or for force equilibrium only, using different interslice force angle distributions including Spencer's, Morgenstern-Price, or one of the methods proposed by the Corps of Engineers. If an analysis requires a search for the most critical failure surface, the simplified Bishop and Janbu methods of analysis are selected due to their relative ease of use. The program may be used to either search for the most critical circular, non-circular, or block-shaped surface, or alternatively, to analyze a single circular or non-circular surface. (<http://www.ggsd.com>)

Program : I.L.A.

Description : I.L.A. is a slope stability analysis program that also incorporates features for retaining system designing. The slope analysis and design can be performed using the Sarma method, whose numerical stability increases the reliability of the calculations. The classic Bishop, Janbu, Morgenstern&Price and Bell methods are also available. The failure surfaces can either be defined as circular or planar surface families or even individually, as polygonal surfaces, and therefore have any shape whatsoever. The analysis can be carried out under drained or undrained conditions, also considering water pressures, surcharges, seismicity. (<http://www.ggsd.com>)

Program : WinStabl

Description : WinStabl is a pre- and post-processor to STABL6. The package supports: Simplified Janbu, Modified Bishop, and Spencer's analyses. Reinforcing layers. Tiebacks. Earthquake (pseudo-static) analysis. Boundary (external) loads. Anisotropic soils. Specific failure surfaces. Circular and irregular surface searching. (<http://www.ggsd.com>)

Program : MStab

Description : MStab carries out stability analysis by the Bishop, Fellenius and Spencer methods. It provides automatic search of the critical slip circle; user-defined zones that the circle will not cross; integration of geotextiles; user-defined non-circular slip plane; temporary and permanent loads; pore pressures and degree of

consolidation; Mohr-Coulomb soil parameters; output of global safety factor; output of safety contours; output of stress components along slip plane. (<http://www.ggsd.com>)

Program : GSTABL7 with STEDwin v.2

Description : GSTABL7 with STEDwin v.2 is a 2D limit equilibrium slope stability program based on STABL6 but which includes geogrid reinforcement, piers/piles, tiebacks, soil nails, applied forces, and surcharge loads. Failure surfaces of any shape can be analyzed with Modified Bishop, Simplified Janbu, Spencer, and Morgenstern-Price methods. (<http://www.ggsd.com>)

Program : GSlope

Description : GSLOPE carries out limit equilibrium slope stability analysis of existing natural slopes, unreinforced man-made slopes, or slopes with soil reinforcement. The program uses Bishop's Modified method and Janbu's Simplified method. Slopes can be analysed in either direction, and a seismic coefficient is provided for pseudo-static analysis. When a non-circular slip surface is drawn, the computed Factor of Safety is displayed immediately. (<http://www.ggsd.com>)

Program : SLOPBG

Description : It allows the analysis of a generalized soil slope using Bishop's modified method. Water pressures are accounted for using either phreatic lines, pore pressure contours or a single pore pressure coefficient. Horizontal and vertical seismic forces are considered. The program can search for the critical minimum factor of safety circle. The program can be run in a deterministic or probabilistic mode. In probabilistic mode several statistical distribution types can be applied to best reflect the range of input variables. A simulation technique is then used to generate pseudo-variables used to calculate the distribution of the factor of safety. (<http://www.ggsd.com>)

Program : Slide

Description : Slide 5.0 is a 2D Limit Equilibrium Analysis program with a CAD based graphical interface and a wide range of modeling and data interpretation options. It now includes sensitivity, probabilistic and back analysis capabilities. Sensitivity analysis allows the user to determine the effect of any parameter on the

factor of safety to discover the most critical parameters, leading to optimization of the slope remediation. Safety factors are calculated based on a number of widely used limit equilibrium techniques including Bishop Simplified, Spencer, and GLE/Morgenstern & Price. (<http://www.ggsd.com>)

Program : Slope-W

Description : Slope-W is a circular and non-circular soil and rock slope stability program. Carries out stability analyses by the methods of Fellenius, Bishop simplified, Janbu simplified, Spencer, Morgenstern-Price, Corps of Engineers, Lowe-Karafiath, General Limit Equilibrium, Finite element stress. It can perform probabilistic stability analyses using the Monte Carlo method. (<http://www.ggsd.com>)

Program : Galena

Description : Galena is a slope stability analysis program incorporating Bishop (circular), Spencer-Wright (circular and non-circular) and Sarma (non-vertical slices) methods for problem solving in soils and rocks. Single and multiple analyses available for all methods. Models can include external forces, distributed loads, and earthquake effects. (<http://www.ggsd.com>)

Program : Slope 2000

Description : Slope 2000 can locate the critical failure surface of a slope under general conditions with general constraints. The shape of the failure surface can be either circular or non-circular. The slope analysis methods include Bishop, Janbu simplified and rigorous, Morgenstern-Price, Sarma, GLE, Corps of Engineers, Lowe Karafiath, wedge. (Geotechnical & Geoenvironmental Software Directory - <http://www.ggsd.com>)

2.7 Slope Stability Analysis Conditions Importance

We know that pore water pressure is a major factor for slope stability check and when carrying out an effective stress analysis the pore water pressures need to be calculated at the base of each slice as the water force is involved in computing the factor of safety. One of the common ways to compute pore water pressure is to use r_u , where r_u is defined as the ratio of the water pressure u to the overburden pressure γh at a given point. This implies that the pore water pressure is related to the

overburden pressure or that the water force U at the base of each slice is proportional to the total weight W of the slice.

Another common way is to use a piezometric surface. A surface may be used in conjunction with a slip circle program that the water pressure, u , at the base of each slice is computed as $\gamma_w h_w$ where h_w is the vertical distance between the piezometric surface and the base of the slice. The use of a piezometric surface for a slope in which seepage is taking place will lead to errors in estimating pore pressures since pore pressures should be determined from a flow net and can't be tied to a single piezometric surface.

The use of a pore water pressure grid can overcome the above problem. Pore pressure values may be specified at points on a regular grid and the values at the base of each slice found from interpolation of values at the nearest grid points. This is particularly useful with seepage problems where finite difference or finite element solutions may be obtained and used to set up a grid pore pressure.

Most of the methods mentioned in the previous sections employ the definition of the factor of safety F_s . As Lowe (1967) pointed out defining the factor of safety as a factor on shear strength is logical because shear strength is usually the quantity that involves the greatest degree of uncertainty. The limitation results from the fact that these methods provide no information regarding the magnitudes of the strains within the slopes or any indication about how they may vary along the slip surface. It is worth noting that the average value of F_s is the same for all practical purposes, even if the factor of safety is assumed to vary from place to place along the slip surface.

3. ARTIFICIAL INTELLIGENCE APPLICATIONS WITH NEURAL NETWORKS

3.1 Introduction

Artificial neural networks are systems and computational devices that are constructed to make use of some organizational principles resembling those of the human brain. Normally there are a large number of highly connected computational nodes (neurons) that are operated and configured in parallel regular architectures. Like human brain an artificial neural network has the ability to learn; recall and generalize from the data which are used to train the system. The pattern of activation at the input units represents the problem being presented to the network; and the pattern of activation at the output processing units, represents computational results achieved by neural network. The neural network propagates the changes in weights of the connection between each linked neuron by minimizing the difference between the actual output and target output. The propagation of the changes in link weight the computation performed by neural network is strongly affected by the topology and strengths of the connections between the neurons. As an example Figure 3.1 shows a simple mathematical model of this network.

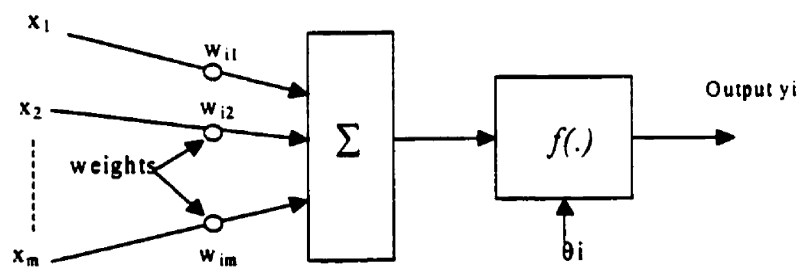


Figure 3.1: Schematic Diagram of A Neuron's Network (McCulloch & Pitts ,1943)

3.2 Neural Network's Properties

3.2.1 Basic Structure of Neural Network

The basic building block of neural network technology is the simulated neuron (depicted in Figure 3.2 as a circle). Independent neurons are of little use, unless they

are interconnected in a network of neurons. The network processes a number of inputs from the outside world in order to produce an output, the network's classifications and predictions. The neurons are connected by weights, (depicted as lines) which are applied to values passed from one neuron on to the next. A group of neurons is called a slab. Neurons are also grouped into layers by their connection to the outside world. For example, if a neuron receives data from outside of the network, it is considered to be in the input layer. If a neuron contains the network's predictions or classifications, it is in the output layer. Neurons in between the input and output layers are in the hidden layer(s). A layer may contain one or more slabs of neurons.

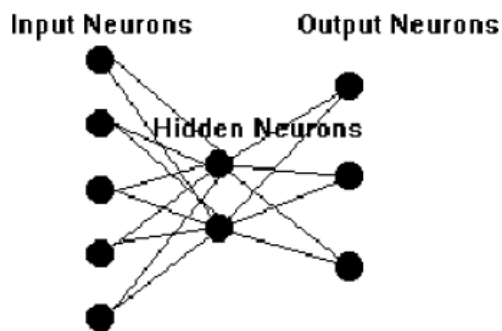


Figure 3.2 : Neural Networks Structure (Ural & Bayrak , 2003)

Neural networks are not programmed; they learn by example. Typically, a neural network is presented with a training set consisting of a group of examples from which the network can learn. The most common training scenarios utilize supervised learning, during which the network is presented with an input pattern together with the target output for that pattern. The target output usually constitutes the correct answer, or correct classification for the input pattern. In response to these paired examples, the neural network adjusts the values of its internal weights. If training is successful, the internal parameters are then adjusted to the point where the network can produce the correct answers in response to each input pattern. Usually the set of training examples is presented many times during training to allow the network to adjust its internal parameters gradually. The neural network approach does not require human development of algorithms and programs that are specific to the classification problem hand, suggesting that time and human effort can be saved. There are drawbacks to the neural network approach, however: the time to train the

network may not be known beforehand, and the process of designing a network that successfully solves an application problem may be involved.

It is possible to develop a network that can generalize on the tasks for which it is trained, enabling the network to provide the correct answer when presented with a new input pattern that is different from the input in the training set. To develop a neural network that can generalize, the training set must include a variety of examples that are good preparation for the generalization task. In addition, the training session must be limited in iterations, so that no “over learning” takes place (i.e., the learning of specific examples instead of classification criteria, which is effective and general). Thus, special considerations in constructing the training set and the training presentations must be made to permit effective generalization behavior from a neural network. All of these characteristics of neural networks may be explained through the simple mathematical structure of neural net models. The computations performed in the neural net may be specified mathematically.

As a summary, an artificial neural network is a parallel computing system with the following characteristics (Lin & Lee , 1996)

1. It is a naturally inspired mathematical model.
2. It consists of a large number of highly interconnected processing units.
3. Its connections (weights) hold the information about the relationship between the inputs and outputs.
4. Each neuron can dynamically respond to its input stimulus and the response completely depends on its local information that is the input signals arrive at the processing element via connections and connection weights.
5. It has the ability to learn recall and generalize from training data by adjusting the connection weights.
6. Its collective behavior demonstrates the computational power while no single neuron carries specific information, the information is distributed among the neurons which have a great deal of computational power.

One of the primary significant properties of neural network is the ability of the network to learn from its environment and to improve its performance through learning. The neural network learns about its environment through an iterative

process of adjustment to its synaptic weights and thresholds. Ideally the network can become more knowledgeable about its environment after each iteration of the learning process. The learning process can be classified as supervised learning or unsupervised learning. For supervised learning we are trying to map the input output pairs according to a given training set. In other words already know what the output will be during the training. The network parameters are updated by a supervised learning rule. For unsupervised learning there is no external instruction available only input vectors can be used for learning. In other words one does not know outputs or classes associated with the input patterns. During the unsupervised learning there is no feedback from the environment to indicate what the outputs of a network should be, or, whether they are correct. The network itself should discover any relationships, such as patterns, features, correlations, or categories that may exist in the input data and translate the discovered relationship outputs.

According to Mendel and McClaren (1970) the definition of learning can be expressed as follows. Learning is a process by which the free parameters of a neural network are adopted through a continuing process of stimulation by the environment in which the network is embedded. The type of learning is determined by the manner in which the parameter changes take place.

The learning can be understood as the process that repeatedly applies input vectors to the network and the finds new weights and biases with the learning rule. The process will be repeated until the sum error based on the cost function falls beneath an acceptable error goal or a maximum number of epochs have occurred. The learning parameters are varied according to different learning rules. But the common parameters which will be used for each supervised learning process are the number of epochs between displaying process the maximum number of epochs to train, the acceptable error goal and the learning rate.

The learning algorithm is defined as a prescribed set of well defined rules for the solution of a learning problem. There are large varieties of learning algorithms which differ from each other in the way to adjust the weight. Each learning algorithm offers an advantage of its own.

3.2.2 Design Choices of Neural Networks

Many design choices are involved in developing a neural network application. Figure 3.3 Shows an example for choosing a design for a neural network application

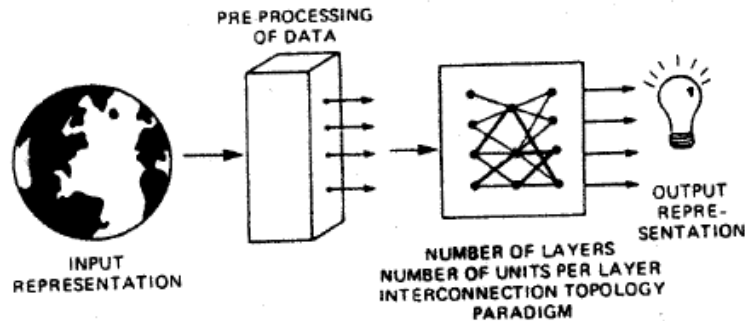


Figure 3.3 : Design Choices For Neural Network application (Dayhoff, 1990)

The first option is in choosing the general area of application. Usually this is an existing problem that appears amenable to solution with a neural network. Next, the problem must be identified, so that a selection of inputs and outputs to the network may be made. Choices for inputs and outputs involve identifying the types of pattern that go into and out of the network. In addition, the researcher must design how those patterns are to represent the needed information (the representation scheme). Next, internal design choices must be made including the topology and size of the network. The number of processing units are specified, along with the specific interconnections that the network is to have. Processing units are usually organized into distinct layers, which are either fully or partially interconnected.

There are additional choices for the dynamic activity of processing units. A variety of neural net paradigms are available; these differ in the specifics of the processing done at each unit and in how their internal parameters are updated. Each paradigm dictates how the readjustments of parameters take place. This readjustment results in “learning” by the network. Next, there are internal parameters that are “tuned” to optimize the neural net design. The value of this parameter influences the rate of learning by the network, and may possibly influence how successful the network learns. These are experiments that indicate “learning” occurs at more successful rates if this parameter is decreased during the learning session. Some paradigms utilize more than one parameter that must be tuned.

Finally, the selection of training of data presented to the neural network influences whether or not the network “learns” a particular task. How well a network will learn depends on the examples presented. A good set of examples, which illustrate the tasks to be learned well, is necessary for the desired learning to take place. A poor set of examples will result in poor learning on the part of the network. The set of training examples must also reflect the variability in the patterns that the network will encounter after training.

3.2.3 Neural Network Architectures

3.2.3.1 GRNN Architecture And Learning Algorithm

General Regression Neural Networks, GRNN, invented by Dr. Donald Specht (1996), is a three-layer network having one hidden neuron for every training pattern, in addition to the total number of neurons equal to sum of input and output number.

Unlike Back-propagation Networks, there is a smoothing factor instead of training parameters; learning rate and momentum. The success of GRNN networks is dependent upon the smoothing factor. The individual smoothing factor adjustments values may be used as a sensitivity analysis tool: inputs with low smoothing factor adjustments are candidates for removal at a later trial, especially if the smoothing factor adjustments approaches zero.

The fact that the GRNN network centers are determined by the training data vectors gives the network stability and it ensures that it is not be over-trained. This is the main feature along with its simplicity that distinguishes it from most other approaches.

GRNN is especially useful for continuous function approximations. GRNN can have multidimensional input, and it will fit multidimensional surfaces through data. GRNN work by measuring how far a given sample pattern is from patterns in the training set in N dimensional space, where N is the number of inputs in the problem. When a new pattern is presented to the network, that input pattern is compared in N dimensional space to all of the patterns in the training set to determine how far in distance it is from those patterns. The output that is predicted by the network, is a proportional amount of all of the outputs in the training set. The proportion is based upon how far the new pattern is, from the given patterns in the training set.

Advantages:

- i. GRNN can handle both linear and non-linear data.
- ii. Adding new samples to the training set does not require re-calibration the model.
- iii. Only one adjustable parameter thereby making overtraining less likely.

Disadvantages:

- i. Requires many training samples to adequately span the variation in the data.
- ii. Requires that all the training samples be stored for future use (i.e., prediction).
- iii. Has trouble with irrelevant inputs.
- iv. No intuitive method for selecting the optimal smoothing parameter.

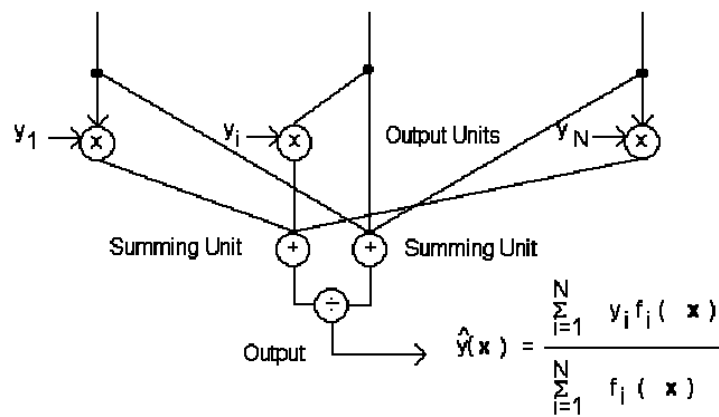


Figure 3.4 : The Basic GRNN Architecture

The general regression neural network (GRNN) is a three layer network having one hidden neuron for every training pattern (Lawrence,1993). (Figure 3.4) In addition to the total number of neurons is equal to the sum of the number of inputs and the outputs (Specht,1991). The regression is the estimation of the least mean squares of variables based on the available data. In other words, the regression decision in the GRNN architecture reveals the most probable value of all the patterns in an N-dimensional space (where N is the number of inputs). Output values correspond to the weighted average of the target values. The target values are weights which exceed from the hidden layers to the output layers. During the GRNN training process, smoothing factors (or bandwidths) are the only weights which need to be calculated. The success of the GRNN is dependent upon the smoothing factor, however, there is no intuitive method for selecting the optimal smoothing factor (Ural and Bayrak, 2003).

The GRNN utilizes a probabilistic model between an independent single training vector in the input space (X) and a dependent scalar output (Y). X_i is defined as the input vector of the i^{th} training data set, and Y_i is the output related to X_i . It is assumed that x and y are defined as measured values of X and Y, respectively, and the regression of Y on x is defined as \hat{y} such that;

$$y(x) = \frac{\sum_{i=1}^p y_i f_i(x)}{\sum_{i=1}^p f_i(x)} \quad (3.1)$$

$$f_i(x) = \exp\left[\frac{-(x-x_i)^T(x-x_i)}{2\sigma^2}\right] \quad (3.2)$$

By substituting Eq. 3.2 in Eq. 3.1

$$y(x) = \frac{\sum_{i=1}^p y_i \exp\left[\frac{-(x-x_i)^T(x-x_i)}{2\sigma^2}\right]}{\sum_{i=1}^p \exp\left[\frac{-(x-x_i)^T(x-x_i)}{2\sigma^2}\right]} \quad (3.3)$$

Eqs. (3) is known as the Specht's GRNN. In Specht's GRNN, σ , is a smoothing factor shared by all the inputs and the pattern nodes. Assigning an independent smoothing factor for each of the variables may improve accuracy; however, this may be impractical in many simulations (Specht, 1996).

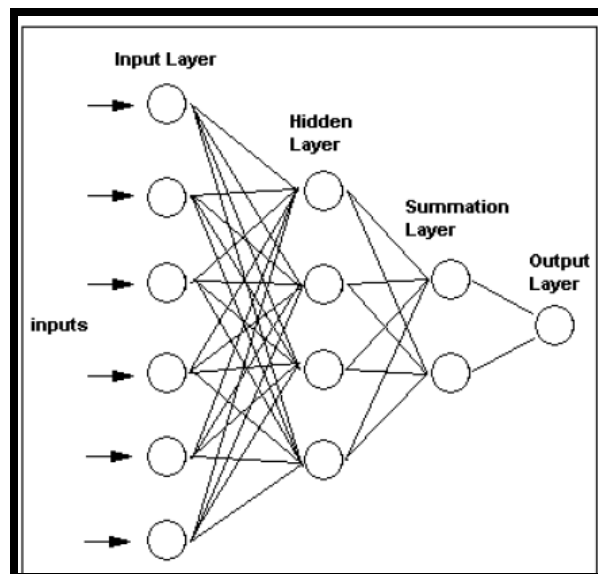


Figure 3.5 : The GRNN Architecture (Specht , 1996)

As shown in Figure 3.5, the GRNN is composed of one input layer, one hidden layer, a summation layer, and one output layer. The GRNN models are trained by a one-pass learning algorithm. In order to estimate an output, the presented input is subtracted from each stored vector in the hidden layers. The probability density functions (PDF) or radial basis functions are applied in order to evaluate the squared or absolute difference between the hidden neurons and inputs. Between these layers activation functions use and the details of them are given below. Activation functions determine neurons behaviour. The formulas of the functions which are used in Neuroshell2 are shown below:

$$\text{Logistic} \rightarrow f(x) = 1/(1 + \exp(-x)) \quad (3.4)$$

$$\text{Linear} \rightarrow f(x) = x \quad (3.5)$$

$$\text{Tanh} \rightarrow f(x) = \tanh(x), \text{ the hyperbolic tangent function} \quad (3.6)$$

$$\text{Tanh15} \rightarrow f(x) = \tanh(1.5x) \quad (3.7)$$

$$\text{Sine} \rightarrow f(x) = \sin(x) \quad (3.8)$$

$$\text{Symmetric Logistic} \rightarrow f(x) = ((2/(1 + \exp(-x))) - 1) \quad (3.9)$$

$$\text{Gaussian} \rightarrow f(x) = \exp(-x^2) \quad (3.10)$$

$$\text{Gaussian Complement} \rightarrow f(x) = 1 - \exp(-x^2) \quad (3.11)$$

The details of these activation functions are given in Figure 3.6, 3.7, 3.8, 3.9 ;

Linear: Use of this function should generally be limited to the output slab. It is useful for problems where the output is continuous variable, as opposed to several outputs which represent categories.

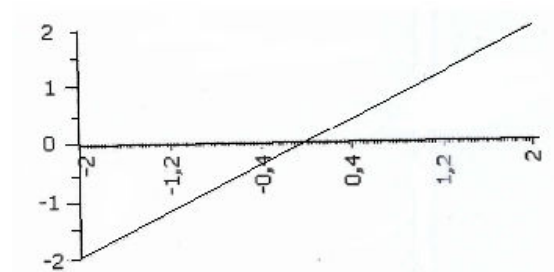


Figure 3.6 : Linear activation function

Logistic (Sigmoid Logistic): This function is useful for most neural network applications, and it maps values into the (0, 1) ranges. It is used when the outputs are in categories.

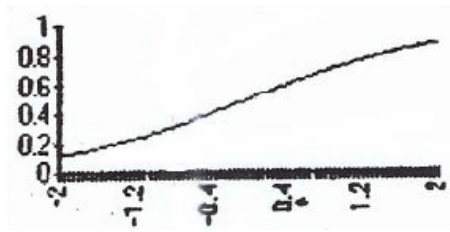


Figure 3.7 : Logistic function

Symmetric Logistic: This is similar to the logistic, except that it maps to (-1, 1) instead of to (0, 1). When the outputs are categories, trying symmetric logistic function instead of the logistic function in the hidden and output layers may be better. In some cases, the network will train to a lower error in the training and test sets.

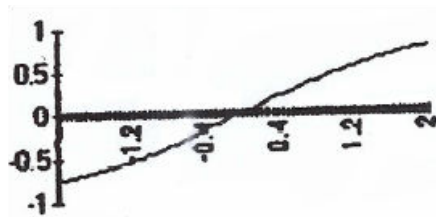


Figure 3.8 : Symmetric logistic function

Gaussian: It is very useful in some set of problems. Trying it in the hidden layer and logistic function in the output layer may give good results.

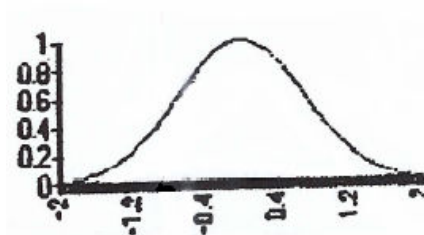


Figure 3.9 : Gaussian function

The summation unit computes the sum of the outputs from all hidden neurons. The network's final output is obtained at the output layer, where a normalization is performed. The normalized output is computed by dividing the value of the weighted sum of hidden layer outputs, by the value in the summation layer.

3.2.3.2 PNN Architecture

Probabilistic Neural Networks (PNN) are known for their ability to train quickly on sparse data sets. PNN separates data into a specified number of output categories. PNN networks are three layer networks wherein the training patterns are presented to the input layer and the output layer has one neuron for each possible category. There must be as many neurons in the hidden layer as there are training patterns. The network produces activations in the output layer corresponding to the probability density function estimate for that category. The highest output represents the most probable category (Frederick, 1996).

The probabilistic neural network (PNN) learns to approximate the PDF of the training examples. More precisely, the PNN is interpreted as a function which approximates the probability density of the underlying examples' distribution (rather than the examples directly by fitting). The PNN consists of nodes allocated in three layers after the inputs (Figure 3.10)

Pattern layer: There is one pattern node for each training example. Each pattern node forms a product of the weight vector and the given example for classification, where the weights entering a node are from a particular example.

Summation layer: Each summation node receives the outputs from pattern nodes associated with a given class

Output layer: The output nodes are binary neurons that produce the classification decision.

The only factor that needs to be selected for training is the smoothing factor, that is if the deviation of the Gaussian functions is too small deviations cause a very spiky approximation which can't generalize well and large deviations smooth out details.

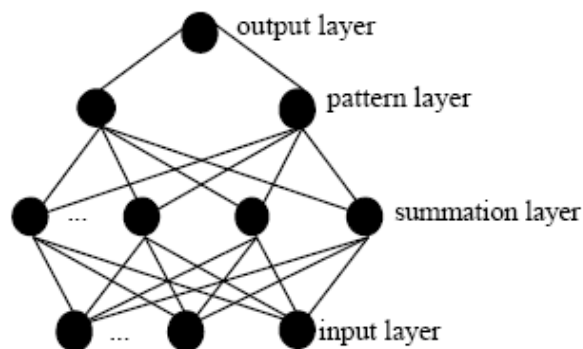


Figure 3.10 : The PNN Architecture

A probabilistic neural network (PNN) has 3 layers of nodes. The Figure 3.11 below, displays the architecture for a PNN that recognizes $K = 2$ classes, but it can be extended to any number K of classes. The input layer (on the left) contains N nodes: one for each of the N input features of a feature vector. These are fan-out nodes that branch at each feature input node to all nodes in the hidden (or middle) layer so that each hidden node receives the complete input feature vector x . The hidden nodes are collected into groups: one group for each of the K classes as shown in the Figure 3.11.

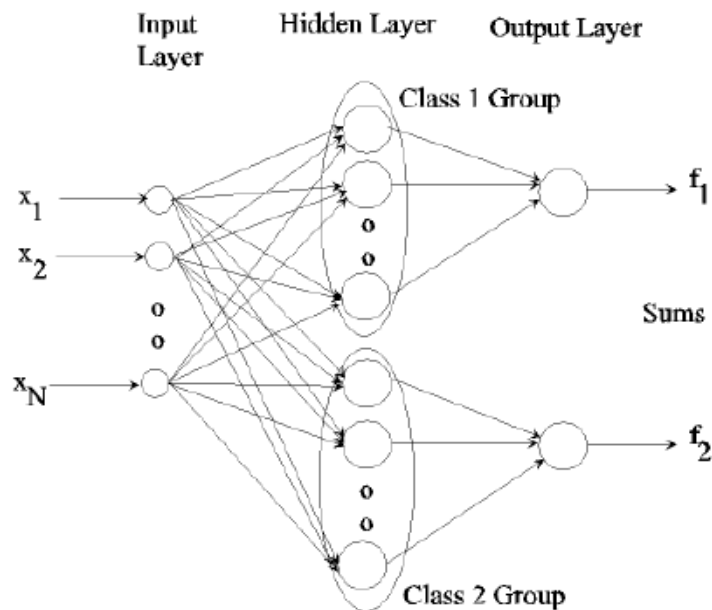


Figure 3.11 : Probabilistic Neural Network Layers

Each hidden node in the group for Class k corresponds to a Gaussian function centered on its associated feature vector (there is a Gaussian for each exemplar feature vector). All of the Gaussians in a class, group feed their functional values to the same output layer node for that class, so there are K output nodes.

At the output node for Class k ($k = 1$ or 2 here), all of the Gaussian values for Class k are summed and the sum is scaled so the probability volume under the sum function is unity so that the sum forms a probability density function. Here we temporarily use special notation for clarity. Let there be P exemplar feature vectors $\{x(p): p = 1, \dots, P\}$ labeled as Class 1 and let there be Q exemplar feature vectors $\{y(r): r = 1, \dots, R\}$ labeled as Class 2. In the hidden layer there are P nodes in the group for Class 1 and R nodes in the group for Class 2. The equations for each

Gaussian centered on the respective Class 1 and Class 2 points $x(p)$ and $y(q)$ (feature vectors) are (where N is the dimension of the vectors) are, for any input vector x

$$g_1(x) = [1/\sqrt{(2\pi\sigma^2)^N}] \exp\{-\|x - x^{(p)}\|^2/(2\sigma^2)\} \quad (3.12)$$

$$g_2(y) = [1/\sqrt{(2\pi\sigma^2)^N}] \exp\{-\|y - y^{(q)}\|^2/(2\sigma^2)\} \quad (3.13)$$

The F values can be taken to be one-half the average distance between the feature vectors in the same group or at each exemplar it can be one-half the distance from the exemplar to its nearest other exemplar vector. The k^{th} output node sums the values received from the hidden nodes in the k^{th} group, called mixed Gaussians or Parzen windows. The sums are defined by

$$f_1(x) = [1/\sqrt{(2\pi\sigma^2)^N}](1/P) \sum_{(p=1,P)} \exp\{-\|x - x^{(p)}\|^2/(2\sigma^2)\} \quad (3.14)$$

$$f_2(y) = [1/\sqrt{(2\pi\sigma^2)^N}](1/Q) \sum_{(q=1,Q)} \exp\{-\|y - y^{(q)}\|^2/(2\sigma^2)\} \quad (3.15)$$

x is any input feature vector, F_1 and F_2 are the spread parameters (standard deviations) for Gaussians in Classes 1 and 2, respectively. N is the dimension of the input vectors, P is the number of center vectors in Class 1 and R is the number of centers in Class 2, $x(p)$ and $y(r)$ are centers in the respective Classes 1 and 2, and $\|x - x(p)\|$ is the Euclidean distance (square root of the sum of squared differences) between x and $x(p)$. Any input vector x is put through both sum functions $f_1(x)$ and $f_2(x)$ and the maximum value (maximum a posteriori, or MAP value) of $f_1(x)$ and $f_2(x)$ decides the class. For $K > 2$ classes the process is analogous. There is no iteration nor computation of weights. For a large number of Gaussians in a sum, the error buildup can be significant. Thus the feature vectors in each class may be reduced by thinning those that are too close to another one and making F larger.

3.2.3.3 Back propagation Neural Network Architecture

The back propagation learning algorithm is one of the most important developments in neural network. Back propagation networks are known for their ability to generalize well on a wide variety of problems. That is why they are used for the vast majority of working neural network applications. Back propagation networks are a supervised type of network, e.g., trained with both inputs and outputs. Depending upon the number of patterns, training may be slower than other paradigms. When using back propagation networks, you can increase the precision of the network by

creating a separate network for each output if your outputs are not categories (Frederick, 1996).

This learning algorithm is applied to multilayer feed forward networks consisting of processing elements with continuous differentiable activation functions. Such networks associated with the back propagation learning algorithm are also called back propagation networks. There are some factors related to this network, these are the initial weights, the learning constant, the cost function, the update rule, the size and nature of the training sets and the network architecture (includes the number of hidden nodes and number of hidden layers) .

The ultimate solutions of multilayer feed forward network are strongly affected by the initial weights. Normally the weight matrices are initialized with the random small values.

The learning constant is another important factor that affects the efficiency and convergence of the back propagation algorithm. A large value of learning constant can speed up the convergence but might result in over shooting, while a small value has an opposite effect. Another problem is that the best values of the learning constant at the beginning of training may not be as good in the later training. Therefore the learning can be improved by using an adaptive learning constant. It can decrease the training time by trying to keep the learning step size as large as possible, while keeping learning stable.

Also , any differentiable function which is minimized when its arguments are equal can be used as the cost function. However the update rule needs to be changed corresponding to different cost functions. The least square cost function is the most popular one that has been used in a large variety of applications because of its simplicity.

The two major requirements on the training data are to be sufficient and proper. However there are no standard procedures or rules for all case when choosing the training data. Normally the training data should be able to cover the entire expected input space. In most situations scaling and normalization is necessary to help the learning. The back propagation artificial neural network is good at generalization, it can explain the input patterns which are new to the network after being well trained. The generalization is important for learning tasks where the number of inputs is large

and the data itself is noisy. In general, we are not looking for a neural network system that can best fit the training input pattern. Instead, we are looking for a system trained with data that can respond to the testing of new input patterns in a satisfactory manner. However, there is one phenomenon called “over fitting“ existing in some network, when the network has too many trainable parameters for the given amount of training data. “Over fitting“ means the network can learn very well on all the training input patterns, but does not perform generalization well. Figure 3.12 demonstrates the network can’t generate reasonable output for the data between the original inputs due to over fitting.

On the other hand, with too few trainable parameters, the network will fail to learn the training data and will also perform very poorly on the testing data. Therefore in the actual practicing we normally introduce the trainable parameters into the system stepwise to figure out the optimum number of input parameters that can perform well at generalization. Another way that may cause over fitting is when we limit the acceptable error goal in the training stage to some small values which are difficult for the system to reach. In this situation the system parameters will be updated in order to specifically fit the training data set but will no longer a good job of fitting the testing data sets. In order to solve this problem we normally decrease the value of acceptable error goal stepwise to check the performance of the system and choose the error goal that can let the system perform best on the testing data. The number of hidden layers and number of hidden nodes are the basic factors we need to determine for setting up the networks. For determination of the number of hidden layers using one to two hidden layers are common and can satisfy most of the problems. For the determination of the number of hidden nodes, it is rather difficult to follow any standard rules due to complexity of network mapping and nondeterministic nature of real world problems.

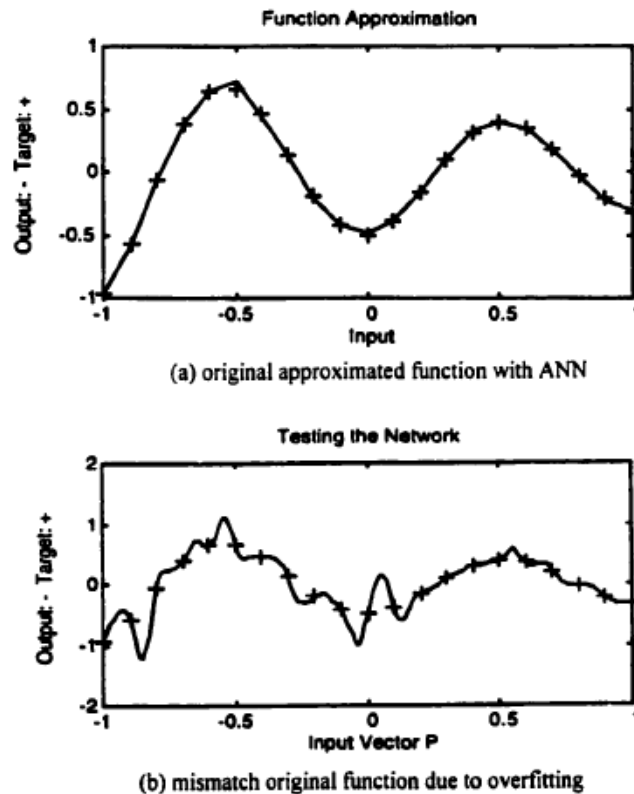


Figure 3.12 : Mismatch The Function Due To The Over fitting

3.2.3.4 Kohonen Architecture

The Kohonen self organizing map network used in numerical programs is a type of unsupervised network, which has the ability to learn without being shown correct outputs in sample patterns. These networks are able to separate data into a specific number of categories. There are only two layers: an input layer and an output layer which has one neuron for each possible output category.

The training patterns are presented to the input layer, then propagated to the output layer and evaluated. One output neuron is the “winner”. The network weights are adjusted during training. This process is repeated for all patterns for a number of epochs chosen in advance. This network is very sensitive to learning rate. It is lowered slightly but steadily as the training progresses, causing smaller and smaller weight changes. This causes the network to stabilize.

The network adjusts the weights for the neurons in a neighborhood around the winning neuron. The neighborhood size is variable, starting off fairly large (sometimes even close to the number of categories) and decreasing with learning until during the last training events the neighborhood is zero, meaning by then only

the winning neuron's weights are changed. By that time the learning rate is very small, and the clusters have been defined. Architecture automatically adjusts learning rate and neighborhood size for you, but you have to specify the initial values as well as the total number of epochs that learning will continue (Frederick, 1996).

3.2.3.5 GMDH Architecture

The technique called Group Method of Data Handling (GMDH) was invented by A.G.Ivakhnenko, but enhanced by others, including A.R.Barron. This technique has also been called "polynomial nets".

GMDH works by building successive layers with complex links (or connections) that are the individual terms of a polynomial. These polynomial terms are created by using linear and non-linear regression. The initial layer is simply the input layer. The first layer created is made by computing regressions of the input variables and then choosing the best ones. The second layer is created by computing regressions of the values in the first layer along with the input variables. Again, only the best are chosen by the algorithm. These are called survivors. This process continues until the net stops getting better (according to a prespecified selection criterion).

The resulting network can be represented as a complex polynomial description of the model. You may view the formula, which contains the most significant input variables. In some respects, it is very much like using regression analysis. GMDH can build very complex models while avoiding over fitting problems.

GMDH contains several evaluation methods, called selection criteria, to determine when it should stop training. One of these, called regularity, is similar to calibration in that the net uses the constructed architecture that works the best on the test set. The other selection criteria do not need a test set because the network automatically penalized models that become too complex in order to prevent overtraining. The advantage of this is that you can use all available data to train the network. A by-product of GMDH is that it recognizes the most significant variables as it trains, and will display a list of them (Frederick, 1996).

3.3 General Applications in Civil Engineering

3.3.1 Dynamic Soil–Structure Interaction Using Neural Networks For Parameter Evaluation

The subject of soil structure interaction has attracted the attention of engineers worldwide over the last four decades. Foundations are subjected to loads, which may induce high pressures in soils causing considerable deformations between soils and structural members. These deformations may eventually affect the forces transferred at the foundation level. This phenomenon is referred to as soil-structure interaction. Thus, to study the behavior of interfaces, it is necessary to characterize the behavior at the interface, model constitutive relationships mathematically, and incorporate the model together with the governing equations of mechanics into numerical procedures such as the finite element method. Such an approach then can be used for solving complex problems that involve dynamic loading, nonlinear material behavior, and the presence of the water, leading to saturated interfaces.

A biased artificial neural network program based on back propagation algorithm has been developed to find saturated Nevada sand aluminum interface parameters from available saturated Ottawa sand steel interface parameters and saturated Sabine clay steel interface parameters.

From the research it is shown that the model can be used to solve complex problems involving dynamic loading, nonlinear material behavior and saturated conditions. It is also shown that artificial neural networks can be used to obtain material parameters for the model from available sets of parameters for different materials.

3.3.2 A Neural Network Approach For Predicting The Structural Behavior of Concrete Slabs

This research investigates the use of Neural Networks (NN) as a preliminary alternative to mathematical modeling or experimental testing for quick prediction of the structural behavior of reinforced concrete slabs. Such predictions could be utilized by a structural engineer on a preliminary basis to determine the initial suitability of a particular slab design. Once this suitability was determined, the engineer could then proceed with further, more traditional methods of design. This will serve to illustrate the simple manner by which neural networks model the impact of a set of parameters (inputs) on a set of simultaneous conclusions (outputs); and

the powerful learn by example and generalization mechanism that neural networks use to detect the hidden relationships linking the inputs to their outputs.

Neural networks are computational models that adopt a training mechanism to extract the relationships that link a set of causal input parameters to their resulting conclusions. Once neural networks are trained, they can predict the results for an unknown case (not used in training) if provided with the input parameters alone. Some characteristics of neural networks that make them potentially useful for many different types of applications are (Moselhi et al., 1992) :

- Neural networks are organized within a parallel, decentralized structure rather than the serial architecture found in conventional computer algorithms. As a result, processing occurs in a rapid manner,
- They have distributed memories; neural network memories are represented by interconnection weights spread over all of the network's processing elements,
- They are fault tolerant, that is, they are still functional even after several processing elements are damaged and become defective,
- They have the ability to learn by example,
- They have the ability to simulate the behavior of systems with limited modeling effort, and
- They can provide speedy and reasonably accurate solutions in complex, uncertain, and subjective situations.

3.3.3 Neural Network Analysis of Structural Damage Due to Corrosion

The need for the maintenance of bridges has been drawing attention in recent years. Many bridges require some kinds of repairs, and the number of such bridges is likely to grow for at least the foreseeable future. When determining whether or not a particular bridge should be repaired, common practice is for a maintenance expert to inspect the bridge visually. This method is therefore time consuming, and the growing number of bridges requiring attention is making the current approach impractical. Under these circumstances, engineers who are not expert in repairing are increasingly called upon to judge the repair time.

In order to help non specialist engineers to make appropriate decisions on the timing of repair, an attempt to develop a practical decision support system for the damage assessment of structural corrosion is made. In this system, it is attempted to apply the neural network technique for the damage assessment. When there are sufficient records of past bridge maintenance, the learning ability of the neural network is useful to save the working time and load necessary in the inspection and analysis. Further reduction of load time can be achieved by utilizing the technique of image processing. Through image processing, one is enabled to assess the damage state of structural corrosion automatically and independent of the subjectivity of inspector, or engineer.

3.3.4 Artificial Neural Networks for Predicting the Response of Structural Systems with Viscoelastic Dampers

The artificial neural networks (ANNs) are emerging as powerful tools for solving problems of an iterative nature. Among the various neural network paradigms available, many problems of civil engineering are solved using multilayer feed forward back-propagation networks. ANN-based methods have been used in environmental and water resources engineering, traffic engineering, highway engineering, and geotechnical engineering. Application of ANNs for structural analysis, design automation, optimization, system identification, condition assessment and monitoring, finite-element mesh generation, structural material characterization, modeling, and structural control has been reported extensively in the literature (Adeli, 2001).

An attempt has been made to estimate the inelastic demand of the structural systems with passive energy dissipators in terms of average peak displacement using a back-propagation neural network. The methodology to arrive at the base shear and roof displacement using the effective damping and effective period predicted by the neural network is also illustrated. Predicting the inelastic demand of structural systems with dampers is a time-consuming process, which involves several iterations. ANN methodology has been effectively tried to quickly predict the inelastic demand in terms of peak displacement, effective damping, and effective time period. The complete methodology to arrive at the design base shear force and roof displacement has been illustrated. The ANN can be effectively used for new designs as well as for checking the response of any retrofitted structure for the

chosen design spectrum. This network is useful in quickly deciding the amount of damping and the number of dampers required to reduce the peak displacement and help in restricting further damage. Sensitivity of input parameters could also be studied which will help in the selection and proportioning of structural members and dampers.

3.3.5 Modeling Ground Motion Using Neural Networks

In view of potential shortcomings of analytical modeling and considering the ever increasing bulk of information on earthquake-induced ground motions within the Valley of Mexico, knowledge-based procedures are being explored to develop alternate ways to analyze the response of Mexico City soil deposits. Modeling earthquake geotechnical problems by means of Artificial Neural Networks (ANNs), when these are trained on a comprehensive set of data, is very appealing because ANNs are capable of capturing and storing the related-phenomenon knowledge directly from the information that originates during the monitoring process.

The information given above demonstrates that ANNs are able to predict with good approximation ground surface responses to seismic events that come from different earthquake sources. After a significant number of trials using different combinations of input functions, learning rules and transfer functions, combined with one and two hidden layers and a variety of processing neurons in each layer, it was found that the architecture with general regression learning rule, was the most accurate.

3.3.6 Analysis Of Soil Water Retention Data Using Artificial Neural Networks

Several approaches for estimating hydraulic properties have been developed over the last three decades (e.g. Husz, 1967; Gupta & Larson, 1979; Vereecken et al., 1989). Tietje & Tapkenhinrichs (1993) reviewed and tested the quality of 13 different pedotransfer functions (PTFs). One of their conclusions was that PTFs which predicted shape parameters such as the Van Genuchten parameters (Van Genuchten, 1980) were inaccurate. All these studies use regression techniques, either linear or non-linear.

When using regression to predict the water retention characteristics, the relations between textural data and hydraulic characteristics need to be described by well-defined, a priori, regression models, which in general is difficult since these models are not known. Neural networks (NNs) do not need such an a priori model. A neural

network is an adaptable non-linear data transfer structure that can learn the relations between input and output data while being insensitive to measurement noise (Hecht-Nielsen, 1990).

Pachepsky et al. (1996) used NNs to estimate points of the water retention curve using textural data from 200 samples and compared the results with the outcomes of regression. Although the differences were not always significant, NNs performed slightly better than regression. Schaap & Bouten (1996) used a neural network to predict Van Genuchten's shape parameters for wetting and drying branches of the water retention curve of sandy forest soils in the Netherlands. However, in none of these studies were the effects of soil structure (i.e. ped-size and shape) considered. The effects of soil structure on the hydraulic characteristics become more important at small suctions, as has been explained by Durner (1994) in his study on the effect of bi-modal pore size distributions on the retentivity and conductivity curve, and by Booltink et al. (1993) who quantified the role of soil structure on water flow in aggregated clay soils.

The first objective of this research is to illustrate the method of neural network modeling by the development and evaluation of PTFs, emphasizing the combined effects of soil textural and structural data (based on available soil data from the Netherlands and Scotland). The second objective is to compare the performance of the NNs with the previously developed regression-based PTFs, as described by Gupta & Larson (1979).

It has been seen that classical statistical regression techniques require an a priori assumption on the model type (e.g. linear, exponential or logarithmic) and that the residuals are independent and identically distributed, whereas neural networks do not. The avoidance of these a priori assumptions and the organizational structure of strongly interconnected nodes make neural networks valuable when non-linear relations have to be described, or when data of different types, quantitative as well as qualitative, have to be included in the analysis. This study illustrates the procedure for predicting points of the water retention curve by the inclusion of soil texture and soil structure data.

Neural network models performed somewhat better than previously developed regression-type transfer functions, although differences were not significant. The neural network models were developed and tested for a limited number of soils.

3.3.7 Neural Network Based Prediction of Ground Surface Settlements due to Tunneling

In this research , a neural network based procedure to predict ground surface settlement during tunneling has been proposed. Incorporating a Gaussian normal distribution function the settlement profiles collected from various tunnel sites (Seoul subway) are analyzed, leading to two representative parameters. These parameters are then stored in a database with background tunnel information for training a neural network. It has been found that the use of both parameters representing monitored raw profile leads to more efficiency in storing as well as in further applications of the database.

Monitored ground surface profiles for a total of '113' monitoring lines have been collected to train an optimal neural network chosen and a parametric study has been performed herein. It leads to a rational prediction based on past tunnel records using pattern recognition and the memorization capability of an ANN. The capabilities enable the neural network based prediction to be automatically improved as further information is accumulated, without any restriction.

In conclusion we can say that , this research has introduced artificial intelligence for prediction of ground surface settlement based on field data accumulated. However, it should be noted that the capabilities of such codes in making accurate predictions, is entirely dependent on the quality and the quantity of data used in training ANNs. If the data is deficient or training is inadequate, the proposed neural network based prediction should be treated with caution. Therefore, the collection and analysis of monitored data should be carefully carried out for guaranteed predictions.

3.3.8 Neural Network Modeling of water table depth fluctuations

Recent literature reviews reveal that ANN specifically the feed forward networks, have been successfully used for water resources variables modeling and prediction [Coulibaly et al., 1999; Maier and Dandy, 2000]. The differences of ANN-based modeling approach against the conventional methods are discussed in detail by many authors [Connor et al., 1994; Sarle, 1994; Weigend and Gershenfeld, 1994; Suykens

et al., 1996] and specifically in hydrological applications by French et al. [1992], Karunanithi et al. [1994], Hsu et al. [1995], Tokar and Markus [2000], and Coulibaly et al. [2000a]. Furthermore, Hornik et al. [1989] established that a three-layer feed forward ANN could be considered as a general nonlinear approximator. The major advantage of an ANN is its ability to represent underlying nonlinear dynamics of the system modeled without any a priori assumption regarding the processes involved. Recently, ANN have been successfully used for modeling complex time-varying patterns, such as low frequency climatic oscillations [Coulibaly et al., 2000b]. In the aquifer system modeling context, ANN approach has been first used to provide maps of conductivity or transmissivity values [Rizzo and Dougherty, 1994; Ranjithan et al., 1995] and to predict water retention curves of sandy soils [Schaap and Bouten, 1996]. Recently, ANN's have been applied to perform inverse groundwater modeling for estimation of different parameters [Morshed and Kaluarachchi, 1998; Lebron et al., 1999]. The purpose of this paper is to identify ANN models that can capture the complex dynamics of large water table fluctuations, even with relatively short length of training (or calibration) data. We specifically focus on temporal neural networks, such as the input delay (IDNN) and the recurrent neural network (RNN) that have different dynamically driven properties.

This study has shown that temporal and probabilistic neural networks are effective at predicting monthly groundwater level fluctuations in the Gondo aquifer located in the Sahel region. A significant advantage of these models is that they can provide satisfactory predictions with short groundwater level records, which are a common occurrence in countries with scarce instrumentation for groundwater monitoring. The prediction results suggest that the RNN can be an effective tool for up to a 3 month ahead forecast of the dry season deep water table depths.

3.4 General Applications in Geotechnical Engineering

The engineering properties of soil and rock exhibit varied and uncertain behaviour due to the complex and imprecise physical processes associated with the formation of these materials (Jaksa 1995). This is in contrast to most other civil engineering materials, such as steel, concrete and timber, which exhibit far greater homogeneity and isotropy. In order to cope with the complexity of geotechnical behaviour, and the spatial variability of these materials, traditional forms of engineering design models

are justifiably simplified. An alternative approach, which has been shown to have some degree of success, is based on the data alone to determine the structure and parameters of the model. The ANN is well suited to model complex problems where the relationship between the model variables is unknown (Hubick 1992).

3.4.1 Pile Capacity

The prediction of the load capacity, particularly those based on pile driving data, has been examined by several ANN researchers. Goh (1994a; 1995b) presented a neural network to predict the friction capacity of piles in clays. The neural network was trained with field data of actual case records. The model inputs were considered to be the pile length, the pile diameter, the mean effective stress and the undrained shear strength. The skin friction resistance was the only model output. The results obtained by utilising the neural network were compared with the results obtained by the method of Semple and Rigden (1986) and the $\hat{\alpha}$ method (Burland 1973).

Goh (1995a; 1996b), soon after, developed another neural network to estimate the ultimate load capacity of driven piles in cohesionless soils. In this study, the data used were derived from the results of actual load tests on timber, precast concrete and steel piles driven into sandy soils. The inputs to the ANN model that were found to be more significant were the hammer weight, the hammer drop, the pile length, the pile weight, the pile cross sectional area, the pile set, the pile modulus of elasticity and the hammer type. The model output was the pile load capacity. When the model was examined with the testing set, it was observed that the neural network successfully modeled the pile load capacity. By examining the connection weights, it was observed that the more important input factors are the pile set, the hammer weight and the hammer type. The study compared the results obtained by the neural networks with the following common relationships: the Engineering News formula (Wellington 1892), the Hiley formula (Hiley 1922) and the Janbu formula (Janbu 1953). Regression analysis was carried out to obtain the coefficients of correlation of predicted versus measured results for neural networks and the traditional methods. Table 3.1 summaries the regression analysis results which indicate that the neural network predictions of the load capacity of driven piles were found to be better than these obtained using the other methods.

Table 3.1 : Summary of regression analysis results of pile capacity prediction
(Goh , 1995)

Method	Coefficient of correlation	
	Training data	Testing data
Neural network	0,96	0,97
Engineering news	0,69	0,61
Hiley	0,48	0,76
Janbu	0,82	0,89

3.4.2 Settlement of Foundations

The design of foundations is generally controlled by the criteria of bearing capacity and settlement; the latter often governing. The problem of estimating the settlement of foundations is very complex, uncertain and not yet entirely understood. This fact encouraged researchers to apply the ANN technique to settlement prediction. Goh (1994) developed a neural network for the prediction of settlement of a vertically loaded pile foundation in a homogeneous soil stratum. The input variables for the proposed neural network consisted of the ratio of the elastic modulus of the pile to the shear modulus of the soil, pile length, pile load, shear modulus of the soil, Poisson's ratio of the soil and radius of the pile. The output variable was the pile settlement. The desired output that was used for the ANN model training was obtained by means of finite element and integral equation analyses developed by Randolph and Wroth (1978).

A comparison of the theoretical and predicted settlements for the training and testing sets is given in Figure 13. The results in Figure 3.13 show that the neural network was able to successfully model the settlement of pile foundations.

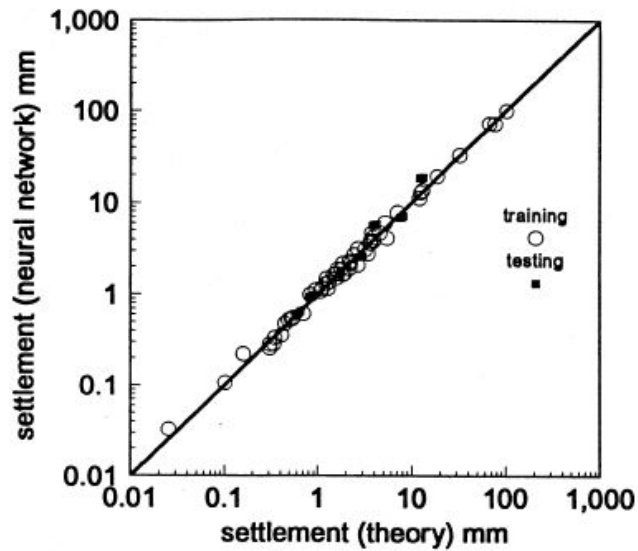


Figure 3.13 : Comparison Of Theoretical Settlement And Neural network Prediction (Goh , 1994)

Also , Sivakugan et al. (1998) explored the possibility of using neural networks to predict the settlement of shallow foundations on granular soils. A neural network was trained with five inputs representing the net applied pressure, average blow count from the standard penetration test, width of foundation, shape of foundation and depth of foundation. The output was the settlement of the foundation. The results obtained by the neural network were compared with methods proposed by Terzaghi and Peck (1967) and Schmertmann (1970). Based on the results obtained, it was shown that the traditional method of Terzaghi and Peck and Schmertmann's method overestimate the settlements by about 2.18 times and 3.39 times respectively as shown in Figure 3.14. In contrast, the predictions using the ANN model were good (Figure 3.15).

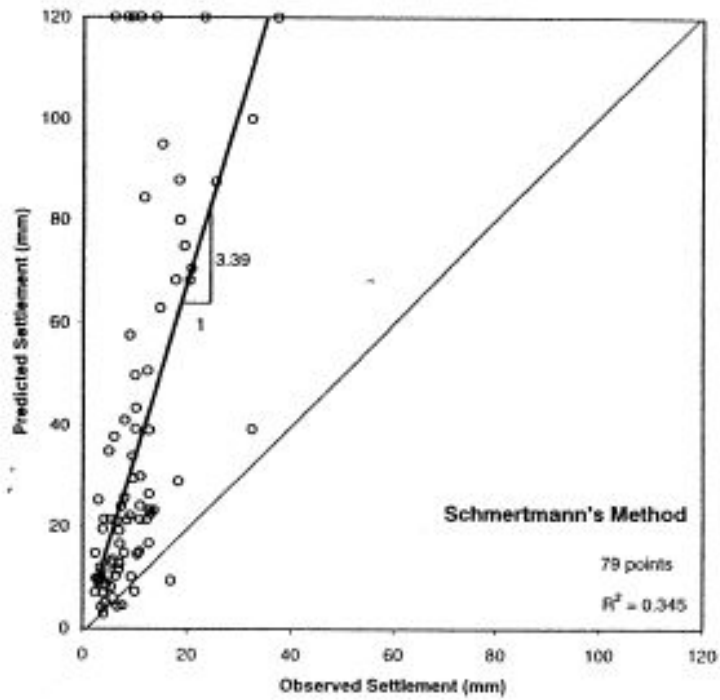


Figure 3.14 : Settlement Predicted using Traditional methods
(Sivakugan et al.1998)

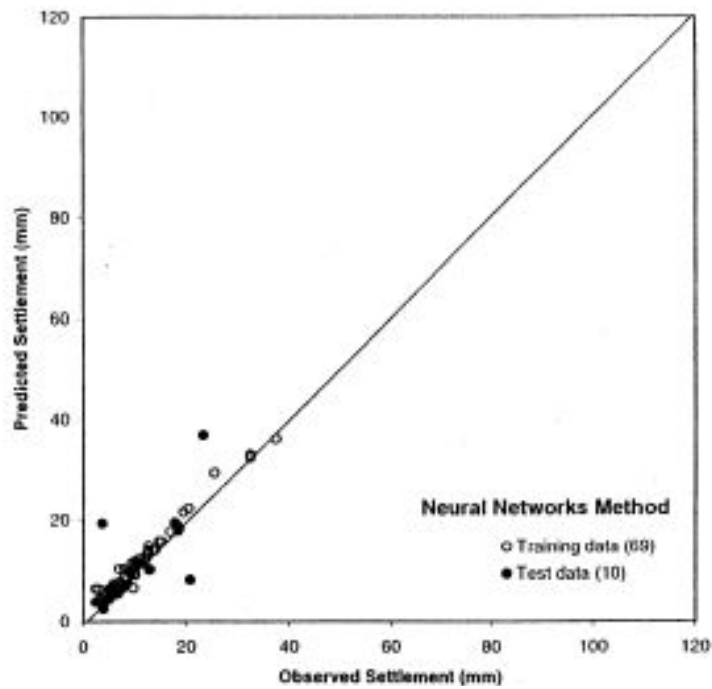


Figure 3.15 : Settlement Prediction Using Artificial Neural Network
(Sivakugan et al.1998)

Most recently, Shahin et al. (2000) carried out similar work for predicting the settlement of shallow foundations on cohesionless soils. In this work, 272 data

records were used for modeling. The input variables considered to have the most significant impact on settlement prediction were the footing width, the footing length, the applied pressure of the footing and the soil compressibility. The results of the ANN were compared with three of the most commonly used traditional methods. These methods were Meyerhof (1965), Schultze and Sherif (1973) and Schmertmann et al. (1978). The results of the study confirmed those found by Sivakugan et al. (1998), in the sense that ANNs were able to predict the settlement well and outperform the traditional methods. As shown in Table 3.2, the ANN produced high coefficients of correlation, r , low root mean squared errors (RMSE) and low mean absolute errors, (MAE) compared with the other methods.

Table 3.2 : Comparison of predicted vs measured settlements (Shahin et al. 2000)

Category	ANN	Meyerhof (1965)	Schultze & Sherif (1973)	Schmertmann et al. (1978)
Correlation , r	0,99	0,33	0,86	0,70
RMSE (mm.)	3,9	27,0	23,8	45,2
MAE (mm.)	2,6	20,8	11,1	29,5

3.4.3 Soil Properties and Behaviour

Soil properties and behaviour is an area that has attracted many researchers to modeling using ANNs. Developing engineering correlations between various soil parameters is an issue discussed by Goh (1995a; 1995c). Goh used neural networks to model the correlation between the relative density and the cone resistance from cone penetration test (CPT), for both normally consolidated and over-consolidated sands. Laboratory data, based on calibration chamber tests, were used to successfully train and test the neural network model. The neural network model used the relative density and the mean effective stress of soils as inputs and the CPT cone resistance as a single output. The ANN model was found to give high coefficients of correlation of 0.97 and 0.91 for the training and testing data, respectively, which indicated that the neural network was successful in modeling the non-linear relationship between the CPT cone resistance and the other parameters.

Ellis et al. (1995) developed an ANN model for sands based on grain size distribution and stress history. Sidarta and Ghaboussi (1998) employed an ANN model within a finite element analysis to extract the geomaterial constitutive behaviour from non-uniform material tests. Penumadu and Jean-Lou (1997) used NNs for representing the behaviour of sand and clay soils. Ghaboussi and Sidarta (1998) used NNs to model both the drained and undrained behaviour of sandy soil subjected to triaxial compression-type testing. Penumadu and Zhao (1999) also used ANNs to model the stress-strain and volume change behaviour of sand and gravel under drained triaxial compression test conditions. Zhu et al. (1998a; 1998b) used neural networks for modeling the shearing behaviour of a fine-grained residual soil, dune sand and Hawaiian volcanic soil. Cal (1995) used a neural network model to generate a quantitative soil classification from three main factors (plastic index, liquid limit and clay content). Najjar et al. (1996a) showed that neural network-based models can be used to accurately assess soil swelling, and that neural network models can provide significant improvements in prediction accuracy over statistical models. Romero and Pamukcu (1996) showed that neural networks are able to effectively characterize and estimate the shear modulus of granular materials. Agrawal et al. (1994); Gribb and Gribb (1994) and Najjar and Basheer (1996b) all used neural network approaches for estimating the permeability of clay liners. Basheer and Najjar (1995) and Najjar et al. (1996b) presented neural network approaches for soil compaction.

Other applications include modeling the mechanical behaviour of medium-to-fine sand (Ellis et al. 1992), modeling rate-dependent behaviour of clay soils (Penumadu et al. (1994), simulating the uniaxial stress-strain constitutive behaviour of fine-grained soils under both monotonic and cyclic loading (Basheer 1998; Basheer and Najjar 1998), characterizing the undrained stress-strain response of Nevada sand subjected to both triaxial compression and extension stress paths (Najjar and Ali 1999; Najjar et al. 1999), predicting the axial and volumetric stress-strain behaviour of sand during loading, unloading and reloading (Zhu and Zaman 1997), predicting the anisotropic stiffness of granular materials from standard repeated load triaxial tests (Tutumluer and Seyhan 1998).

3.4.4 Liquefaction

Liquefaction is a phenomenon which occurs mainly in loose and saturated sands as a result of earthquakes. It causes the soil to lose its shear strength due to an increase in pore water pressure, often resulting in large amounts of damage to most civil engineering structures. Determination of liquefaction potential due to earthquakes is a complex geotechnical engineering problem. Goh (1994b) used neural networks to model the complex relationship between seismic and soil parameters in order to investigate liquefaction potential. The neural network used in this work was trained using case records from 13 earthquakes that occurred in Japan, United States and Pan-America during the period 1891–1980. The study used eight input variables and only one output variable. The input variables were the SPT-value, the fines content, the mean grain size, the total stress, the effective stress, the equivalent dynamic shear stress, the earthquake magnitude and the maximum horizontal acceleration at ground surface. The output was assigned a binary value of 1, for sites with extensive or moderate liquefaction, and a value of 0 for marginal or no liquefaction. The results obtained by the neural network model were compared with the method of Seed et al. (1985). The study showed that the neural network gave correct predictions in 95% of cases, whereas Seed et al. (1985) gave a success rate of 84%. Goh (1996a) also used neural networks to assess liquefaction potential from cone penetration test (CPT) resistance data. The data records were taken for sites of sand and silty sand deposits in Japan, China, United States and Romania, representing five earthquakes that occurred during the period 1964–1983. A similar neural network modeling strategy, as used in Goh (1994b), was used for this study and the results were compared with the method of Shibata and Teparaksa (1988). The neural network showed a 94% success rate, which is equivalent to the same number of error predictions as the conventional method by Shibata and Teparaksa (1988).

Two other works (Najjar and Ali 1998; Ural and Saka 1998) also used CPT data to evaluate soil liquefaction potential and resistance. Najjar and Ali (1998) used neural networks to characterize the soil liquefaction resistance utilizing field data sets representing various earthquake sites from around the world. The ANN model that was developed in this work was generated to produce a liquefaction potential assessment chart that could be used by geotechnical engineers in liquefaction assessment tasks. Ural and Saka (1998) used neural networks to analyze liquefaction.

Comparison between this approach and a simplified liquefaction procedure indicated a similar rate of success for the neural network approach as the conventional approach.

Other applications of ANNs for liquefaction prediction include the prediction of liquefaction resistance and potential (Juang and Chen 1999), investigation of the accuracy of liquefaction prediction of ANNs compared with fuzzy logic and statistical approaches (Ali and Najjar 1998) and assessment of liquefaction potential using standard penetration test results (Agrawal et al. 1997).

3.4.5 Site Characterization

Site characterization is an area concerned with the analysis and interpretation of geotechnical site investigation data. Zhou and Wu (1994) used a neural network model to characterize the spatial distribution of rockhead elevations. The data used to train the model were taken from seismic refraction surveys on more than 11 km of transverse lines. The network used the spatial position (x- and y-coordinate) and the surface elevation as inputs, and was used to estimate the rockhead elevation at that location as the output. The trained network was tested to estimate the rockhead elevations for all locations within the area of investigation by producing a contour map. Results from the neural network model compared well with similar contour maps, with the additional benefit that neural networks do not make assumptions or simplify spatial variations.

A similar application relevant to ground water characterization was described by Basheer et al. (1996). Basheer et al. (1996) indicated that neural networks can be used to map and logically predict the variation of soil permeability in order to identify landfill boundaries and construct a waste landfill. Rizzo et al. (1996) presented a new site characterization method called SCANN (Site Characterization using Artificial Neural Networks) that is based on the use of neural networks to map discrete spatially-distributed fields.

3.4.6 Earth Retaining Structures

Goh et al. (1995) developed a neural network model to provide initial estimates of maximum wall deflections for braced excavations in soft clay. The neural network was used to synthesis data derived from finite element studies on braced excavations in clay. The input parameters used in the model were the excavation width, soil

thickness/excavation width ratio, wall stiffness, height of excavation, soil undrained shear strength, undrained soil modulus/shear strength ratio and soil unit weight. The maximum wall deflection was the only output. Using regression analysis, the scatter of the predicted neural network deflections relative to the deflections obtained using the finite element method were assessed. The results produced high coefficients of correlation for the training and testing data of 0.984 and 0.967, respectively. Some additional testing data from actual case records were also used to confirm the performance of the trained neural network model. The study intended to use the neural network model as a time-saving and user-friendly alternative to the finite element method.

3.4.7 Tunnels and Underground Openings

Shi et al. (1998) presented a study of neural networks for predicting settlements of tunnels. A general NN model was trained and tested using data from the 6.5 km Brasilia Tunnel, Brazil. The study identified many factors to be used as the model inputs and three settlement parameters as the model outputs. The input parameters were the length of excavation from drive start, the depth of soil cover above tunnel crown, the area of tunnel section, the delay for closing invert, the water level depth, the rate of advance of excavation, the construction method, the mean blow count from standard penetration test at tunnel crown level, the tunnel spring-line level and the tunnel inverted arch level. The three output parameters were the settlement at the face passage, the settlement at the invert closing and the final settlement after stabilization. The results showed that the NN model could not achieve a high level of accuracy. To improve the prediction accuracy, the study proposed a modular NN model based on the concept of integrating multiple neural network modules in one system, with each module being constrained to operate at one specific situation of a complicated real world problem. The modular concept showed an improvement in terms of model convergence and prediction. The capability to improve the models developed in this work was later extended by Shi (2000) by applying input data transformation. This extended study indicated that distribution transformation of the input variables reduced the prediction error by more than 13%.

4. NEURAL NETWORK APPROACHES FOR SLOPE STABILITY

4.1 Introduction

In this chapter, application of neural networks for slope stability is discussed. There are 5 models introduced for neural network approaches. Model 1 and 2 are Back-Propagation Neural Network (BPNN) approaches, and model 3, 4, 5 are General Regression Neural Network (GRNN) approaches. Data and case studies are given for Neural Network (NN). Factor of safety and seismic coefficients will be examined by NN approaches which are the BPNN and GRNN approaches. Values are obtained from a doctorate thesis (Cao , 2002). These values will be used in NN approaches. Neural Network parameters and case study are given in section 4.2.

4.2 Input Parameters Information

In this study, there are nine data parameter important for factor of safety, that are presented for NN approaches. All data parameters are given below.

- 1 - H (m.) : The height of slope,
- 2- H_w (m.) : The height of water level,
- 3- H_b (m.) : The distance of firm base,
- 4- γ (kN/m^3) : The unit weight of soil,
- 5- β (deg.) : The inclination of slope,
- 6- c (kPa.) : The cohesion of soil,
- 7- ϕ (deg.) : The friction angle of soil,
- 8- k_h : Horizontal seismic coefficient ,
- 9- k_v : Vertical seismic coefficient,
- 10- F.S. : Factor of Safety (with Bishop's method)

There were 170 data patterns for Neural Network approaches (Given in Appendix A) and the input – output values range for Neural Network is given below in Figure 4.1. To see the common effects of parameters the slope profile has taken only one soil layer and its parameters.

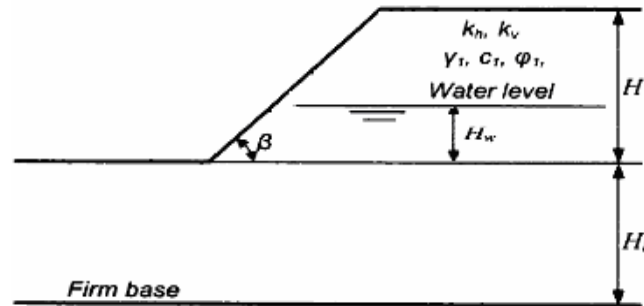


Figure 4.1 : Basic Slope Profile and Slope Parameters

First of all we have to define the output and input parameters in the program , then we define the values range. So the program will use min, max, mean values while the program is learning the model. This input and output values range table is given below in Table 4.1.

Table 4.1 : Input and output values range for Neural Network

Parameters	The height of slope	The height of water level	The depth of firm base	The inclination of slope	The unit weight of soil
Variable Name	H (m.)	Hw (m.)	Hb (m.)	β (deg.)	γ (kN/m³)
Variable Type	I	I	I	I	I
Min	3,65	0,0	0,00	11	9,00
Max	214,00	45,0	164,00	71	28,44
Mean	23,95	2,0	6,00	29	19,08
Std. Deviation	30,10	6,2	22,90	10	2,69
Parameters	The cohesion of soil	The friction angle of soil	Horizontal seismic coefficient	Vertical seismic coefficient	Factor of Safety
Variable Name	c (kPa)	Φ (deg.)	kh	kv	F.S.
Variable Type	I	I	I	I	A
Min	0,0	0,000	0,035	0,050	0,620
Max	150,0	45,0	0,510	0,250	2,150
Mean	15,3	23,1	0,273	0,146	1,190
Std. Deviation	20,0	9,5	0,138	0,071	0,335

I is input value and A is actual output value in Table 4.1. We define which parameters are input and output so these parameters used in the model as we defined.

4.3 Analysis

Analysis results are presented in output tables, error through pattern graphics. r^2 , defined in Neuroshell2, is a statistical indicator usually applied to multiple regression analysis. It compares the accuracy of the model to the accuracy of a trivial benchmark model, and the prediction is just the mean of all of the samples. A perfect fit would result in an r squared value of 1, a very good fit near 1, and a very poor fit near 0. The formula that Neuroshell2 uses is defined as the following:

$$r^2 = 1 - \frac{SSE}{SS_{YY}} \quad \text{Where} \quad (4.1)$$

$$SSE = \sum (y - \hat{y})^2 \quad (4.2)$$

$$SS_{YY} = \sum (y - \bar{y})^2 \quad (4.3)$$

Where y is the actual value, \hat{y} is the predicted value of y, and \bar{y} is the mean of the y values.

4.3.1 BPNN approaches

4.3.1.1 Model 1

In Table 4.2, training calibration for model 1 is given. Architecture is 3 hidden slabs, and different activation functions used in this model. Activation function is linear function. Pattern selection is rotational, not random from 145 pattern processed for training.

Table 4.2 : Model 1 approach for training

Architecture	3 hidden slabs , different activation function
% Test Set Extraction	15
# of Hidden Layer	2
# of Neurons In One Hidden Layer	18
Learning Rate	0,2
Momentum Factor	0,6
Initial weight	0,3

Calibration Interval	400
Scale Function	Linear [-1,1]
Missing Values	Error Condition
Pattern Selection	Rotation
Pattern Processed	170

As it is seen from Table 4.3 the most important parameter is the height of slope but after the height parameter the seismic coefficients are coming. So for model 1 the earthquake effect on slope can be seen.

Table 4.3 : The contribution factors for Model 1

Parameters	The Contribution Function	Orders of The Contribution Function
H (m.)	0,27667	1
kh	0,10485	2
kv	0,10008	3
Hw (m.)	0,09826	4
Hb (m.)	0,09587	5
γ (kN/m³)	0,08857	6
β (deg.)	0,08404	7
c (kPa)	0,07862	8
Φ (deg.)	0,07305	9

After we made approximately 100 model approaches we get the results from Model 1 analysis. From these results as we can see from Table 4.4 our success rate is % 79,31 and the correlation coefficient is 0,8912.

Table 4.4 : The results of Model 1

R squared:	0,7931
r squared:	0,7943
Mean squared error:	0,023
Mean absolute error:	0,109
Min. absolute error:	0
Max. absolute error:	0,667
Correlation coefficient r:	0,8912

r^2 value is best fit correlation coefficient from Excel and same value from that Neuroshell2 's r^2 . This show that the process which has been performed is correct.

The black line is best fit line and green lines are 20% error limits is taken from bestfit line. In Figure 4.1, 20% error limit means that when the difference the target output the network result is greater than 20% green lines, the network is considered as an incorrectsimulation (Bayrak, 2004). According to this assumption, if the error graphs of each mode is considered and this best network gives 10 incorrect simulations, out of 170 data set for model 1. The error percentage 5.88 % which correspond to a success percentage is 94.12 % for this simulation shown in Figure 4.2.

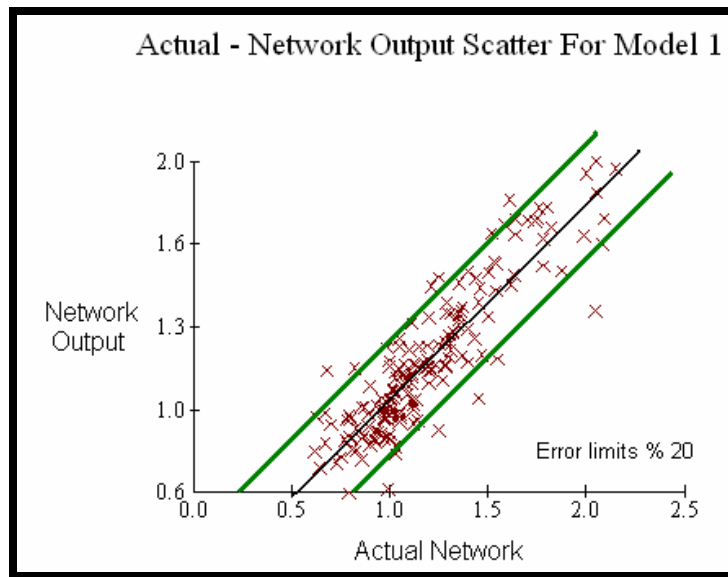


Figure 4.2 : Actual – Network output scatter for Model 1 and error limits

There are 24 incorrect simulations this means simulation success percentages 85 % according to Figure 4.3.

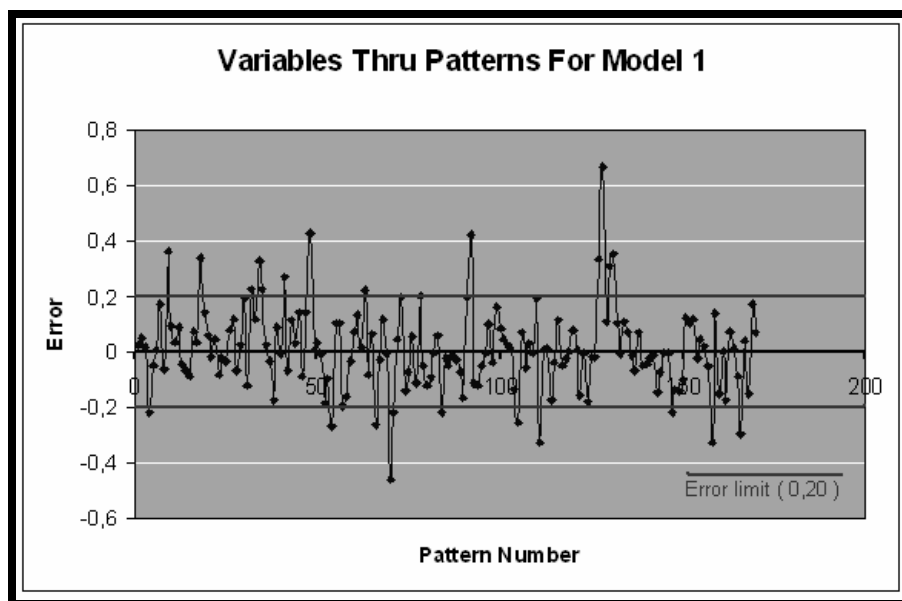


Figure 4.3 : Variables error through pattern and error limits for model 1

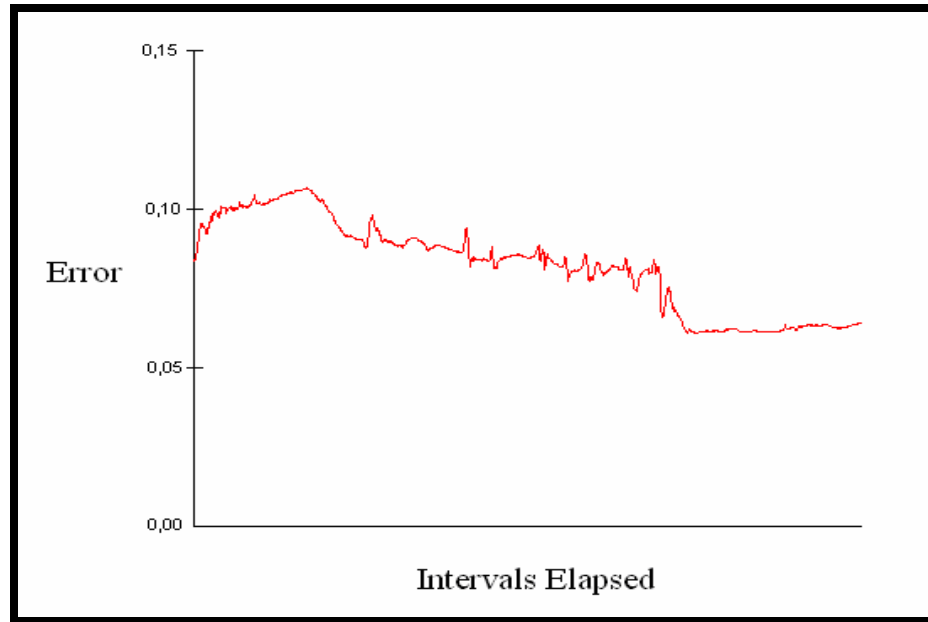


Figure 4.4 : Test set error graph for Model 1

There are not so many big peaks and graph is decreased also after 0.05 graph is generally constant in Figure 4.4, this means that over-learning did not occur.

A piece of model 1 outputs are given below in table 4.5 and all of the datas are given in Appendix B. In Table 4.5 the Actual (1) is the factor of safety values that we define , the network (1) is the simulation results of factor of safety and Act-Net (1) is the difference between Actual (1) – Network (1). We can see how the model success by looking Act-net (1) values then we can accept it successful.

Table 4.5 : A pieces of Model 1 output table

Actual(1)	Network(1)	Act-Net(1)
1,3200	1,2958	0,0242
0,9400	0,8895	0,0505
0,9700	0,9517	0,0183
1,6100	1,8270	-0,2170
1,6400	1,6866	-0,0466
1,3500	1,3435	0,0065
1,2700	1,0988	0,1712
1,0600	1,1224	-0,0624
1,5500	1,1839	0,3661
1,4000	1,3054	0,0946
1,1800	1,1452	0,0348
1,3100	1,2206	0,0894
0,7500	0,7897	-0,0397
0,8000	0,8660	-0,0660
0,7700	0,8582	-0,0882

This model has % 80 success percentage but Back Propagation Neural Network is not an appropriate method for evaluation of Slope Stability and the Seismic coefficients effects.

4.3.1.2 Model 2

There are certain differences between Model 2 from Model 1. Pattern extraction is same 15% in Model 2 but momentum factor is 0.7 and calibration interval is 600 in Model 2. These training model approach differences are given in Table 4.6.

Table 4.6 : Model 2 approach for training

Architecture	3 hidden slabs , different activation function
% Test Set Extraction	15
# of Hidden Layer	2
# of Neurons In One Hidden Layer	18
Learning Rate	0,2
Momentum Factor	0,7
Initial weight	0,3
Calibration Interval	600
Scale Function	Linear << -1,1 >>
Missing Values	Error Condition
Pattern Selection	Rotation
Pattern Processed	170

As it is seen from Table 4.7 the most important parameter is the height of slope but after the height parameter the seismic coefficients are coming. So like model 1 in this model 2 the earthquake effect on slope can be seen.

Table 4.7 : The contribution factors for Model 2

Parameters	The Contribution Function	Orders of The Cont.Func.
H (m.)	0,27258	1
kh	0,10545	2
kv	0,10157	3
Hw (m.)	0,09792	4
Hb (m.)	0,09673	5
γ (kN/m ³)	0,08959	6
β (deg.)	0,08754	7
c (kPa)	0,07771	8
Φ (deg.)	0,07091	9

After we made approximately 100 model approaches we get the results from Model 2. From these results as we can see from Table 4.8 our success rate is % 80,30 and the correlation coefficient is 0,8974 .

Table 4.8 : The results of Model

R squared:	0,8030
r squared:	0,8053
Mean squared error:	0,022
Mean absolute error:	0,106
Min. absolute error:	0,002
Max. absolute error:	0,594
Correlation coefficient r:	0,8974

There are 20 incorrect simulations in Figure 4.5, and the simulation success percentage is 88 %.

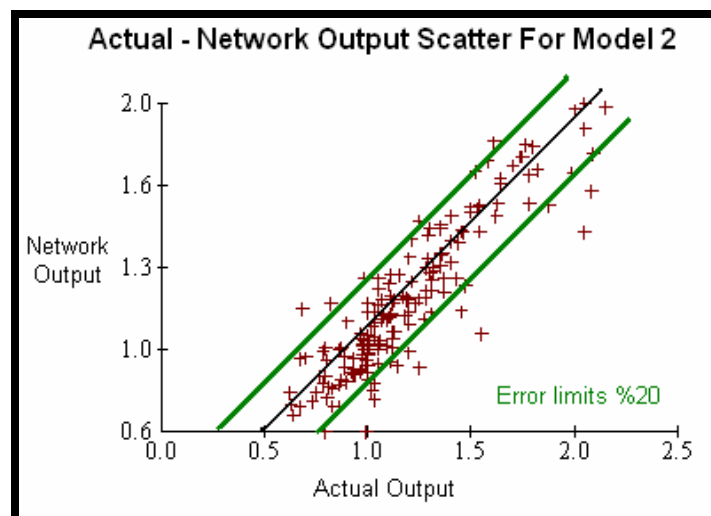


Figure 4.5 : Actual-Network output scatter for Model 2 and error limits

There are 25 incorrect simulations this means simulation success percentages 85 % according to Figure 4.6.

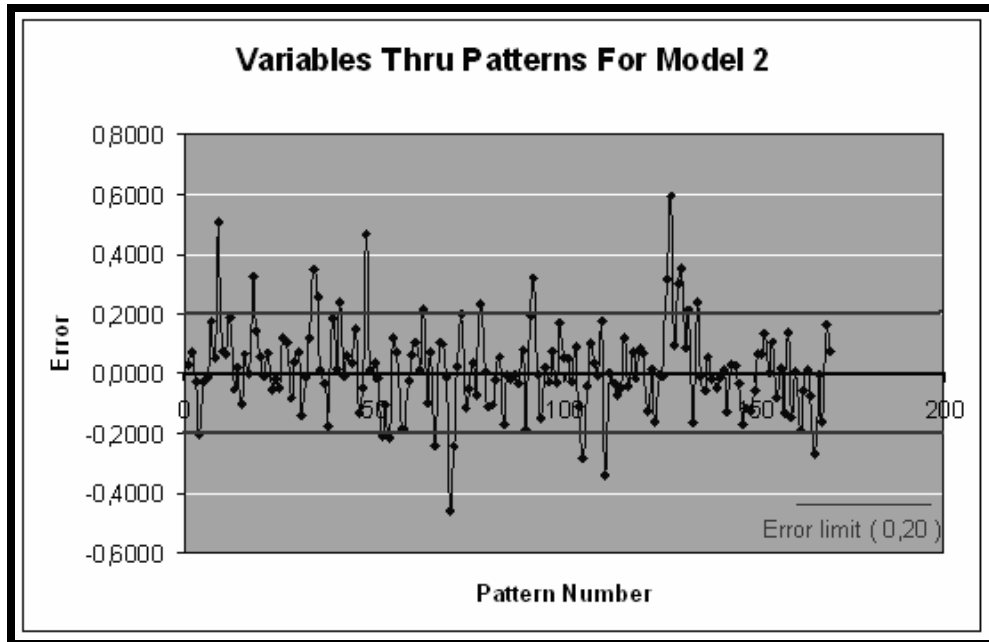


Figure 4.6 : Variables error through pattern and error limits for model 2

As it is seen from Figure 4.7 over-learning occurred with local peaks but generally graph is decreased after the local peaks. This model has the challenge same model 1.

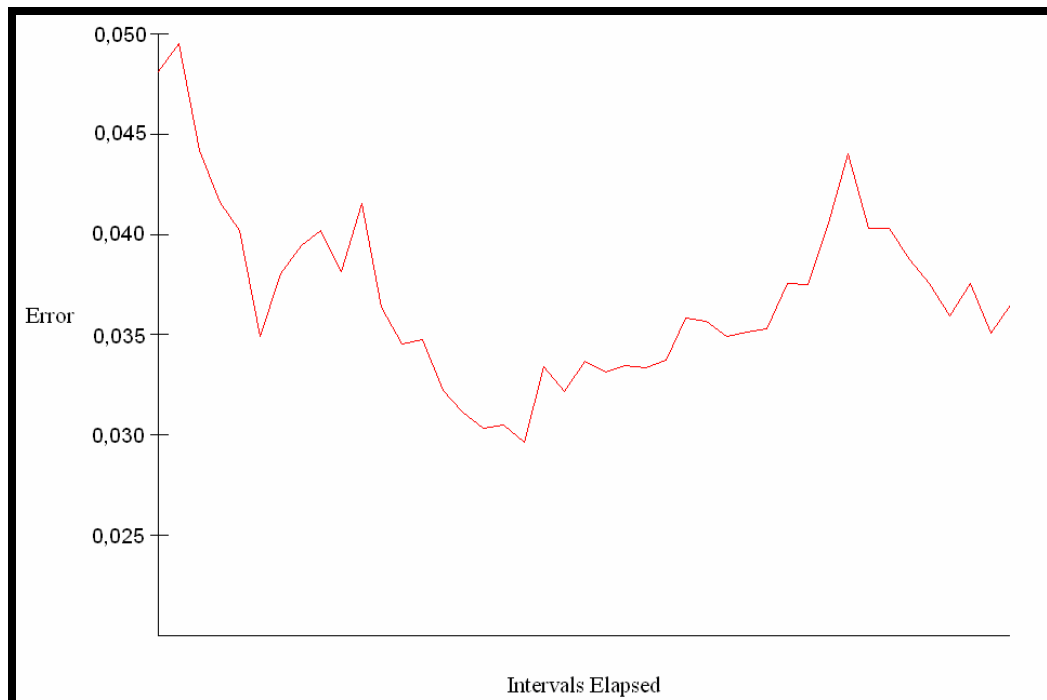


Figure 4.7 : Test set error graph for Model 2

4.3.2 GRNN approaches

4.3.2.1 Model 3

In Table 4.9, the GRNN architecture properties are shown for Model 3. The GRNN method differs from BPNN methods by the existence of smoothing factors. On the other hand, there are no learning rate, momentum factor, and initial weights in the GRNN method. Extraction for training is 20%. There are 136 patterns for training and 34 patterns for test patterns. Genetic breeding pool size can be taken values 20, 50, 75, 100, 200, 300 respectively for Neuroshell2. In this model genetic pool size is taken 200. Missing values is taken error conditions. It should be noted that smoothing factor is taken values in a range from 0 to 1 ($0 < \text{smoothing factor} < 1$).

Table 4.9 : The architecture and the configuration of the Model

Smoothing Factor	0,01821
Activation Function	linear [0,1]
Distance Metric	City Block
Calibraiton	Genetic , Adaptive
Missing Values	Error condition
Genetic Breeding Pool Size	200
% Test Set Extraction	20
Number of Inputs	9
Number of Outputs	1
Number of Training Patterns	136
Number of Test Pattern	34
Pattern Processed	170

All the network parameters and the smoothing factors defined by program and given in Table 4.10. As it is seen from Table 4.10 the most important parameter is the unit weight of soil but after the unit weight of soil parameter the height and the water level come. The seismic coefficients are coming after these parameters. So in model 3 the earthquake effect can be seen after these 3 parameters.

Table 4.10 : Individual smoothing factors for Model 3

Network type:	GRNN, genetic adaptive	
Problem name:	C:\NSHELL2\GRNN-1\GRNN-1	
Number of inputs:	9	
Number of outputs:	1	
Number of training patterns:	136	
Number of test patterns:	34	
current best smoothing factor:	0,0721176	
smoothing test generations:	85	
last mean squared error:	0,028048	
minimum mean squared error:	0,027964	
generations since min. ms. error:	20	
Input name	Individual smoothing factor	Orders
γ (kN/m ³)	3,0000	1
H (m.)	1,9412	2
Hw (m.)	1,2000	3
kh	0,7177	4
Hb (m.)	0,6118	5
kv	0,3059	6
c (kPa)	0,1059	7
Φ (deg.)	0,0235	8
β (deg.)	0,0118	9

After we made approximately 216 model approaches we get the results from Model 3. From these results as we can see from Table 4.11 our success rate is % 90,29 and the correlation coefficient is 0,9505 .

Table 4.11 : The results of Model 3

R squared:	0,9029
r squared:	0,9034
Mean squared error:	0,011
Mean absolute error:	0,038
Min. absolute error:	0
Max. absolute error:	0,510
Correlation coefficient r:	0,9505

There are 10 incorrect simulations in Figure 4.8 and the simulation success percentage is 94.11 %.

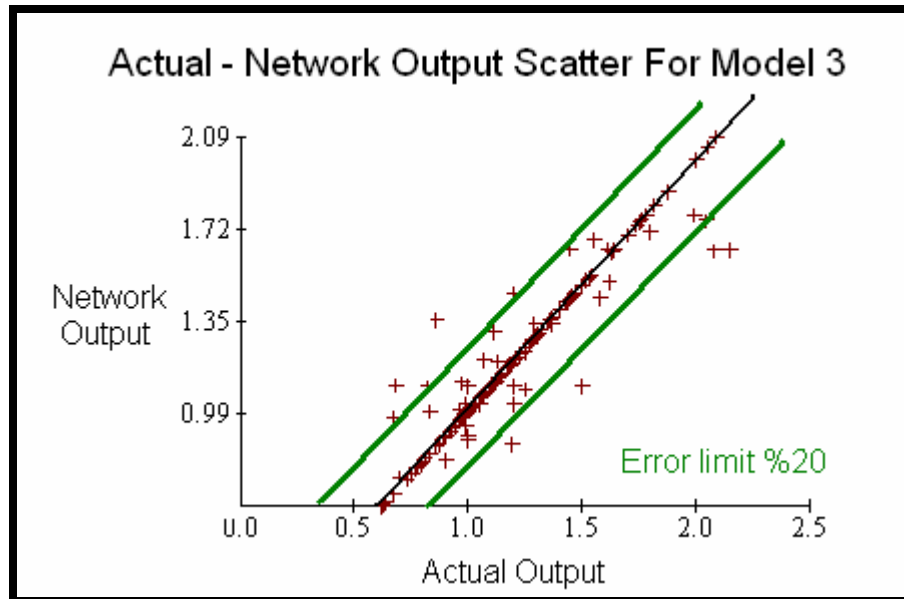


Figure 4.8 : Actual-Network output scatter for model 3 and error limits

There are 10 incorrect simulations in Figure 4.9, and the simulation success percentage is 94.11%.

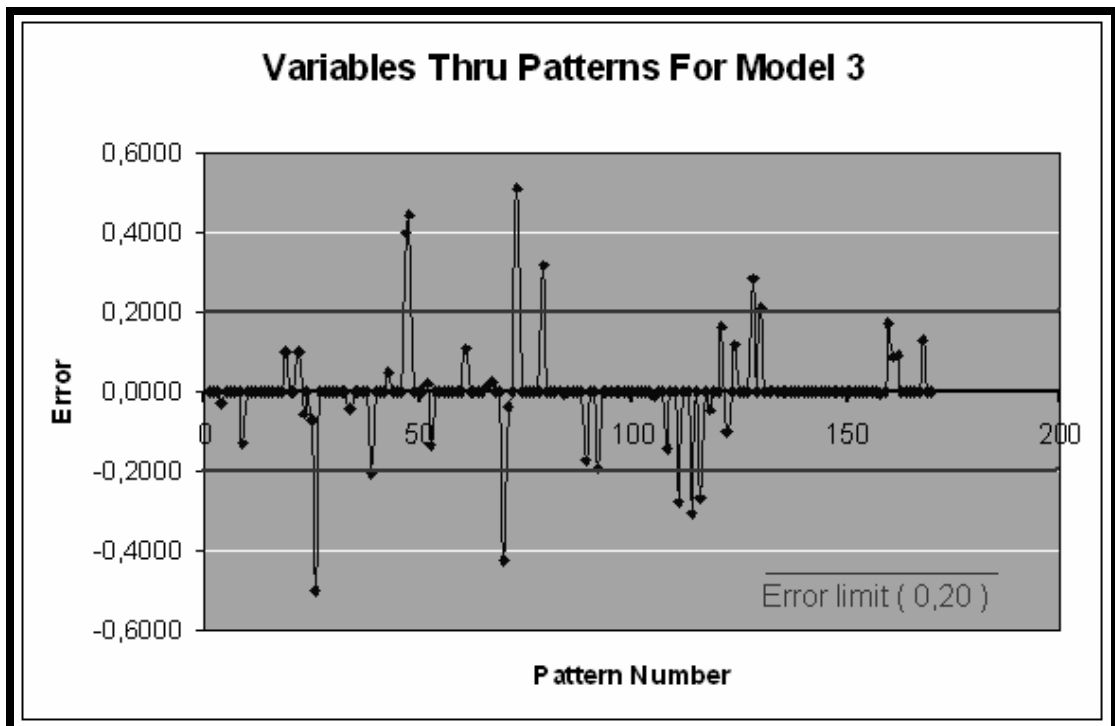


Figure 4.9 : Variables error through pattern and error limits for model 3

As it is seen from Figure 4.10 over-learning did not occur and the error gradually decreases.



Figure 4.10 : Test set error graph for model 3

4.3.2.2 Model 4

In model 4, activation function , distance metric and genetic breeding pool size are different from model 3 architecture. Genetic breeding pool size is 50, distance metric is vanilla and activation function is tanh. All the factors for Model 4 is given in Table 4.12.

Table 4.12 : The architecture and the configuration of the Model 4

Smoothing Factor	0,2196471
Activation Function	tanh
Distance Metric	Vanilla
Calibraiton	Genetic , Adaptive
Missing Values	Average Values
Genetic Breeding Pool Size	50
% Test Set Extraction	15
Number of Inputs	9
Number of Outputs	1
Number of Training Patterns	145
Number of Test Pattern	25
Pattern Processed	170

All the network parameters and the smoothing factors defined by program and given in Table 4.13. As it is seen from Table 4.13 the most important parameter is the cohesion of soil but after the cohesion of soil parameter the inclination of slope come. The seismic coefficients are coming after these parameters. So in model 4 the earthquake effect can be seen after these 4 parameters. If we compare model 4 between other models the seismic coefficient effect in model 4 is less than others.

Table 4.13 : Individual smoothing factors for Model 4

Network type:	GRNN, genetic adaptive	
Problem name:	C:\NSHELL2\GRNN-2\GRNN-2	
Number of inputs:	9	
Number of outputs:	1	
Number of training patterns:	145	
Number of test patterns:	25	
current best smoothing factor:	0,2196471	
smoothing test generations:	66	
last mean squared error:	0,021763	
minimum mean squared error:	0,021742	
generations since min. ms. error:	20	
Input name	Individual smoothing factor	Orders
c (kPa)	3,00000	1
β (deg.)	2,02353	2
Φ (deg.)	1,57647	3
Hb (m.)	1,41176	4
kh	1,23529	5
kv	0,78824	6
H (m.)	0,50588	7
Hw (m.)	0,30588	8
γ (kN/m³)	0,03529	9

After making approximately 216 model approaches we get the results from Model 4. From these results as we can see from Table 4.14 our success rate is % 91,37 and the correlation coefficient is 0,9570.

Table 4.14 : The results of the Model 4

R squared:	0,9137
r squared:	0,9158
Mean squared error:	0,010
Mean absolute error:	0,040
Min. absolute error:	0
Max. absolute error:	0,510
Correlation coefficient r:	0,9570

There are 9 incorrect simulation in Figure 4.11, and the success simulation percentage is 94.70%.

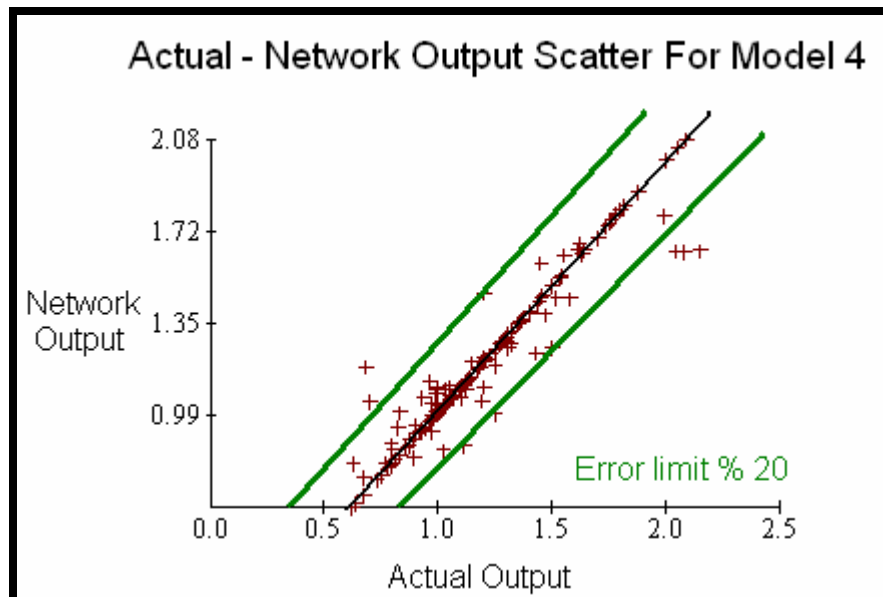


Figure 4.11 : Actual-Network output scatter for model 4 and error limits

There are 10 incorrect simulations in Figure 4.12, and the success simulation percentage is 94.11%.

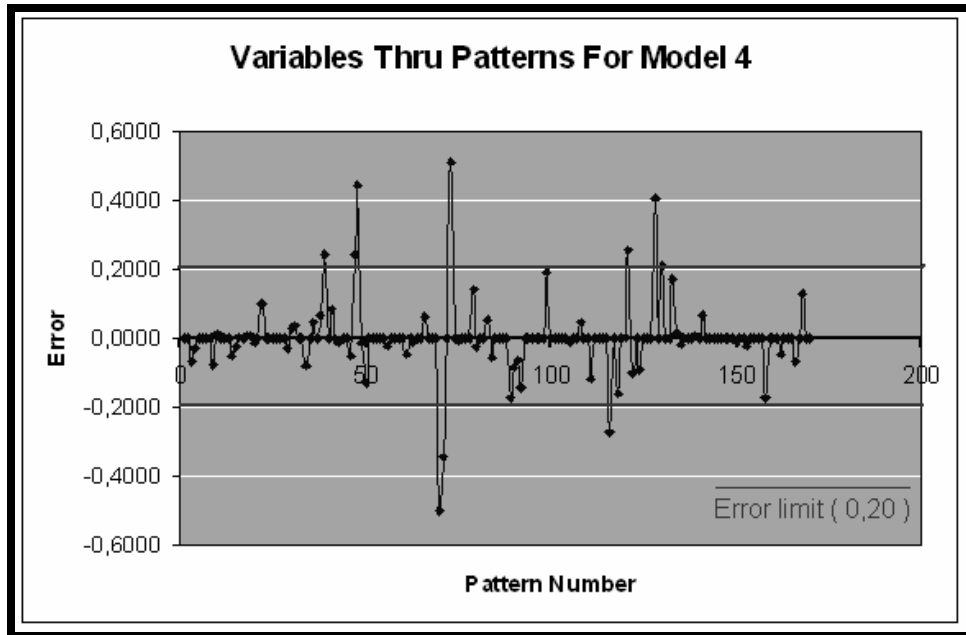


Figure 4.12 : Variables error through pattern and error limits for Model 4

As it is seen from Figure 4.13 over-learning did not occur. Graph is close to 0,025 that means error is very little.

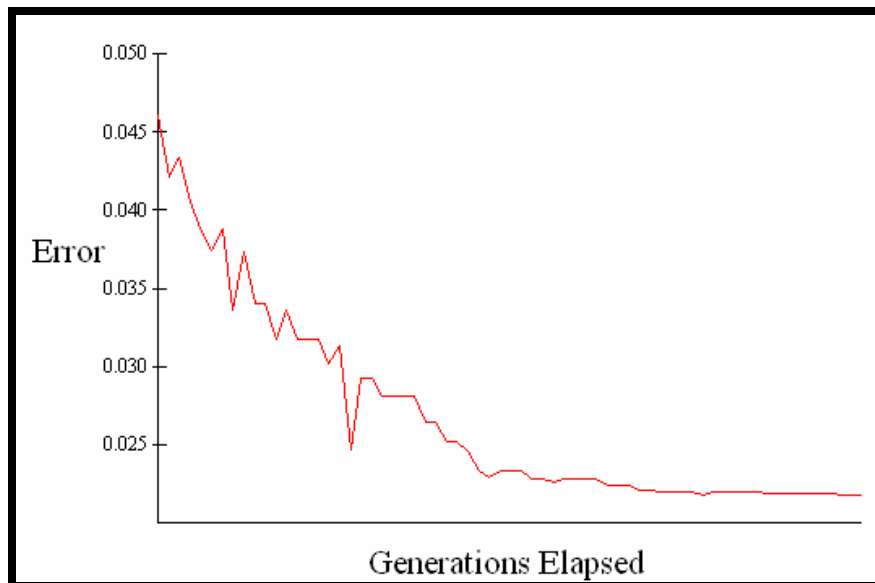


Figure 4.13 : Test set error graph for model 4

4.3.2.3 Model 5

Model 4 activation function is also different from Model 3 and Model 4 activation function. This model's activation function is linear [-1,1]. Model 5 have the same extraction at 20% like Model 4. Number of training patterns are 145 patterns and number of test patterns are 25 patterns like Model 4. Genetic breeding pool size is 100 in Table 4.15.

Table 4.15 : The architecture and the configuration of the Model 5

Smoothing Factor	0,11201
Activation Function	Linear [-1,1]
Distance Metric	Vanilla
Calibraiton	Genetic , Adaptive
Missing Values	Error Condition
Genetic Breeding Pool Size	100
% Test Set Extraction	15
Number of Inputs	9
Number of Outputs	1
Number of Training Patterns	145
Number of Test Pattern	25
Pattern Processed	170

All the network parameters and the smoothing factors for Model 5 defined by program and given in Table 4.16. As it is seen from Table 4.16 the most important parameter is the cohesion of soil but after the cohesion of soil parameter, the inclination of slope come. The seismic coefficients are coming after these parameters. So in model 5 the earthquake effect can be seen after these 4 parameters. If we compare model 5 between other models the seismic coefficient effect in model 5 is less than others.

Table 4.16 : Individual Smoothing Factors for Model 5

Network type:	GRNN, genetic adaptive
Problem name:	C:\NSHELL2\GRNN-3\GRNN-3
Number of inputs:	9
Number of outputs:	1
Number of training patterns:	145
Number of test patterns:	25
current best smoothing factor:	0,1458824
smoothing test generations:	58
last mean squared error:	0,020391
minimum mean squared error:	0,020346
generations since min. ms. error:	20

Input name	Individual smoothing factor	Orders
c (kPa)	2,97647	1
β (deg.)	2,14118	2
Hb (m.)	1,61176	3
Φ (deg.)	0,90588	4
kh	0,72941	5
H (m.)	0,71765	6
kv	0,49412	7
γ (kN/m3)	0,45882	8
Hw (m.)	0,36471	9

After making approximately 216 model approaches we get the results from Model 5. From these results as we can see from Table 4.17 our success rate is % 92,25 and the correlation coefficient is 0,9618 .

Table 4.17 : The results of the Model 5

R squared:	0,9225
r squared:	0,9250
Mean squared error:	0,009
Mean absolute error:	0,036
Min. absolute error:	0
Max. absolute error:	0,510
Correlation coefficient r:	0,9618

There are 6 incorrect simulation. Simulation success percentage is 96.47% as depicted in Figure 4.14.

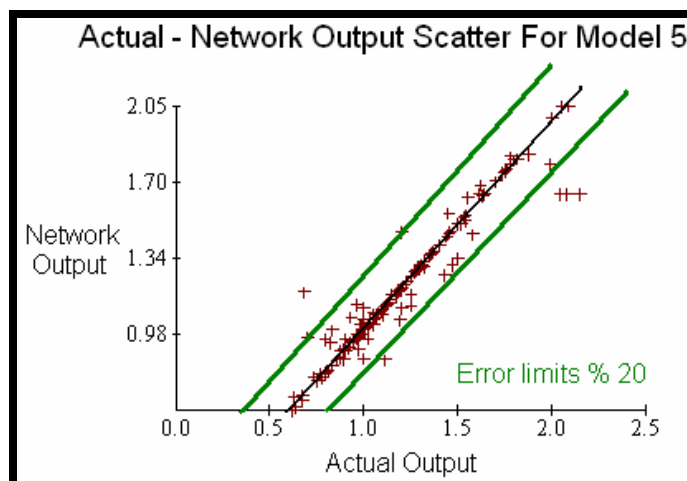


Figure 4.14 : Actual-Network output scatter for Model 5 and error limits

There are 8 incorrect simulations in Figure 4.15, and the success simulation percentage is 95,29 %.

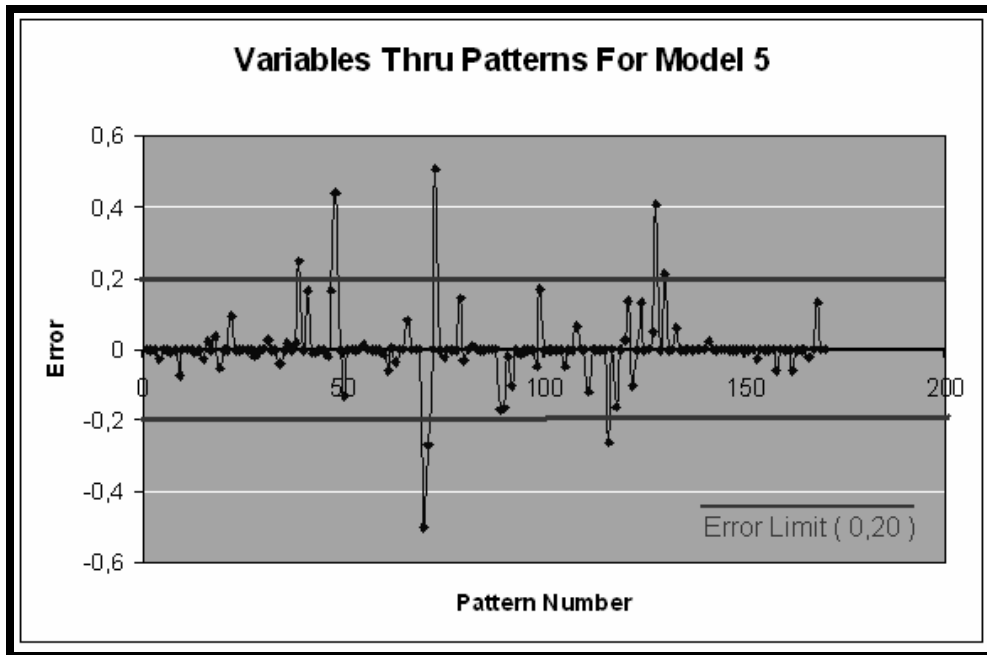


Figure 4.15 : Variables error through pattern and error limits for Model 5

As it is seen from Figure 4.16 over-learning did not occur and graph is close to 0,015 that means error is very little.

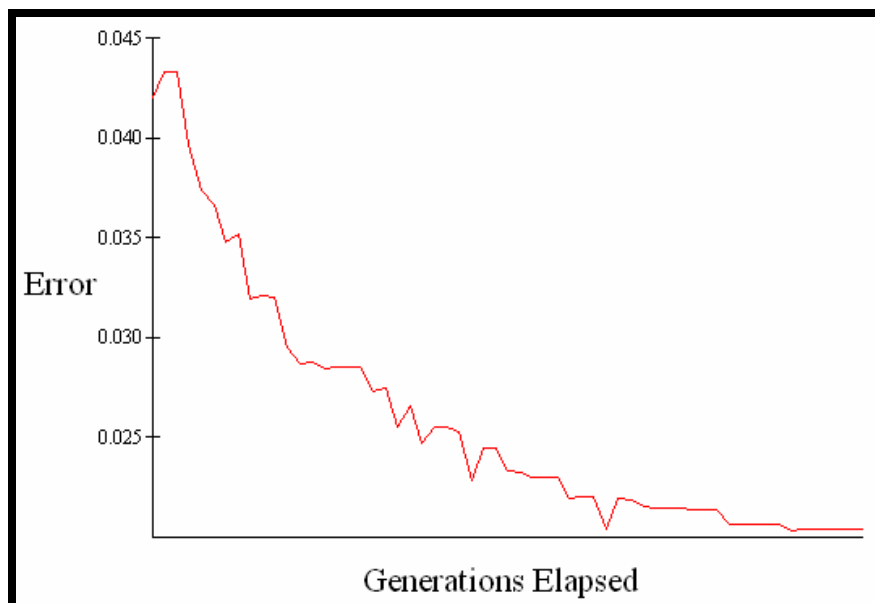


Figure 4.16 : Test set error graph for model 5

5. RESULTS

To reach the best results, different configurations and architectures are trained. In chapter 4, the best configurations, architectures, and error graphs for BPNN and GRNN approaches are presented. In this chapter, all models results are evaluated. Model 1 and Model 2 approach architectures are given in Table 5.1.

Table 5.1 : Model 1 and Model 2 approach configurations and architecture

	MODEL 1	MODEL 2
Architecture	3 hidden slabs , different activation function	3 hidden slabs , different activation function
% Test Set Extraction	15	15
# of Hidden Layer	2	2
# of Neurons In One Hidden Layer	18	18
Learning Rate	0	0,2
Momentum Factor	0,6	0,7
Initial weight	0	0,3
Calibration Interval	400	600
Scale Function	Linear [-1,1]	Linear << -1,1 >>
Missing Values	Error Condition	Error Condition
Pattern Selection	Rotation	Rotation
Pattern Processed	170	170

There are not a different extraction percentage for each other for training. Model's extraction percentage is 15%. Momentum factors are differ from each other. 0.6, 0.7 are momentum factors for model 1 and model 2, respectively. In Addition, there is a different calibration interval for Model 1 and Model 2 in Table 5.1.As in Table 5.2, Model 2 results are better compared to Model 1. If we look at the success rate of Model 1 and Model 2 in Table 5.2, we can say that there are not too much difference.

Table 5.2 : Output R^2 values for Model 1 and 2

	R squared:	r squared:
Model 1	0,7931	0,7943
Model 2	0,803	0,8053

The Model 1 calibration interval is 400, and error graph is quite good, however Model 2 calibration interval is 600 and error graph is not acceptable. In Model 2, there are several local over-learning points. In summary, increasing calibration interval could lead to over-learning situations for BPNN approaches. This can be seen from Figure 5.1 and 5.2.

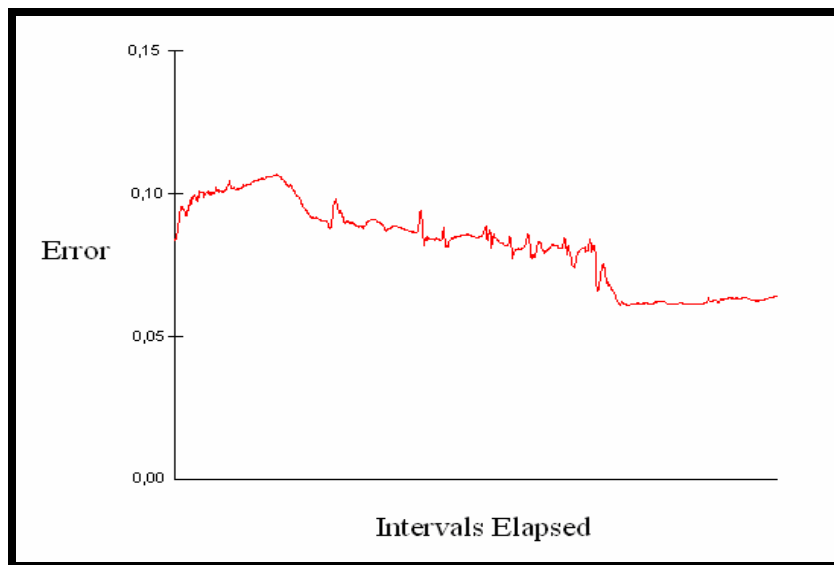


Figure 5.1 : Test set error graph for Model 1

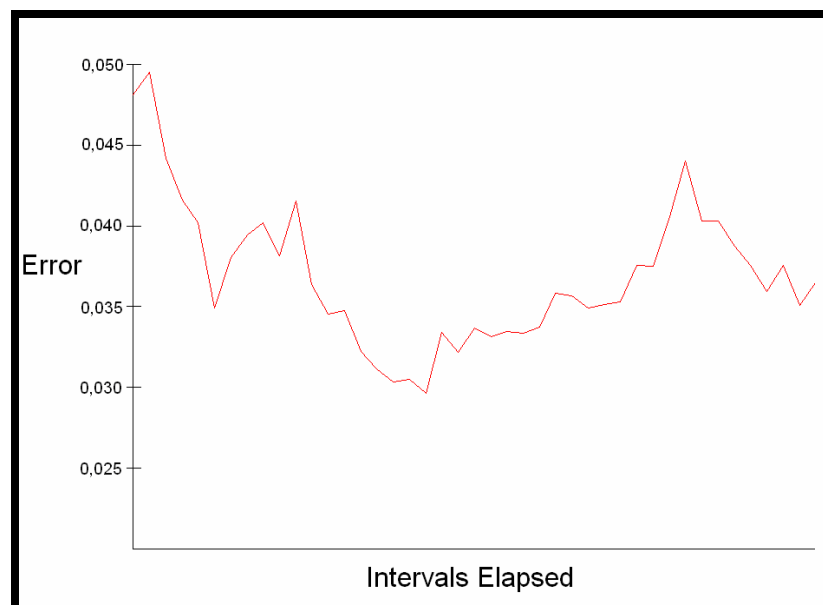


Figure 5.2 : Test set error graph for Model 2

As seen in Table 5.3, the first five of contribution factors of Model 1 and Model 2 are the same parameters in output. This shows that results are generally meaningful for evaluation of contribution factors for BPNN approaches.

Table 5.3 : The first five contribution factors for Model 1 and Model 2

Order	Model 1	Model 2
1	H (m.)	H m.)
2	kh	kh
3	kv	kv
4	Hw (m.)	Hw (m.)
5	Hb (m.)	Hb (m.)

In this GRNN approaches, all models results are evaluated. Model 3, Model 4 and Model 5 approach architectures are given in Table 5.4.

Table 5.4 : The architecture and the configuration of Models 3, 4 and 5

	MODEL 3	MODEL 4	MODEL 5
Smoothing Factor	0,01821	0,2196471	0,11201
Activation Function	linear [0,1]	tanh	Linear [-1,1]
Distance Metric	City Block	Vanilla	Vanilla
Calibraton	Genetic , Adaptive	Genetic , Adaptive	Genetic , Adaptive
Missing Values	Error condition	Average Values	Error Condition
Genetic Breeding Pool Size	200	50	100
% Test Set Extraction	20	15	15
Number of Inputs	9	9	9
Number of Outputs	1	1	1
Number of Training Patterns	136	145	145
Number of Test Pattern	34	25	25
Pattern Processed	170	170	170

If we look at the success rate of Model 3 , Model 4 and Model 5 in Table 5.5, we can say that Model 5 is the best approach for slope stability.

Table 5.5 : Output R² values for Model 3, 4, and 5

	R squared:	r squared:
Model 3	0,9029	0,9034
Model 4	0,9137	0,9158
Model 5	0,9225	0,9250

The activation function “ Linear [-1,1] ” gives better results compared to “Linear [0 , 1]” for the GRNN models in Table 5.5. In Model 3 and Model 5 all configuration parameters are the same, except activation function and genetic breeding pool size. For GRNN approaches, when activation function changes and genetic breeding pool size decreases, success ratio gets better as seen in Table 5.5. The architecture and the configuration of the Model 3, 4 and 5 are given in Table 5.4. As seen in Table 5.6, the first five parameters are generally same in Model 3 and 5, however they have different activation functions.

Table 5.6 : The first five of sensitivity factors for Models 3, 4, and 5

Order	Model 3	Model 4	Model 5
1	β (deg.)	c (kPa)	c (kPa)
2	H (m.)	β (deg.)	β (deg.)
3	Hw (m.)	Φ (deg.)	H (m.)
4	kh	H (m.)	Φ (deg.)
5	Hb (m.)	kh	kh

Results are meaningful for individual smoothing parameters. But model 3 gives different parameters from other models because of its genetic breeding pool size is larger than other models. (Figure 5.3, Figure 5.4 and Figure 5.5)

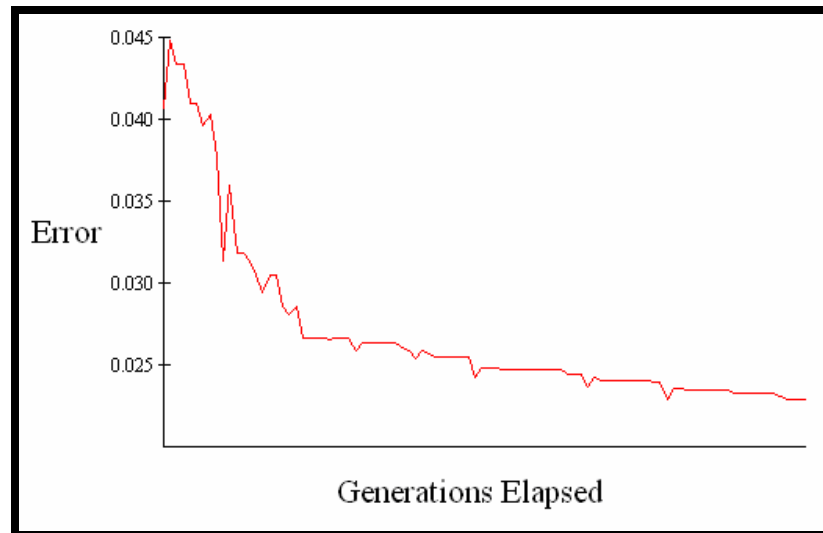


Figure 5.3 : Test set error graph for model 3

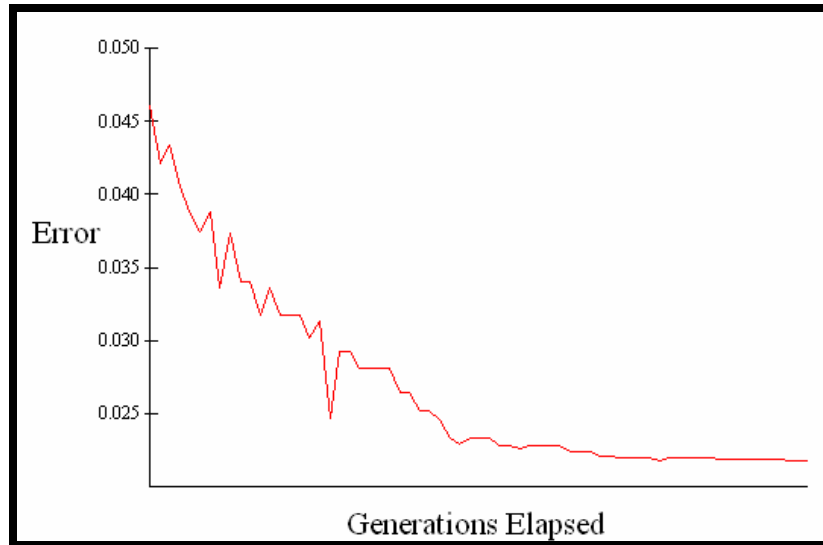


Figure 5.4 : Test set error graph for model 4

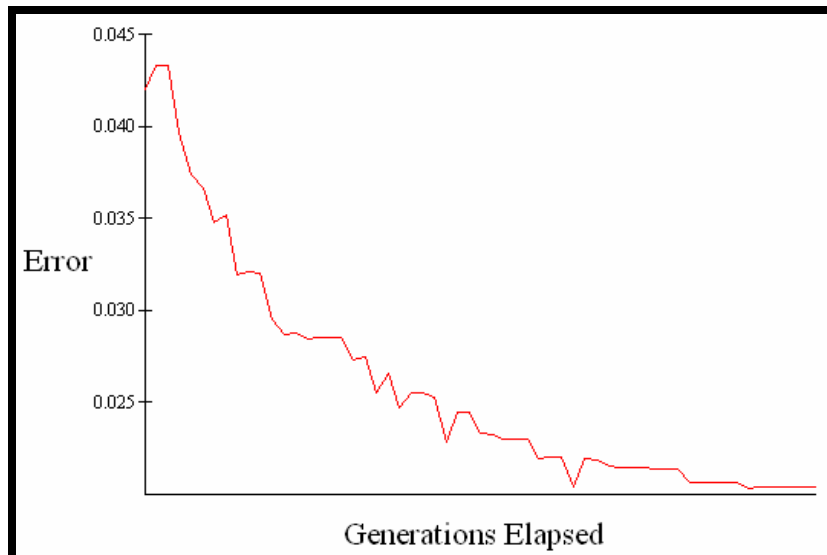


Figure 5.5 : Test set error graph for Model 5

From model 3 through model 5, test set error decreases. The best model number 5 has the smallest test set error value. This shows that test set improves with different calibrations. The smallest values are approximately 0.25 for model 3, 0.015 for model 4, 0.01 for model 5. On the contrary like this comparison is not made for BPNN. All the simulation success rates are given in Table 5.7.

Table 5.7 : Simulation success rates for each model

BPNN	Model 1 (R squared)	0,7943
	Model 1 (Number of incorrect simulations)	24
	Model 1 (Simulation success rate %)	85,88
BPNN	Model 2 (R squared)	0,8053
	Model 2 (Number of incorrect simulations)	20
	Model 2 (Simulation success rate %)	88,24
GRNN	Model 3 (R squared)	0,9034
	Model 3 (Number of incorrect simulations)	10
	Model 3 (Simulation success rate %)	94,11
GRNN	Model 4 (R squared)	0,9158
	Model 4 (Number of incorrect simulations)	10
	Model 4 (Simulation success rate %)	94,11
GRNN	Model 5 (R squared)	0,9250
	Model 5 (Number of incorrect simulations)	6
	Model 5 (Simulation success rate %)	96,47

Model 1 and 2 are Back-Propagation Neural Network (BPNN) approaches, and model 3, 4, 5 are General Regression Neural Network (GRNN) approaches and in Model 2 sometimes over learning patterns happen but this is not seen in Model 3, 4, and 5 for GRNN approaches.

Neural network is generally used in Hydrology branch of civil engineering disciplines and in Geotechnical discipline etc. which is given in Chapter 3. By the way of this study Geotechnical, Earthquake Engineering work with together. Because this study is slope stability by using seismic coefficients data and concerns with these disciplines. Earthquake, and soil properties are used with together in this study as input parameters. This study brings new view point to Earthquake Engineering, and Geotechnical Engineering.

In this study , the aim is to find the parameters effects and which parameter is the important factor for slope stability. Because of finding the seismic coefficients effects importance for earthquake and geotechnical engineering, this study have done.

In conclusion, from this study it has seen that seismic coefficients effects are important in slope stability but not a determining parameter for evaluation of slope stability and the effects of seismic coefficient. We can say that the slope height and the water level are more important. For evaluation of slope stability and the effects of seismic coefficient GRNN is very good and suitable approach. Model 5 have the best success rate but model 3 have the best contribution factors because of model 4 and model 5 parameters are chosen from clay soil. As a result for Model 4 and 5 cohesion (c) is in the first order of contribution factor. On the contrary, BPNN is not suitable approaches for this study. In future, forecasting can be done by using these models. For example, there are 9 input parameters in this study, and using these 9 parameters factor of safety and seismic coefficient effects can be solved by the way of Neural Network. Therefore solving and forecasting engineering problems get easy for slope stability investigation.

REFERENCES

Agrawal , G. Chameau , J.L. & Baurdeau P.L. (1997) Assessing the liquefaction susceptibility at a site based on information from penetration testing , In: Artificial Neural Networks for applications , ASCE Monograph , Newyork , 185-214.

Bayrak, B., 2002. Liquefaction Potential: A neural network approach. *Senior Thesis*, I.T.U. Civil Engineering Faculty, Istanbul.

Bayrak, B., 2004. Strong Ground Motion Attenuation Relationship Model by Using Neural Network Methodology, *M.S.c Thesis*, I.T.U. Institute of Science and Technology, Istanbul

Cao Jinggang (2002), Neural Network and Analytical Modeling of Slope Stability , Doctorate Thesis, Oklahoma University , Oklahoma

Chen Z. and Shao C. (1988) , Evaluation of minimum factor of safety in slope stability analysis. *Can. Geotech. J.* , 20(1). 104-119

Chen, Y.H., and Tsai, C.C.P., 2002. A new method for estimation of the attenuation relationship with variance components, *Bulletin of the Seismological Society of America*, Vol.92, No.5. 1984-1991 (13).

Das., B.M., 1993. “ Principles of Soil Dynamics” Thomson Learning Academic Resource Center. ISBN 0-534-93129-4

Duncan, M.,(1969) , Soil slope stability analysis, Landslides Investigation and Mitigation, Transportation Research Board Special Report 247, pp. 337–371.

Efe, Ö., Kaynak O., 2000. “Yapay Sınır Ağları ve Uygulamaları”, Bogazici Üniversitesi

Ellis, G. W., Yao, C., Zhao, R., and Penumadu, D., 1995, Stress-strain modelling of sands using artificial neural networks, *J. of Geotech. Eng.* 121(5), 429–435.

Fellenius Y. (1927) , Erdstatische berechnungen mit reibung und kohaesion. Ernst. Berlin (in English)

Feng, X., 1991, A neural network approach to comprehensive classification of rock stability, blastability and drillability, *Int. J. Surface Mining, Reclamation and Environment* 9, 57–62.

Frederick, M.D., 1996. Neuroshell2 user’s manual version 3.0. Ward Systems Group

- Goh A.T.C.**, (1996) “Neural Network modeling of CPT seismic liquefaction data, Journal of Geotechnical and Geoenvironmental Engineering Division, 122, No.1, 70-73.
- Goh, A.T.C.** (1994). “Empirical design in geotechnics using Neural Networks.” *Geotechnique*, 45(4), 709-714.
- Goh, A.T.C.**, (1995) “Seismic liquefaction potential assessed by Neural Networks. Journal of Geotechnical and Geoenvironmental Engineering Division, ASCE, 120 (9), 1467- 1480.
- Goh, A.T.C., and Chua, C.G.**, 2003. “A hybrid Bayesian back-propagation neural network approach to multivariate modeling”, *Int. J. Numer. Anal. Meth. Geomech.*, 27: 000-000.
- Goh, A.T.C., and Chua, C.G.**, 2003. “Quantifying uncertainty in predictions using a Bayesian neural network”, *GALAYAA B.V./MIT2_453:pp. 1-3*
- Goh, A.T.C., and Chua, C.G.**, 2004. “Nonlinear modeling with confidence estimation using Bayesian neural networks”, eJSE.
- Goh, A.T.C., and Chua, C.G.**, 2005. “Estimating wall deflections in deep excavations using Bayesian Neural Networks”, Tunneling and Underground Space Technology.
- Goh, A.T.C., Kulhawy, F.H., and Chua, C.G.**, 2005. “Bayesian Neural Network Analysis of Undrained Side Resistance of Drilled Shafts”, *Journal of Geotechnical and Geoenvironmental Engineering*, Vol. 131, No. 1,
- Hecht-Nielsen, R.** (1990). Neurocomputing, Addison-Wesely Publishing Company.
- Hecht-Nielson, R.:** 1990, Theory of the back-propagation neural network, in Proc. of Int. Joint Conf.on Neural Networks, Addison Wesley, New York, pp. I:595–611.
- Hubick, K. T.** (1992). Artificial neural networks in Australia, Department of Industry, Technology and Commerce, Commonwealth of Australia, Canberra.
- Jaksa, M. B.** (1995). “The influence of spatial variability on the geotechnical design properties of a stiff, overconsolidated clay,” PhD thesis, The University of Adelaide, Adelaide.
- Kramer, S.L.**, 1996. “Earthquake Geotechnical Engineering”, Prentice-Hall International Series in Civil Engineering Mechanics, New Jersey, USA
- Lin C. T. and Lee C. S. G.** (1996) . , Neural fuzzy systems – A neuro-fuzzy synergism to intelligent systems. , Prentice Hall Inc.
- Lowe J.** (1967) , Stability anlysis of embankments.J Soil Mech. And Found. Div. , ASCE , 93(4), 1-33

McCullock W. S. and Pitts W.H. (1943) , A Logical calculus at the ideas imminent in nervous activity. *Bull. Math. Biophy* 5:115-133

Mendel J. M. and R. W. McLaren (1970) , Reinforced learning control and pattern recognition system , In *adaptive learning and pattern recognition systems : Theory and applications* , New York Academic Press, pp.287-318

Morgensten N. (1963) , Stability charts for earth slopes during rapid drawdown. *Geotechnique*, V13. pp.121-131

Morgenstern N.R. and Price V.E. (1965) ,The analysis of the stability of general slip surface. *Geotechnique*. London 15(1),79-93

Mostyn G.R. and Small J.C. (1987) , Methods of stability analysis. *Soil slope instability and stabilization* , Walker & Fell (eds.) , Balkema , Rotterdam.

Özaydın, K., 1995. “Zemin Mekaniği (Soil Mechanics)” Yıldız Tek. Üni. İnşaat fak., İnşaat Müh. Blm. Geoteknik Anabilim Dalı, ISBN 975-511-145-X

Randolph, M. F., and Wroth, C. P. (1978). “Analysis of deformation of vertically loaded piles.” *J. Geotech. Engrg., ASCE*, 104(12), 1465-1488.

Schaap, M.G. & Bouten, W. 1996. Modeling water retention curves of sandy soils using neural networks. *Water Resources Research*, 32, 3033–3040.

Shahin, M. A., Jaksa, M. B., and Maier, H. R. (2000). “Predicting the settlement of shallow foundations on cohesionless soils using back-propagation neural networks.” *Research Report No. R 167*, The University of Adelaide, Adelaide.

Shi, J. J. (2000). “Reducing prediction error by transforming input data for neural networks.” *J. Computing in Civil Engrg., ASCE*, 14(2), 109-116.

Shibata, T., and Teparaksa, W. (1988). “Evaluation of liquefaction potentials of soils using cone penetration tests.” *Soils and Foundations*, 28(2), 49-60.

Sidarta, D. E., and Ghaboussi, J. (1998). “Constitutive modeling of geomaterials from non-uniform material tests.” *J. Computers & Geomechanics*, 22(10), 53-71.

Sivakugan, N., Eckersley, J. D., and Li, H. (1998). “Settlement predictions using neural networks.” *Australian Civil Engineering Transactions*, CE40, 49-52.

Skempton A.W. (1964) , Long-Term stability of clay slopes. *Gewotechnique*, 14. 77-102

Skempton A.W. and Hutchinson J.N. (1967) , Stability of natural slopes and embankment foundations. *Proc. 7th Int. Conf. Soil mech. And Found. Eng. Mexico City* , State of the Art Volume , pp.291 - 340

Specht D.F. (1996) "Fuzzy logic and Neural Network Handbook: Chapter 3- Probabilistic and General Regression Neural Networks" McGraw-Hill Companies, Inc., New York.

Specht, D.F., 1991. A generalized regression neural network, IEEE Transactions on Neural Network, 568-576.

Specht, D.F., 1996. Fuzzy Logic and Neural Network Handbook, Mc Graw-Hill Companies, Inc.,

Spencer E. (1969), Effect of tension on the stability of embankments. ASCE, Journal of the soil mech. And found. Division , V94 , pp.1159-1173

Spencer E. (1973) ,Thrust line criterion in embankment stability stability anlysis. Geotech.,V23 ,1, pp.85-100

Spencer, E., (1969), A method of analysis of the stability of embankments assuming parallel inter-slice forces, Geotechnique, 1711–26.

Tutumluer, E., and Seyhan, U. (1998). "Neural network modeling of anisotropic aggregate behavior from repeated load triaxial tests. " Transportation Research Record 1615, National Research Council, Washington, D.C.

Ural, D., and Saka, H., 1998. "Liquefaction Prediction by Neural Networks", Electronic Journal of Geotechnical Engineering, ISSN 1089-3032, Vol. 3, pp.1- 4.

Web Pages :

<http://www.ggsd.com> - Geotechnical & Geoenvironmental Software Directory

APPENDIXES

Appendix A. BPNN Approach Output Tables for Model 1

Appendix B. BPNN Approach Output Tables for Model 2

Appendix C. Error Through Patterns Graphs for Model 1 and 2.

Appendix D. GRNN Approach Output Tables for Model 3

Appendix E. GRNN Approach Output Tables for Model 4

Appendix F. GRNN Approach Output Tables for Model 5

Appendix G. Error Through Patterns Graphs for Model 3,4 and 5.

Appendix H. Slope Data Used In Program

Appendix A. BPNN Approach Output Tables for Model 1

Actual(1)	Network(1)	Act-Net(1)
1,3200	1,2958	0,0242
0,9400	0,8895	0,0505
0,9700	0,9517	0,0183
1,6100	1,8270	-0,2170
1,6400	1,6866	-0,0466
1,3500	1,3435	0,0065
1,2700	1,0988	0,1712
1,0600	1,1224	-0,0624
1,5500	1,1839	0,3661
1,4000	1,3054	0,0946
1,1800	1,1452	0,0348
1,3100	1,2206	0,0894
0,7500	0,7897	-0,0397
0,8000	0,8660	-0,0660
0,7700	0,8582	-0,0882
1,0500	0,9742	0,0758
0,9800	0,9446	0,0354
2,0900	1,7515	0,3385
1,0000	0,8538	0,1462
0,9000	0,8390	0,0610
1,1000	1,1197	-0,0197
1,2000	1,1544	0,0456
1,2900	1,3711	-0,0811
0,9700	0,9905	-0,0205
1,1300	1,1630	-0,0330
0,8600	0,7813	0,0787
1,1200	0,9997	0,1203
0,9600	1,0255	-0,0655
1,0000	0,9741	0,0259
1,1200	0,9246	0,1954
1,1000	1,2209	-0,1209
1,4000	1,1703	0,2297
1,0000	0,8796	0,1204
0,9900	0,6597	0,3303
1,0300	0,8021	0,2279
1,3200	1,2953	0,0247
1,5000	1,5342	-0,0342
1,5200	1,6925	-0,1725
1,1100	1,0193	0,0907
0,9700	0,9785	-0,0085
1,4700	1,1997	0,2703
0,9300	0,9949	-0,0649
0,9900	0,8729	0,1171
1,3500	1,3186	0,0314
0,7900	0,6446	0,1454

Actual(1)	Network(1)	Act-Net(1)
1,1500	1,2354	-0,0854
1,5000	1,3546	0,1454
2,0800	1,6502	0,4298
1,1900	1,1815	0,0085
0,9300	0,8940	0,0360
0,8100	0,8183	-0,0083
1,0500	1,2325	-0,1825
1,0700	1,1660	-0,0960
1,2100	1,4773	-0,2673
1,8200	1,7137	0,1063
0,9700	0,8637	0,1063
0,6200	0,8119	-0,1919
0,7800	0,9401	-0,1601
1,5400	1,5714	-0,0314
0,9300	0,8530	0,0770
1,6200	1,4839	0,1361
1,3000	1,2828	0,0172
1,7800	1,5596	0,2204
1,0300	1,1087	-0,0787
1,2300	1,1622	0,0678
1,2500	1,5146	-0,2646
1,3700	1,3961	-0,0261
1,2800	1,1608	0,1192
1,1100	1,1166	-0,0066
0,6800	1,1390	-0,4590
0,7000	0,9199	-0,2199
1,2000	1,1550	0,0450
2,1500	1,9525	0,1975
1,3500	1,4915	-0,1415
0,8900	0,9602	-0,0702
0,9200	0,8619	0,0581
0,6400	0,7483	-0,1083
1,1400	0,9359	0,2041
1,1900	1,2367	-0,0467
0,8700	0,9913	-0,1213
1,0500	1,1412	-0,0912
1,1700	1,1725	-0,0025
1,3100	1,2478	0,0622
1,0500	1,2664	-0,2164
1,3600	1,3803	-0,0203
1,5300	1,5754	-0,0454
1,3500	1,3638	-0,0138
1,0000	1,0266	-0,0266
0,8300	0,9026	-0,0726

Actual(1)	Network(1)	Act-Net(1)
0,7900	0,9566	-0,1666
1,0300	0,8343	0,1957
1,4500	1,0252	0,4248
1,6400	1,7485	-0,1085
1,2900	1,4117	-0,1217
1,0100	1,0574	-0,0474
1,0700	1,0724	-0,0024
1,0500	0,9476	0,1024
0,7300	0,7682	-0,0382
1,4300	1,2680	0,1620
1,0500	0,9638	0,0862
1,0000	0,9559	0,0441
1,2800	1,2553	0,0247
1,0000	0,9909	0,0091
0,8600	0,9928	-0,1328
0,9800	1,2301	-0,2501
1,2100	1,1395	0,0705
1,3100	1,3678	-0,0578
0,9700	0,9401	0,0299
1,7500	1,7513	-0,0013
2,0500	1,8548	0,1952
0,8200	1,1464	-0,3264
1,0000	0,9933	0,0067
0,9800	0,9676	0,0124
0,6700	0,8458	-0,1758
1,7600	1,7963	-0,0363
1,2000	1,0843	0,1157
1,1200	1,1657	-0,0457
0,9600	0,9827	-0,0227
1,7400	1,7397	0,0003
1,5400	1,4608	0,0792
1,2500	1,2440	0,0060
1,0000	1,1544	-0,1544
0,8700	0,8734	-0,0034
1,0000	1,1777	-0,1777
1,1100	1,1262	-0,0162
1,0000	1,0193	-0,0193
1,8750	1,5406	0,3344
2,0450	1,3778	0,6672
1,7800	1,6699	0,1101
1,9900	1,6817	0,3083
1,2500	0,8968	0,3532
1,1300	1,0239	0,1061
1,0200	1,0277	-0,0077

Actual(1)	Network(1)	Act-Net(1)
1,3000	1,1923	0,1077
1,2000	1,1305	0,0695
1,0900	1,1039	-0,0139
0,7800	0,8460	-0,0660
2,0000	1,9302	0,0698
1,7000	1,7450	-0,0450
1,0200	1,0602	-0,0402
0,8900	0,9100	-0,0200
1,4600	1,4707	-0,0107
0,8000	0,9442	-0,1442
1,4400	1,5093	-0,0693
0,8600	0,8622	-0,0022
1,0800	1,0844	-0,0044
1,1100	1,3293	-0,2193
1,4000	1,5357	-0,1357
1,3500	1,4917	-0,1417
1,0300	1,1319	-0,1019
1,2800	1,1535	0,1265
1,6300	1,5245	0,1055
1,0500	0,9304	0,1196
1,0300	1,0503	-0,0203
1,0900	1,0421	0,0479
1,1100	1,0893	0,0207
1,0100	1,0628	-0,0528
0,6250	0,9493	-0,3243
1,1200	0,9816	0,1384
1,2000	1,3517	-0,1517
1,8000	1,7990	0,0010
0,9000	1,0747	-0,1747
0,9600	0,8864	0,0736
0,8300	0,8157	0,0143
0,7900	0,8746	-0,0846
0,6700	0,9665	-0,2965
1,4500	1,4097	0,0403
1,5800	1,7291	-0,1491
1,3700	1,1987	0,1713
2,0500	1,9812	0,0688

Appendix B. BPNN Approach Output Tables for Model 2

Actual(1)	Network(1)	Act-Net(1)
1,3200	1,2902	0,0298
0,9400	0,8705	0,0695
0,9700	0,9951	-0,0251
1,6100	1,8157	-0,2057
1,6400	1,6686	-0,0286
1,3500	1,3615	-0,0115
1,2700	1,0968	0,1732
1,0600	1,0110	0,0490
1,5500	1,0413	0,5087
1,4000	1,3269	0,0731
1,1800	1,1132	0,0668
1,3100	1,1234	0,1866
0,7500	0,8022	-0,0522
0,8000	0,7761	0,0239
0,7700	0,8684	-0,0984
1,0500	0,9861	0,0639
0,9800	0,9767	0,0033
2,0900	1,7669	0,3231
1,0000	0,8540	0,1460
0,9000	0,8432	0,0568
1,1000	1,1075	-0,0075
1,2000	1,1274	0,0726
1,2900	1,3427	-0,0527
0,9700	0,9871	-0,0171
1,1300	1,1749	-0,0449
0,8600	0,7428	0,1172
1,1200	1,0157	0,1043
0,9600	1,0419	-0,0819
1,0000	0,9572	0,0428
1,1200	1,0469	0,0731
1,1000	1,2385	-0,1385
1,4000	1,4137	-0,0137
1,0000	0,8827	0,1173
0,9900	0,6425	0,3475
1,0300	0,7725	0,2575
1,3200	1,3082	0,0118
1,5000	1,5323	-0,0323
1,5200	1,6958	-0,1758
1,1100	0,9272	0,1828
0,9700	0,9550	0,0150
1,4700	1,2335	0,2365
0,9300	0,9400	-0,0100
0,9900	0,9304	0,0596
1,3500	1,3143	0,0357
0,7900	0,6401	0,1499

Actual(1)	Network(1)	Act-Net(1)
1,1500	1,2788	-0,1288
1,5000	1,5479	-0,0479
2,0800	1,6139	0,4661
1,1900	1,1773	0,0127
0,9300	0,8961	0,0339
0,8100	0,8212	-0,0112
1,0500	1,2598	-0,2098
1,0700	1,1753	-0,1053
1,2100	1,4223	-0,2123
1,8200	1,7024	0,1176
0,9700	0,8981	0,0719
0,6200	0,8027	-0,1827
0,7800	0,9687	-0,1887
1,5400	1,5612	-0,0212
0,9300	0,8704	0,0596
1,6200	1,5151	0,1049
1,3000	1,2875	0,0125
1,7800	1,5672	0,2128
1,0300	1,1244	-0,0944
1,2300	1,1601	0,0699
1,2500	1,4925	-0,2425
1,3700	1,2647	0,1053
1,2800	1,1822	0,0978
1,1100	1,1223	-0,0123
0,6800	1,1398	-0,4598
0,7000	0,9422	-0,2422
1,2000	1,1770	0,0230
2,1500	1,9544	0,1956
1,3500	1,4645	-0,1145
0,8900	0,9434	-0,0534
0,9200	0,8834	0,0366
0,6400	0,7107	-0,0707
1,1400	0,9095	0,2305
1,1900	1,1823	0,0077
0,8700	0,9799	-0,1099
1,0500	1,1542	-0,1042
1,1700	1,1911	-0,0211
1,3100	1,2531	0,0569
1,0500	1,2177	-0,1677
1,3600	1,3643	-0,0043
1,5300	1,5485	-0,0185
1,3500	1,3536	-0,0036
1,0000	1,0344	-0,0344
0,8300	0,7472	0,0828

Actual(1)	Network(1)	Act-Net(1)
0,7900	0,9798	-0,1898
1,0300	0,8383	0,1917
1,4500	1,1300	0,3200
1,6400	1,6420	-0,0020
1,2900	1,4378	-0,1478
1,0100	0,9903	0,0197
1,0700	1,0979	-0,0279
1,0500	0,9765	0,0735
0,7300	0,7640	-0,0340
1,4300	1,2638	0,1662
1,0500	0,9944	0,0556
1,0000	0,9497	0,0503
1,2800	1,3068	-0,0268
1,0000	0,9119	0,0881
0,8600	0,9723	-0,1123
0,9800	1,2635	-0,2835
1,2100	1,2521	-0,0421
1,3100	1,2112	0,0988
0,9700	0,9352	0,0348
1,7500	1,7563	-0,0063
2,0500	1,8710	0,1790
0,8200	1,1625	-0,3425
1,0000	0,9973	0,0027
0,9800	1,0114	-0,0314
0,6700	0,7422	-0,0722
1,7600	1,8047	-0,0447
1,2000	1,0784	0,1216
1,1200	1,1640	-0,0440
0,9600	0,8880	0,0720
1,7400	1,7563	-0,0163
1,5400	1,4523	0,0877
1,2500	1,1815	0,0685
1,0000	1,1274	-0,1274
0,8700	0,8529	0,0171
1,0000	1,1600	-0,1600
1,1100	1,1135	-0,0035
1,0000	1,0068	-0,0068
1,8750	1,5603	0,3147
2,0450	1,4507	0,5943
1,7800	1,6828	0,0972
1,9900	1,6904	0,2996
1,2500	0,9014	0,3486
1,1300	1,0458	0,0842
1,0200	0,8087	0,2113

Actual(1)	Network(1)	Act-Net(1)
1,3000	1,4622	-0,1622
1,2000	0,9646	0,2354
1,0900	1,0982	-0,0082
0,7800	0,8374	-0,0574
2,0000	1,9444	0,0556
1,7000	1,7199	-0,0199
1,0200	1,0648	-0,0448
0,8900	0,9039	-0,0139
1,4600	1,4480	0,0120
0,8000	0,9294	-0,1294
1,4400	1,4070	0,0330
0,8600	0,8334	0,0266
1,0800	1,1135	-0,0335
1,1100	1,2793	-0,1693
1,4000	1,5170	-0,1170
1,3500	1,4758	-0,1258
1,0300	1,0846	-0,0546
1,2800	1,2118	0,0682
1,6300	1,5631	0,0669
1,0500	0,9170	0,1330
1,0300	1,0282	0,0018
1,0900	0,9852	0,1048
1,1100	1,1896	-0,0796
1,0100	0,9953	0,0147
0,6250	0,7538	-0,1288
1,1200	0,9799	0,1401
1,2000	1,3455	-0,1455
1,8000	1,7952	0,0048
0,9000	1,0872	-0,1872
0,9600	1,0154	-0,0554
0,8300	0,8182	0,0118
0,7900	0,8685	-0,0785
0,6700	0,9388	-0,2688
1,4500	1,4539	-0,0039
1,5800	1,7386	-0,1586
1,3700	1,2078	0,1622
2,0500	1,9722	0,0778

Appendix C. Error Through Patterns Graphs for Model 1 and 2.

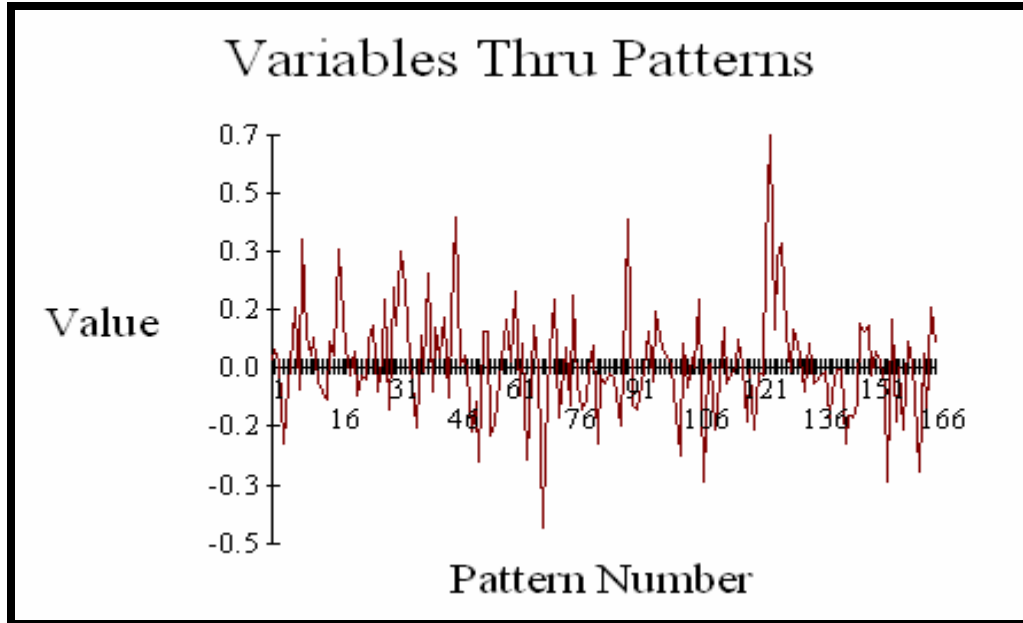


Figure App. C1 : Error through patterns for act-net for Model 1

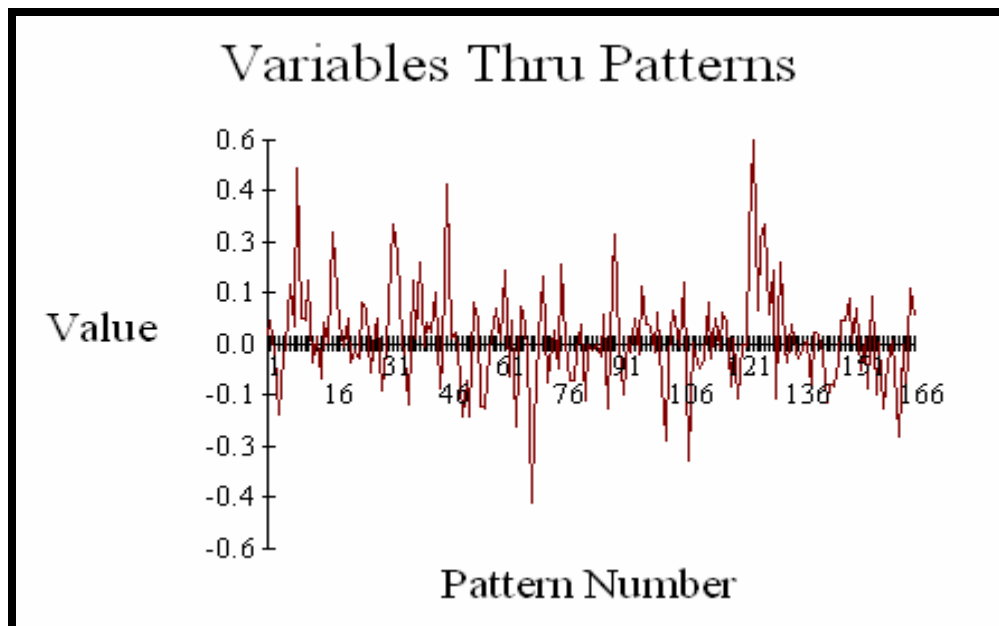


Figure App. C2 : Error through patterns for act-net for Model 2

Appendix D. GRNN Approach Output Tables for Model 3

Actual(1)	Network(1)	Act-Net(1)
1,3200	1,3200	0,0000
0,9400	0,9400	0,0000
0,9700	0,9700	0,0000
1,6100	1,6400	-0,0300
1,6400	1,6400	0,0000
1,3500	1,3500	0,0000
1,2700	1,2700	0,0000
1,0600	1,0600	0,0000
1,5500	1,6799	-0,1299
1,4000	1,4000	0,0000
1,1800	1,1800	0,0000
1,3100	1,3100	0,0000
0,7500	0,7500	0,0000
0,8000	0,8000	0,0000
0,7700	0,7700	0,0000
1,0500	1,0500	0,0000
0,9800	0,9800	0,0000
2,0900	2,0897	0,0003
1,0000	0,9000	0,1000
0,9000	0,9000	0,0000
1,1000	1,0999	0,0001
1,2000	1,0998	0,1002
1,2900	1,3452	-0,0552
0,9700	0,9700	0,0000
1,1300	1,1996	-0,0696
0,8600	1,3600	-0,5000
1,1200	1,1188	0,0012
0,9600	0,9613	-0,0013
1,0000	1,0021	-0,0021
1,1200	1,1185	0,0015
1,1000	1,1000	0,0000
1,4000	1,4000	0,0000
1,0000	1,0000	0,0000
0,9900	1,0300	-0,0400
1,0300	1,0300	0,0000
1,3200	1,3200	0,0000
1,5000	1,5000	0,0000
1,5200	1,5200	0,0000
1,1100	1,3155	-0,2055
0,9700	0,9700	0,0000
1,4700	1,4696	0,0004
0,9300	0,9300	0,0000
0,9900	0,9398	0,0502
1,3500	1,3500	0,0000
0,7900	0,7900	0,0000

Actual(1)	Network(1)	Act-Net(1)
1,1500	1,1500	0,0000
1,5000	1,0997	0,4003
2,0800	1,6372	0,4428
1,1900	1,1900	0,0000
0,9300	0,9301	-0,0001
0,8100	0,8100	0,0000
1,0500	1,0305	0,0195
1,0700	1,2051	-0,1351
1,2100	1,2100	0,0000
1,8200	1,8202	-0,0002
0,9700	0,9700	0,0000
0,6200	0,6200	0,0000
0,7800	0,7800	0,0000
1,5400	1,5400	0,0000
0,9300	0,9300	0,0000
1,6200	1,5115	0,1085
1,3000	1,3000	0,0000
1,7800	1,7801	-0,0001
1,0300	1,0300	0,0000
1,2300	1,2300	0,0000
1,2500	1,2361	0,0139
1,3700	1,3443	0,0257
1,2800	1,2800	0,0000
1,1100	1,1100	0,0000
0,6800	1,1030	-0,4230
0,7000	0,7385	-0,0385
1,2000	1,2000	0,0000
2,1500	1,6400	0,5100
1,3500	1,3500	0,0000
0,8900	0,8900	0,0000
0,9200	0,9199	0,0001
0,6400	0,6401	-0,0001
1,1400	1,1400	0,0000
1,1900	0,8712	0,3188
0,8700	0,8700	0,0000
1,0500	1,0500	0,0000
1,1700	1,1700	0,0000
1,3100	1,3062	0,0038
1,0500	1,0538	-0,0038
1,3600	1,3600	0,0000
1,5300	1,5299	0,0001
1,3500	1,3500	0,0000
1,0000	1,0000	0,0000
0,8300	1,0000	-0,1700

Actual(1)	Network(1)	Act-Net(1)
0,7900	0,7904	-0,0004
1,0300	1,0300	0,0000
1,4500	1,6447	-0,1947
1,6400	1,6400	0,0000
1,2900	1,2900	0,0000
1,0100	1,0100	0,0000
1,0700	1,0700	0,0000
1,0500	1,0500	0,0000
0,7300	0,7300	0,0000
1,4300	1,4299	0,0001
1,0500	1,0500	0,0000
1,0000	1,0000	0,0000
1,2800	1,2800	0,0000
1,0000	1,0000	0,0000
0,8600	0,8600	0,0000
0,9800	0,9919	-0,0119
1,2100	1,2100	0,0000
1,3100	1,3100	0,0000
0,9700	1,1125	-0,1425
1,7500	1,7500	0,0000
2,0500	2,0500	0,0000
0,8200	1,0971	-0,2771
1,0000	1,0000	0,0000
0,9800	0,9800	0,0000
0,6700	0,9746	-0,3046
1,7600	1,7600	0,0000
1,2000	1,4688	-0,2688
1,1200	1,1199	0,0001
0,9600	1,0059	-0,0459
1,7400	1,7400	0,0000
1,5400	1,5400	0,0000
1,2500	1,0883	0,1617
1,0000	1,0998	-0,0998
0,8700	0,8710	-0,0010
1,0000	0,8813	0,1187
1,1100	1,1100	0,0000
1,0000	1,0000	0,0000
1,8750	1,8738	0,0012
2,0450	1,7580	0,2870
1,7800	1,7800	0,0000
1,9900	1,7800	0,2100
1,2500	1,2500	0,0000
1,1300	1,1300	0,0000
1,0200	1,0155	0,0045

Actual(1)	Network(1)	Act-Net(1)
1,3000	1,3000	0,0000
1,2000	1,2000	0,0000
1,0900	1,0900	0,0000
0,7800	0,7800	0,0000
2,0000	2,0000	0,0000
1,7000	1,7000	0,0000
1,0200	1,0200	0,0000
0,8900	0,8898	0,0002
1,4600	1,4600	0,0000
0,8000	0,8000	0,0000
1,4400	1,4400	0,0000
0,8600	0,8600	0,0000
1,0800	1,0800	0,0000
1,1100	1,1100	0,0000
1,4000	1,4000	0,0000
1,3500	1,3500	0,0000
1,0300	1,0300	0,0000
1,2800	1,2800	0,0000
1,6300	1,6300	0,0000
1,0500	1,0500	0,0000
1,0300	1,0300	0,0000
1,0900	1,0900	0,0000
1,1100	1,1112	-0,0012
1,0100	1,0100	0,0000
0,6250	0,6295	-0,0045
1,1200	1,1200	0,0000
1,2000	1,0300	0,1700
1,8000	1,7125	0,0875
0,9000	0,8076	0,0924
0,9600	0,9600	0,0000
0,8300	0,8300	0,0000
0,7900	0,7883	0,0017
0,6700	0,6720	-0,0020
1,4500	1,4500	0,0000
1,5800	1,4500	0,1300
1,3700	1,3700	0,0000
2,0500	2,0500	0,0000

Appendix E. GRNN Approach Output Tables for Model 4

Actual(1)	Network(1)	Act-Net(1)
1,3200	1,3200	0,0000
0,9400	0,9412	-0,0012
0,9700	1,0355	-0,0655
1,6100	1,6400	-0,0300
1,6400	1,6400	0,0000
1,3500	1,3500	0,0000
1,2700	1,2712	-0,0012
1,0600	1,0600	0,0000
1,5500	1,6237	-0,0737
1,4000	1,3864	0,0136
1,1800	1,1807	-0,0007
1,3100	1,3108	-0,0008
0,7500	0,7514	-0,0014
0,8000	0,8491	-0,0491
0,7700	0,7945	-0,0245
1,0500	1,0471	0,0029
0,9800	0,9816	-0,0016
2,0900	2,0822	0,0078
1,0000	0,9934	0,0066
0,9000	0,9134	-0,0134
1,1000	1,1006	-0,0006
1,2000	1,1006	0,0994
1,2900	1,2900	0,0000
0,9700	0,9704	-0,0004
1,1300	1,1300	0,0000
0,8600	0,8600	0,0000
1,1200	1,1197	0,0003
0,9600	0,9605	-0,0005
1,0000	1,0289	-0,0289
1,1200	1,0917	0,0283
1,1000	1,0606	0,0394
1,4000	1,4000	0,0000
1,0000	1,0000	0,0000
0,9900	1,0706	-0,0806
1,0300	1,0300	0,0000
1,3200	1,2733	0,0467
1,5000	1,4989	0,0011
1,5200	1,4540	0,0660
1,1100	0,8666	0,2434
0,9700	0,9700	0,0000
1,4700	1,3871	0,0829
0,9300	0,9340	-0,0040
0,9900	0,9999	-0,0099
1,3500	1,3505	-0,0005
0,7900	0,7900	0,0000

Actual(1)	Network(1)	Act-Net(1)
1,1500	1,1984	-0,0484
1,5000	1,2577	0,2423
2,0800	1,6368	0,4432
1,1900	1,2036	-0,0136
0,9300	1,0598	-0,1298
0,8100	0,8100	0,0000
1,0500	1,0500	0,0000
1,0700	1,0700	0,0000
1,2100	1,2100	0,0000
1,8200	1,8199	0,0001
0,9700	0,9895	-0,0195
0,6200	0,6200	0,0000
0,7800	0,7803	-0,0003
1,5400	1,5400	0,0000
0,9300	0,9283	0,0017
1,6200	1,6651	-0,0451
1,3000	1,2953	0,0047
1,7800	1,7878	-0,0078
1,0300	1,0300	0,0000
1,2300	1,2300	0,0000
1,2500	1,1865	0,0635
1,3700	1,3679	0,0021
1,2800	1,2800	0,0000
1,1100	1,1096	0,0004
0,6800	1,1807	-0,5007
0,7000	1,0421	-0,3421
1,2000	1,2000	0,0000
2,1500	1,6400	0,5100
1,3500	1,3500	0,0000
0,8900	0,8929	-0,0029
0,9200	0,9200	0,0000
0,6400	0,6404	-0,0004
1,1400	1,1400	0,0000
1,1900	1,0455	0,1445
0,8700	0,8953	-0,0253
1,0500	1,0497	0,0003
1,1700	1,1682	0,0018
1,3100	1,2570	0,0530
1,0500	1,1030	-0,0530
1,3600	1,3600	0,0000
1,5300	1,5290	0,0010
1,3500	1,3500	0,0000
1,0000	0,9999	0,0001
0,8300	1,0001	-0,1701

Actual(1)	Network(1)	Act-Net(1)
0,7900	0,8729	-0,0829
1,0300	1,0924	-0,0624
1,4500	1,5917	-0,1417
1,6400	1,6400	0,0000
1,2900	1,2900	0,0000
1,0100	1,0100	0,0000
1,0700	1,0700	0,0000
1,0500	1,0500	0,0000
0,7300	0,7307	-0,0007
1,4300	1,2366	0,1934
1,0500	1,0505	-0,0005
1,0000	1,0000	0,0000
1,2800	1,2800	0,0000
1,0000	1,0000	0,0000
0,8600	0,8600	0,0000
0,9800	0,9870	-0,0070
1,2100	1,2100	0,0000
1,3100	1,3100	0,0000
0,9700	0,9221	0,0479
1,7500	1,7495	0,0005
2,0500	2,0500	0,0000
0,8200	0,9396	-0,1196
1,0000	0,9999	0,0001
0,9800	0,9800	0,0000
0,6700	0,6702	-0,0002
1,7600	1,7600	0,0000
1,2000	1,4727	-0,2727
1,1200	1,1199	0,0001
0,9600	1,1200	-0,1600
1,7400	1,7388	0,0012
1,5400	1,5365	0,0035
1,2500	0,9959	0,2541
1,0000	1,1006	-0,1006
0,8700	0,8700	0,0000
1,0000	1,0914	-0,0914
1,1100	1,1100	0,0000
1,0000	0,9999	0,0001
1,8750	1,8744	0,0006
2,0450	1,6395	0,4055
1,7800	1,7800	0,0000
1,9900	1,7800	0,2100
1,2500	1,2500	0,0000
1,1300	1,1297	0,0003
1,0200	0,8481	0,1719

Actual(1)	Network(1)	Act-Net(1)
1,3000	1,2830	0,0170
1,2000	1,2170	-0,0170
1,0900	1,0900	0,0000
0,7800	0,7801	-0,0001
2,0000	1,9999	0,0001
1,7000	1,6928	0,0072
1,0200	1,0198	0,0002
0,8900	0,8215	0,0685
1,4600	1,4598	0,0002
0,8000	0,8000	0,0000
1,4400	1,4391	0,0009
0,8600	0,8601	-0,0001
1,0800	1,0796	0,0004
1,1100	1,1100	0,0000
1,4000	1,4000	0,0000
1,3500	1,3500	0,0000
1,0300	1,0371	-0,0071
1,2800	1,2800	0,0000
1,6300	1,6300	0,0000
1,0500	1,0693	-0,0193
1,0300	1,0280	0,0020
1,0900	1,0900	0,0000
1,1100	1,1102	-0,0002
1,0100	1,0100	0,0000
0,6250	0,7969	-0,1719
1,1200	1,1200	0,0000
1,2000	1,1992	0,0008
1,8000	1,8000	0,0000
0,9000	0,9470	-0,0470
0,9600	0,9600	0,0000
0,8300	0,8303	-0,0003
0,7900	0,7899	0,0001
0,6700	0,7388	-0,0688
1,4500	1,4502	-0,0002
1,5800	1,4502	0,1298
1,3700	1,3698	0,0002
2,0500	2,0500	0,0000

Appendix F. GRNN Approach Output Tables for Model 5

Actual(1)	Network(1)	Act-Net(1)
1,3200	1,3200	0,0000
0,9400	0,9400	0,0000
0,9700	0,9701	-0,0001
1,6100	1,6391	-0,0291
1,6400	1,6384	0,0016
1,3500	1,3500	0,0000
1,2700	1,2762	-0,0062
1,0600	1,0600	0,0000
1,5500	1,6252	-0,0752
1,4000	1,3999	0,0001
1,1800	1,1800	0,0000
1,3100	1,3089	0,0011
0,7500	0,7617	-0,0117
0,8000	0,8011	-0,0011
0,7700	0,7954	-0,0254
1,0500	1,0279	0,0221
0,9800	0,9801	-0,0001
2,0900	2,0545	0,0355
1,0000	1,0528	-0,0528
0,9000	0,9016	-0,0016
1,1000	1,1002	-0,0002
1,2000	1,1045	0,0955
1,2900	1,2900	0,0000
0,9700	0,9700	0,0000
1,1300	1,1300	0,0000
0,8600	0,8600	0,0000
1,1200	1,1196	0,0004
0,9600	0,9785	-0,0185
1,0000	1,0007	-0,0007
1,1200	1,1196	0,0004
1,1000	1,0722	0,0278
1,4000	1,4000	0,0000
1,0000	1,0000	0,0000
0,9900	1,0300	-0,0400
1,0300	1,0300	0,0000
1,3200	1,3003	0,0197
1,5000	1,5011	-0,0011
1,5200	1,5016	0,0184
1,1100	0,8600	0,2500
0,9700	0,9700	0,0000
1,4700	1,3046	0,1654
0,9300	0,9403	-0,0103
0,9900	1,0010	-0,0110
1,3500	1,3500	0,0000
0,7900	0,7900	0,0000

Actual(1)	Network(1)	Act-Net(1)
1,1500	1,1695	-0,0195
1,5000	1,3352	0,1648
2,0800	1,6400	0,4400
1,1900	1,1901	-0,0001
0,9300	1,0614	-0,1314
0,8100	0,8101	-0,0001
1,0500	1,0496	0,0004
1,0700	1,0700	0,0000
1,2100	1,2100	0,0000
1,8200	1,8061	0,0139
0,9700	0,9666	0,0034
0,6200	0,6200	0,0000
0,7800	0,7800	0,0000
1,5400	1,5400	0,0000
0,9300	0,9451	-0,0151
1,6200	1,6816	-0,0616
1,3000	1,2922	0,0078
1,7800	1,8154	-0,0354
1,0300	1,0299	0,0001
1,2300	1,2300	0,0000
1,2500	1,1684	0,0816
1,3700	1,3663	0,0037
1,2800	1,2800	0,0000
1,1100	1,1100	0,0000
0,6800	1,1792	-0,4992
0,7000	0,9682	-0,2682
1,2000	1,1999	0,0001
2,1500	1,6400	0,5100
1,3500	1,3514	-0,0014
0,8900	0,9126	-0,0226
0,9200	0,9196	0,0004
0,6400	0,6408	-0,0008
1,1400	1,1400	0,0000
1,1900	1,0465	0,1435
0,8700	0,8998	-0,0298
1,0500	1,0499	0,0001
1,1700	1,1582	0,0118
1,3100	1,3092	0,0008
1,0500	1,0508	-0,0008
1,3600	1,3600	0,0000
1,5300	1,5286	0,0014
1,3500	1,3499	0,0001
1,0000	1,0000	0,0000
0,8300	1,0007	-0,1707

Actual(1)	Network(1)	Act-Net(1)
0,7900	0,9554	-0,1654
1,0300	1,0509	-0,0209
1,4500	1,5504	-0,1004
1,6400	1,6400	0,0000
1,2900	1,3039	-0,0139
1,0100	1,0100	0,0000
1,0700	1,0730	-0,0030
1,0500	1,0501	-0,0001
0,7300	0,7772	-0,0472
1,4300	1,2599	0,1701
1,0500	1,0524	-0,0024
1,0000	1,0000	0,0000
1,2800	1,2800	0,0000
1,0000	1,0001	-0,0001
0,8600	0,8600	0,0000
0,9800	1,0267	-0,0467
1,2100	1,2100	0,0000
1,3100	1,3100	0,0000
0,9700	0,9065	0,0635
1,7500	1,7500	0,0000
2,0500	2,0500	0,0000
0,8200	0,9389	-0,1189
1,0000	0,9997	0,0003
0,9800	0,9800	0,0000
0,6700	0,6700	0,0000
1,7600	1,7600	0,0000
1,2000	1,4620	-0,2620
1,1200	1,1200	0,0000
0,9600	1,1200	-0,1600
1,7400	1,7400	0,0000
1,5400	1,5120	0,0280
1,2500	1,1160	0,1340
1,0000	1,1045	-0,1045
0,8700	0,8700	0,0000
1,0000	0,8669	0,1331
1,1100	1,1100	0,0000
1,0000	0,9999	0,0001
1,8750	1,8273	0,0477
2,0450	1,6390	0,4060
1,7800	1,7800	0,0000
1,9900	1,7800	0,2100
1,2500	1,2500	0,0000
1,1300	1,1300	0,0000
1,0200	0,9603	0,0597

Actual(1)	Network(1)	Act-Net(1)
1,3000	1,3000	0,0000
1,2000	1,2000	0,0000
1,0900	1,0900	0,0000
0,7800	0,7801	-0,0001
2,0000	2,0000	0,0000
1,7000	1,6997	0,0003
1,0200	1,0200	0,0000
0,8900	0,8656	0,0244
1,4600	1,4600	0,0000
0,8000	0,8000	0,0000
1,4400	1,4400	0,0000
0,8600	0,8600	0,0000
1,0800	1,0800	0,0000
1,1100	1,1100	0,0000
1,4000	1,4001	-0,0001
1,3500	1,3500	0,0000
1,0300	1,0307	-0,0007
1,2800	1,2800	0,0000
1,6300	1,6300	0,0000
1,0500	1,0786	-0,0286
1,0300	1,0299	0,0001
1,0900	1,0911	-0,0011
1,1100	1,1107	-0,0007
1,0100	1,0100	0,0000
0,6250	0,6847	-0,0597
1,1200	1,1200	0,0000
1,2000	1,2000	0,0000
1,8000	1,8000	0,0000
0,9000	0,9596	-0,0596
0,9600	0,9600	0,0000
0,8300	0,8300	0,0000
0,7900	0,7896	0,0004
0,6700	0,6947	-0,0247
1,4500	1,4500	0,0000
1,5800	1,4502	0,1298
1,3700	1,3699	0,0001
2,0500	2,0500	0,0000

Appendix G. Error Through Patterns Graphs for Model 3,4 and 5.

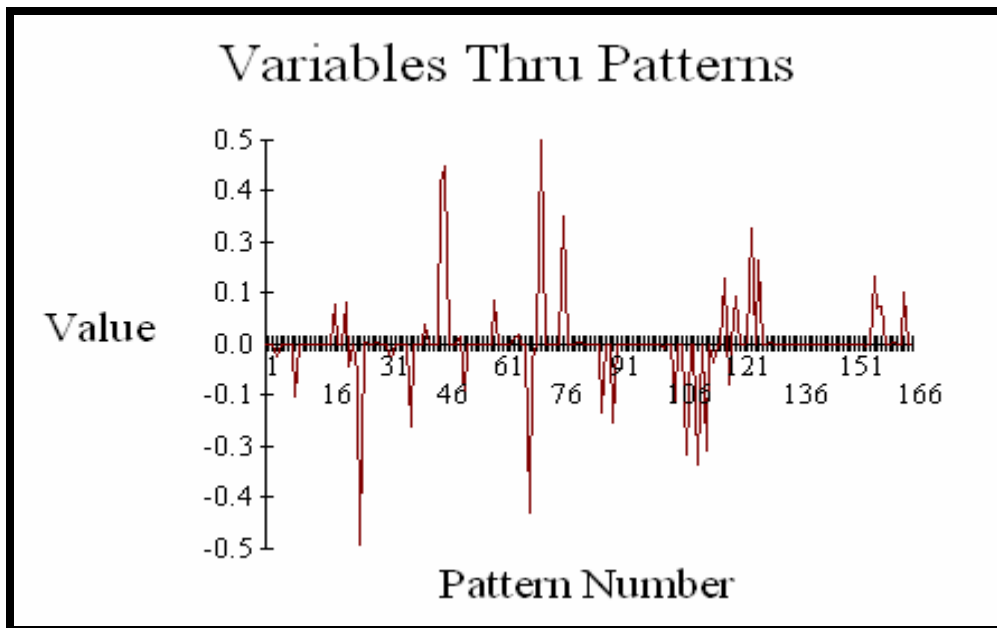


Figure App. G1 : Error through patterns for act-net for Model 3

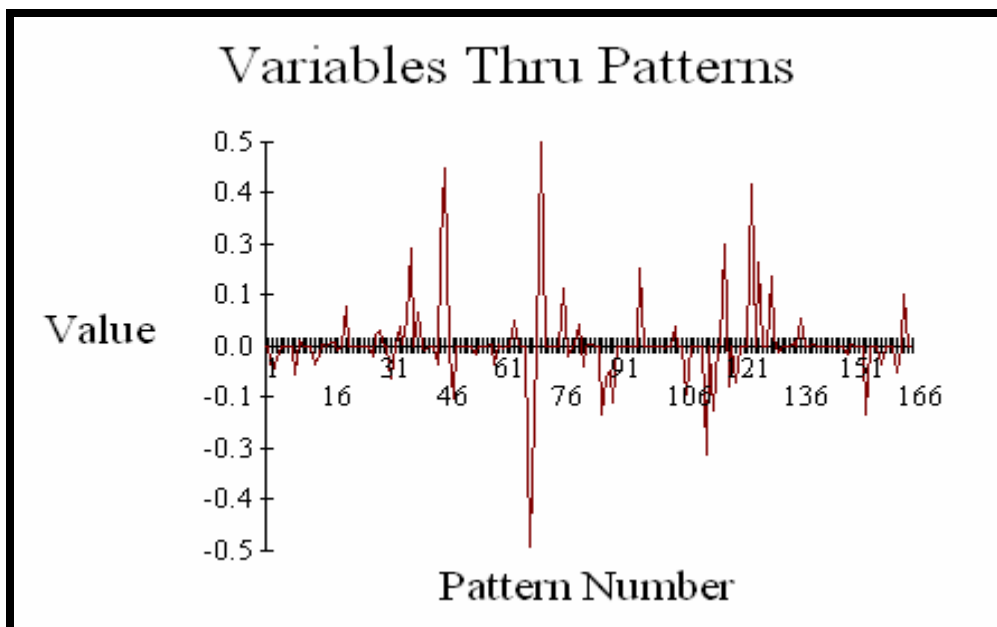


Figure App. G2 : Error through patterns for act-net for Model 4

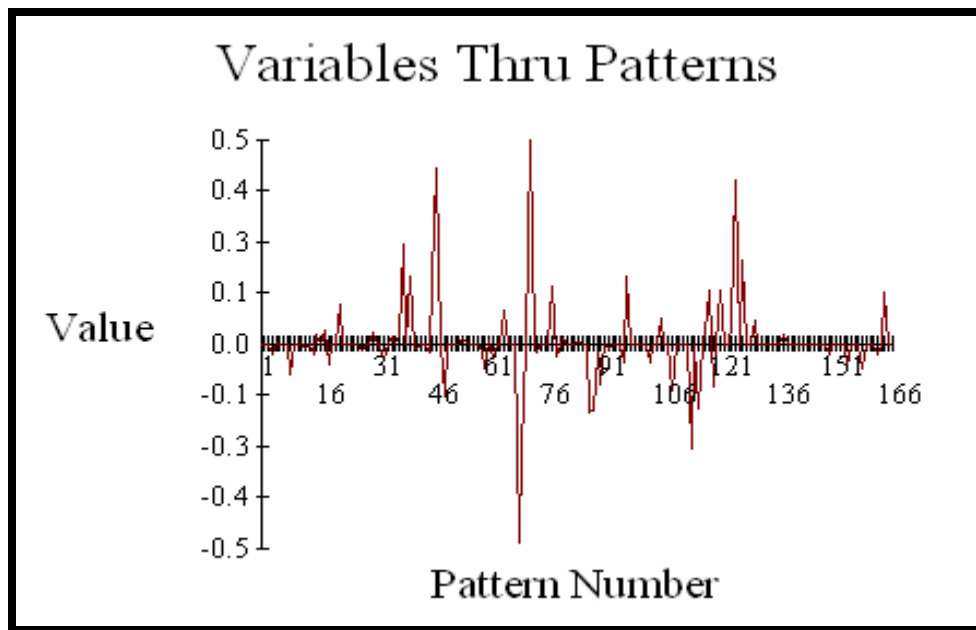


Figure App. G3 : Error through patterns for act-net for Model 5

Appendix H. Slope Data Used In Program (Cao Jinggang , 2002)

H (m.)	Hw (m.)	Hb (m.)	β (deg.)	γ (kN/m³)	c (kPa)	Φ (deg.)	kh	kv	F.S.
10,00	0,00	10,00	33,69	20,00	10,00	20,00	0,100	0,050	1,32
15,20	0,00	0,00	71,60	18,00	20,00	20,00	0,150	0,100	0,94
50,00	0,00	0,00	21,80	11,00	15,00	21,00	0,200	0,150	0,97
10,00	9,00	0,00	26,57	19,61	31,70	13,00	0,250	0,200	1,61
10,50	0,00	0,00	26,57	20,27	31,70	13,00	0,300	0,250	1,64
5,00	0,00	30,00	20,00	20,00	40,00	30,00	0,350	0,050	1,35
8,05	0,00	0,00	26,57	18,50	15,00	10,00	0,400	0,100	1,27
23,75	6,30	0,00	29,20	17,65	0,00	37,00	0,450	0,150	1,06
10,00	9,00	2,00	30,00	18,00	25,00	10,00	0,500	0,200	1,55
6,00	6,00	0,00	33,69	19,80	4,00	32,00	0,100	0,250	1,40
44,20	12,00	0,00	19,98	22,76	16,76	37,50	0,150	0,050	1,18
20,00	0,00	0,00	33,69	19,65	4,31	32,00	0,200	0,100	1,31
6,20	0,00	0,00	16,72	18,80	0,00	20,00	0,250	0,150	0,75
7,20	0,00	0,00	19,98	18,80	1,00	20,00	0,300	0,200	0,80
7,00	0,00	0,00	18,43	18,80	1,00	20,00	0,350	0,250	0,77
7,80	0,00	3,20	44,50	18,60	10,20	20,00	0,400	0,050	1,05
12,20	0,00	0,00	17,10	18,80	1,50	20,00	0,450	0,100	0,98
8,00	0,00	0,00	26,57	18,50	20,00	20,00	0,500	0,150	2,09
20,00	0,00	0,00	22,00	20,00	0,00	20,00	0,035	0,200	1,00
20,00	10,00	0,00	22,00	20,00	0,00	20,00	0,035	0,250	0,90
11,50	0,00	10,80	27,60	17,71	9,09	20,35	0,200	0,050	1,10
11,50	0,00	10,80	27,60	17,71	9,09	20,35	0,100	0,100	1,20
8,00	0,00	0,00	45,00	18,50	15,00	20,00	0,100	0,150	1,29
8,00	5,60	5,60	45,00	19,50	17,50	7,50	0,150	0,200	0,97
7,62	6,73	2,31	26,57	18,53	0,00	30,00	0,200	0,250	1,13
32,80	26,90	164,00	18,16	17,00	12,00	16,30	0,250	0,050	0,86

H (m.)	Hw (m.)	Hb (m.)	β (deg.)	γ (kN/m ³)	c (kPa)	Φ (deg.)	kh	kv	F.S.
20,40	10,00	0,00	22,00	20,00	20,00	20,00	0,035	0,100	1,12
20,40	10,00	0,00	22,00	20,00	20,00	20,00	0,100	0,150	0,96
44,20	0,00	0,00	19,98	22,80	16,80	37,50	0,100	0,200	1,00
44,20	0,00	0,00	19,98	22,80	16,80	37,50	0,150	0,250	1,12
4,90	0,00	0,00	18,43	18,80	1,20	20,00	0,200	0,050	1,10
20,00	0,00	100,00	33,69	18,80	41,70	15,00	0,250	0,100	1,40
15,20	0,00	0,00	63,40	18,00	20,00	20,00	0,300	0,150	1,00
46,00	0,00	0,00	41,01	9,00	25,00	20,00	0,350	0,200	0,99
45,50	0,00	0,00	41,01	12,00	23,00	25,00	0,400	0,250	1,03
8,00	0,00	0,00	45,00	18,50	20,00	15,00	0,450	0,050	1,32
8,00	0,00	0,00	45,00	18,50	20,00	20,00	0,500	0,100	1,50
30,00	0,00	0,00	20,56	19,61	14,71	20,00	0,100	0,150	1,52
32,80	26,90	164,00	18,16	17,00	12,00	16,30	0,150	0,200	1,11
17,00	0,00	0,00	33,69	18,80	1,00	20,00	0,200	0,250	0,97
6,10	0,00	30,50	33,69	19,62	4,31	32,00	0,250	0,050	1,47
10,00	0,00	5,00	26,57	16,00	10,00	15,00	0,300	0,100	0,93
9,10	4,00	5,00	26,60	16,50	8,50	10,60	0,350	0,150	0,99
8,00	0,00	0,00	45,00	18,50	25,00	10,00	0,400	0,200	1,35
17,68	17,68	88,40	26,57	19,65	10,06	27,00	0,450	0,250	0,79
8,56	0,00	0,00	45,00	18,50	20,00	10,00	0,500	0,050	1,15
44,00	0,00	0,00	19,98	22,80	16,80	37,50	0,100	0,100	1,50
13,50	0,00	0,00	26,57	17,30	57,50	7,00	0,150	0,150	2,08
6,10	0,00	0,00	33,69	19,65	4,31	32,00	0,200	0,200	1,19
6,00	0,00	0,00	23,96	18,80	1,00	20,00	0,250	0,250	0,93
7,00	0,00	0,00	26,57	18,80	1,00	20,00	0,300	0,050	0,81
10,00	0,00	0,00	26,57	18,93	11,97	32,00	0,350	0,100	1,05
10,00	0,00	5,00	33,69	17,66	7,85	25,00	0,400	0,150	1,07
8,00	0,00	0,00	26,57	18,50	5,00	20,00	0,450	0,200	1,21
8,00	0,00	0,00	26,57	18,50	15,00	20,00	0,500	0,250	1,82
10,40	0,00	0,00	15,24	18,80	0,00	20,00	0,100	0,050	0,97

H (m.)	Hw (m.)	Hb (m.)	β (deg.)	γ (kN/m ³)	c (kPa)	Φ (deg.)	kh	kv	F.S.
5,10	3,27	25,50	25,25	18,84	0,00	34,00	0,150	0,100	0,62
4,00	0,00	0,00	20,00	17,95	5,00	15,00	0,200	0,150	0,78
20,00	0,00	0,00	20,00	19,72	30,00	30,00	0,250	0,200	1,54
4,50	0,00	1,30	20,00	15,92	2,16	17,33	0,300	0,250	0,93
12,19	0,00	0,00	33,69	19,24	22,80	35,00	0,350	0,050	1,62
9,50	0,00	0,00	25,50	20,00	11,50	9,60	0,400	0,100	1,30
8,00	0,00	0,00	26,57	18,50	20,00	15,00	0,450	0,150	1,78
20,00	0,00	0,00	26,57	18,71	0,00	23,50	0,510	0,100	1,03
21,50	0,00	0,00	24,13	17,40	5,00	10,00	0,100	0,050	1,23
44,20	0,00	0,00	20,00	22,00	16,80	37,50	0,150	0,100	1,25
44,20	0,00	0,00	20,00	22,00	16,80	37,50	0,200	0,150	1,37
13,70	0,00	0,00	26,57	18,71	0,00	14,00	0,050	0,200	1,28
8,20	0,00	0,00	45,00	18,50	15,00	15,00	0,100	0,250	1,11
44,10	0,00	0,00	19,98	22,80	16,50	37,50	0,150	0,050	0,68
44,10	0,00	0,00	19,98	22,80	16,50	37,50	0,200	0,100	0,70
12,19	0,00	7,62	27,15	18,87	0,00	33,00	0,250	0,150	1,20
12,19	0,00	7,62	27,15	18,87	67,00	0,00	0,300	0,200	2,15
12,19	0,00	7,62	27,15	18,87	28,70	20,00	0,350	0,250	1,35
8,45	0,00	0,00	45,00	18,50	10,00	15,00	0,400	0,050	0,89
21,50	0,00	0,00	24,13	17,40	0,00	14,00	0,450	0,100	0,92
21,50	0,00	0,00	24,13	17,40	0,00	17,20	0,500	0,150	0,64
46,00	0,00	0,00	38,66	14,00	20,00	26,30	0,100	0,200	1,14
22,70	0,00	0,00	16,27	18,20	0,00	14,10	0,150	0,250	1,19
22,70	0,00	0,00	16,27	18,20	0,00	17,20	0,200	0,050	0,87
15,50	0,00	0,00	15,01	18,00	5,00	10,00	0,250	0,100	1,05
15,50	0,00	0,00	15,01	18,00	0,00	14,00	0,300	0,150	1,17
15,00	0,00	0,00	12,99	22,00	0,00	26,00	0,350	0,200	1,31
15,00	0,00	0,00	12,99	22,00	0,00	26,00	0,400	0,250	1,05
25,00	6,25	125,00	22,00	18,80	30,00	20,00	0,450	0,050	1,36
8,00	0,00	0,00	45,00	18,50	25,00	15,00	0,500	0,100	1,53

H (m.)	Hw (m.)	Hb (m.)	β (deg.)	γ (kN/m³)	c (kPa)	Φ (deg.)	kh	kv	F.S.
8,00	0,00	0,00	26,50	18,50	15,00	15,00	0,100	0,150	1,35
10,06	30,38	0,00	21,80	18,44	0,96	24,50	0,150	0,200	1,00
10,06	30,38	0,00	21,80	18,44	0,72	25,60	0,200	0,250	0,83
6,00	6,00	30,00	33,69	19,65	1,50	30,00	0,250	0,050	0,79
12,80	0,00	0,00	27,76	21,85	8,62	32,00	0,300	0,100	1,03
27,43	0,00	0,00	26,40	17,29	44,54	12,00	0,350	0,150	1,45
14,33	15,14	3,05	36,53	20,47	68,00	0,00	0,400	0,200	1,64
8,00	0,00	0,00	26,57	18,50	10,00	15,00	0,450	0,250	1,29
10,00	7,00	0,00	39,81	20,36	0,98	32,50	0,500	0,050	1,01
18,00	0,00	0,00	26,57	19,50	9,81	27,00	0,100	0,100	1,07
12,80	0,00	6,10	28,50	21,55	8,62	30,00	0,150	0,150	1,05
10,06	0,00	0,00	21,80	18,01	15,33	20,00	0,200	0,200	0,73
10,06	0,00	0,00	21,80	18,84	0,00	20,00	0,250	0,250	1,43
7,01	0,00	0,00	18,43	21,29	0,00	20,00	0,300	0,050	1,05
7,01	0,00	0,00	18,43	19,79	0,96	13,00	0,350	0,100	1,00
18,29	0,00	0,00	11,00	22,32	15,33	21,00	0,400	0,150	1,28
12,10	10,00	0,00	24,38	16,10	25,00	20,00	0,450	0,200	1,00
30,00	0,00	20,00	30,00	21,00	22,11	18,29	0,500	0,250	0,86
5,00	0,00	30,00	33,69	19,60	2,56	27,60	0,100	0,050	0,98
67,80	0,00	0,00	29,05	19,00	33,00	29,50	0,150	0,100	1,21
67,80	45,00	0,00	29,05	16,00	25,00	20,00	0,200	0,150	1,31
14,30	13,30	0,00	27,00	19,60	9,60	25,00	0,250	0,200	0,97
8,00	0,00	0,00	45,00	18,50	30,00	15,00	0,300	0,250	1,75
8,00	0,00	0,00	26,57	18,50	25,00	15,00	0,350	0,050	2,05
11,50	0,00	10,80	27,60	17,71	9,09	20,35	0,400	0,100	0,82
5,00	1,00	3,00	26,57	17,64	4,90	10,00	0,450	0,150	1,00
12,80	8,09	8,09	28,00	21,67	7,82	32,00	0,500	0,200	0,98
10,00	0,00	0,00	14,04	20,00	10,00	25,00	0,100	0,250	0,67
6,00	0,00	30,00	45,00	18,00	10,00	37,00	0,150	0,050	1,76
6,00	0,00	30,00	33,69	18,00	10,00	37,00	0,200	0,100	1,20

H (m.)	Hw (m.)	Hb (m.)	β (deg.)	γ (kN/m ³)	c (kPa)	Φ (deg.)	kh	kv	F.S.
20,15	10,00	0,00	22,00	20,00	20,00	20,00	0,035	0,250	1,12
20,15	10,00	0,00	22,00	20,00	20,00	20,00	0,100	0,050	0,96
8,00	0,00	0,00	45,00	18,50	25,00	20,00	0,100	0,050	1,74
8,30	0,00	0,00	26,57	18,50	10,00	20,00	0,200	0,100	1,54
11,50	0,00	10,80	27,60	17,71	9,09	20,35	0,050	0,150	1,25
11,50	0,00	10,80	27,60	17,71	9,09	20,35	0,100	0,100	1,00
11,50	0,00	10,80	27,60	17,71	9,09	20,35	0,150	0,200	0,87
10,20	0,00	5,00	45,00	19,60	11,80	30,00	0,200	0,050	1,00
8,23	0,00	0,00	35,00	18,67	26,34	15,00	0,100	0,100	1,11
3,66	0,00	0,00	30,00	16,50	11,49	0,00	0,150	0,150	1,00
30,50	0,00	0,00	20,00	18,84	14,40	25,00	0,200	0,200	1,88
30,50	0,00	0,00	20,00	18,84	57,46	20,00	0,250	0,250	2,05
100,00	0,00	0,00	35,00	28,44	29,42	35,00	0,300	0,050	1,78
100,00	0,00	0,00	35,00	28,44	39,23	38,00	0,350	0,100	1,99
40,00	0,00	0,00	30,00	20,60	16,28	26,50	0,400	0,150	1,25
50,00	0,00	0,00	20,00	14,80	0,00	17,00	0,450	0,200	1,13
88,00	0,00	0,00	30,00	14,00	11,97	26,00	0,500	0,250	1,02
120,00	0,00	0,00	53,00	25,00	120,00	45,00	0,100	0,050	1,30
200,00	0,00	0,00	50,00	26,00	150,05	45,00	0,150	0,100	1,20
6,00	0,00	0,00	30,00	18,50	25,00	0,00	0,200	0,150	1,09
6,00	0,00	0,00	30,00	18,50	12,00	0,00	0,250	0,200	0,78
10,00	0,00	0,00	30,00	22,40	10,00	35,00	0,300	0,250	2,00
20,00	0,00	0,00	30,00	21,40	10,00	30,34	0,350	0,050	1,70
50,00	0,00	0,00	45,00	22,00	20,00	36,00	0,400	0,100	1,02
50,00	0,00	0,00	45,00	22,00	0,00	36,00	0,450	0,150	0,89
4,00	0,00	0,00	35,00	12,00	0,00	30,00	0,500	0,200	1,46
8,00	0,00	0,00	45,00	12,00	0,00	30,00	0,100	0,250	0,80
4,00	0,00	0,00	35,00	12,00	0,00	30,00	0,150	0,050	1,44
8,00	0,00	0,00	45,00	12,00	0,00	30,00	0,200	0,100	0,86
214,00	0,00	0,00	37,00	23,47	0,00	32,00	0,250	0,150	1,08

H (m.)	Hw (m.)	Hb (m.)	β (deg.)	γ (kN/m³)	c (kPa)	Φ (deg.)	kh	kv	F.S.
115,00	0,00	0,00	40,00	16,00	70,00	20,00	0,300	0,200	1,11
10,67	0,00	0,00	22,00	20,41	24,90	13,00	0,350	0,250	1,40
12,19	0,00	0,00	22,00	19,63	11,97	20,00	0,400	0,050	1,35
12,80	0,00	0,00	28,00	21,82	8,62	32,00	0,450	0,100	1,03
45,72	0,00	0,00	16,00	20,41	33,52	11,00	0,500	0,150	1,28
10,67	0,00	0,00	25,00	18,84	15,32	30,00	0,100	0,200	1,63
7,62	0,00	0,00	20,00	18,84	0,00	20,00	0,150	0,250	1,05
61,00	0,00	0,00	20,00	21,43	0,00	20,00	0,200	0,050	1,03
21,00	0,00	0,00	35,00	19,06	11,71	28,00	0,250	0,100	1,09
30,50	0,00	0,00	20,00	18,84	14,36	25,00	0,300	0,150	1,11
76,81	0,00	0,00	31,00	21,51	6,94	30,00	0,350	0,200	1,01
88,00	0,00	0,00	30,00	14,00	11,97	26,00	0,400	0,250	0,63
20,00	0,00	0,00	45,00	18,00	24,00	30,15	0,450	0,050	1,12
100,00	0,00	0,00	20,00	23,00	0,00	20,00	0,500	0,100	1,20
15,00	0,00	0,00	45,00	22,40	100,00	45,00	0,100	0,150	1,80
10,00	0,00	0,00	45,00	22,40	10,00	35,00	0,150	0,200	0,90
50,00	0,00	0,00	45,00	20,00	20,00	36,00	0,200	0,250	0,96
50,00	0,00	0,00	45,00	20,00	20,00	36,00	0,250	0,050	0,83
50,00	0,00	0,00	45,00	20,00	0,00	36,00	0,300	0,100	0,79
50,00	0,00	0,00	45,00	20,00	0,00	36,00	0,350	0,150	0,67
8,00	0,00	0,00	33,00	22,00	0,00	40,00	0,400	0,200	1,45
8,00	0,00	0,00	33,00	24,00	0,00	40,00	0,450	0,250	1,58
8,00	0,00	0,00	20,00	20,00	0,00	24,50	0,500	0,050	1,37
8,00	0,00	0,00	20,00	18,00	5,00	30,00	0,100	0,100	2,05

CURRICULLUM VITAE

Mert TOLON was born on August 19, 1983 in İstanbul. He completed his primary school in 1994 and his secondary school in Evrim Secondary School in 1998, and his high school in Evrim High School in 2001 in İstanbul. He started his BS degree at the Civil Engineering Department of the Yıldız Technical University and completed a four-year undergraduate education and graduated in 2005. At the same year, he started his MS education as a graduate student in the Earthquake Engineering Division of Civil Engineering Department at the Istanbul Technical University.

ÖZGEÇMİŞ

İnş. Müh. Mert TOLON 19.08.1983 'de İstanbul'da doğdu. İlkokulu 1994'de, ortaokulu 1998'de , liseyi de 2001'de Özel Evrim Lisesi'nde (İstanbul) bitirdi. Lisans eğitimini Yıldız Teknik Üniversitesi İnşaat Mühendisliği bölümünde 4 yılda 2005 yılında tamamladı. Yine aynı yıl İstanbul Teknik Üniversitesi Fen Bilimleri Enstitüsü Deprem Mühendisliği Anabilim Dalında yüksek lisans eğitimine başladı.